machines

MDPI

Review

Parallel–Serial Robotic Manipulators: A Review of Architectures, Applications, and Methods of Design and Analysis

Anton Antonov

Mechanisms Theory and Machines Structure Laboratory, Mechanical Engineering Research Institute of the Russian Academy of Sciences (IMASH RAN), 101000 Moscow, Russia; antonov.av@imash.ru; Tel.: +7-495-623-3273

Abstract: Parallel–serial (hybrid) manipulators represent robotic systems composed of kinematic chains with parallel and serial structures. These manipulators combine the benefits of both parallel and serial mechanisms, such as increased stiffness, high positioning accuracy, and a large workspace. This study discusses the existing architectures and applications of parallel–serial robots and the methods of their design and analysis. The paper reviews around 500 articles and presents over 150 architectures of manipulators used in machining, medicine, and pick-and-place tasks, humanoids and legged systems, haptic devices, simulators, and other applications, covering both lower mobility and kinematically redundant robots. After that, the paper considers how researchers have developed and analyzed these manipulators. In particular, it examines methods of type synthesis, mobility, kinematic, and dynamic analysis, workspace and singularity determination, performance evaluation, optimal design, control, and calibration. The review concludes with a discussion of current trends in the field of parallel–serial manipulators and potential directions for future studies.

Keywords: parallel–serial (hybrid) manipulator; machine tools; medicine robotics; kinematic redundancy; type synthesis; kinematic and dynamic analysis; optimal design; calibration; robot control

Citation: Antonov, A. Parallel–Serial Robotic Manipulators: A Review of Architectures, Applications, and Methods of Design and Analysis. *Machines* **2024**, *12*, 811. https://doi.org/10.3390/machines12110811

Academic Editor: Zheng Chen

Received: 21 October 2024
Revised: 7 November 2024
Accepted: 11 November 2024
Published: 14 November 2024

1. Introduction

The rapid growth of modern technologies promotes the development of novel technological and robotic systems. Among them are robotic manipulators that have now become widespread in industrial [1], medical [2], service [3], and other applications [4,5].

These manipulators usually have a serial or a parallel architecture [6,7]. In the first one, the manipulator end-effector (output link) attaches to the base by a series of links connected with 1-DOF (one degree of freedom) actuated joints. The serial architecture provides the end-effector with a large workspace and high versatility, making these manipulators suitable for welding [8], pick-and-place [9], or assembling [10] operations. At the same time, serial robots have low payload capacity and stiffness and may be unsuitable for high-precision tasks since the drive motion errors "accumulate" from the base towards the end-effector. The design of parallel manipulators, where the output link connects to the base with multiple kinematic chains (branches), mitigates these limitations, making them useful in machining [11] and precise positioning [12] operations. On the other hand, parallel robots have a smaller workspace compared to serial ones. Singular configurations [13] represent another issue that limits the applications of parallel manipulators.

In search of "optimal" robotic architectures that do not have the limitations of serial and parallel mechanisms, scholars have proposed various parallel–serial manipulators. These mechanical systems, composed of parallel and serial kinematic chains, combine the features of both architectures. The parallel part enhances the robot stiffness and motion accuracy, while the serial part expands its workspace. These benefits have encouraged the development of parallel–serial robots for diverse applications, including machining [14], medicine [15], object capturing [16], and other operations, which are considered in the current paper.

With the growing interest in parallel–serial manipulators, this article aims to review the existing architectures of these systems, their applications, and the methods that scholars have applied to design and analyze them. To our knowledge, there have been no similar reviews in recent years as discussed in the next section. The rest of the paper has the following organization. Section 2 describes the search methodology used to select the articles for this review. Section 3 considers various applications of parallel–serial manipulators and the architectures proposed for these applications. Section 4 focuses on the methods used for designing and analyzing parallel–serial manipulators. Section 5 discusses trends and perspectives in this field. Finally, Section 6 outlines the review results.

2. Methodology

In robotic literature, the term "parallel–serial" is used to name various architectures of manipulators which differ in their underlying mechanisms. We can distinguish the following types of these architectures:

1. Multiple parallel mechanisms connected in series (Figure 1a). These systems are also known as parallel–parallel manipulators [17].
2. A parallel mechanism connected with a serial kinematic chain (Figure 1b). The parallel mechanism can be placed near the base [18], at the end-effector [19], or between two serial chains [20].
3. Parallel and serial mechanisms operating as two independent modules [21] (Figure 1c).
4. A serial mechanism, typically with revolute joints, where these joints are actuated by additional kinematic chains, which often include actuated prismatic joints or have a parallelogram structure (Figure 1d). These systems are also known as quasi-serial manipulators [22].
5. A mechanism where kinematic chains between the base and the end-effector are also coupled, and it is challenging to distinguish parallel and serial parts (Figure 1e). These systems are also known as interconnected manipulators [23].

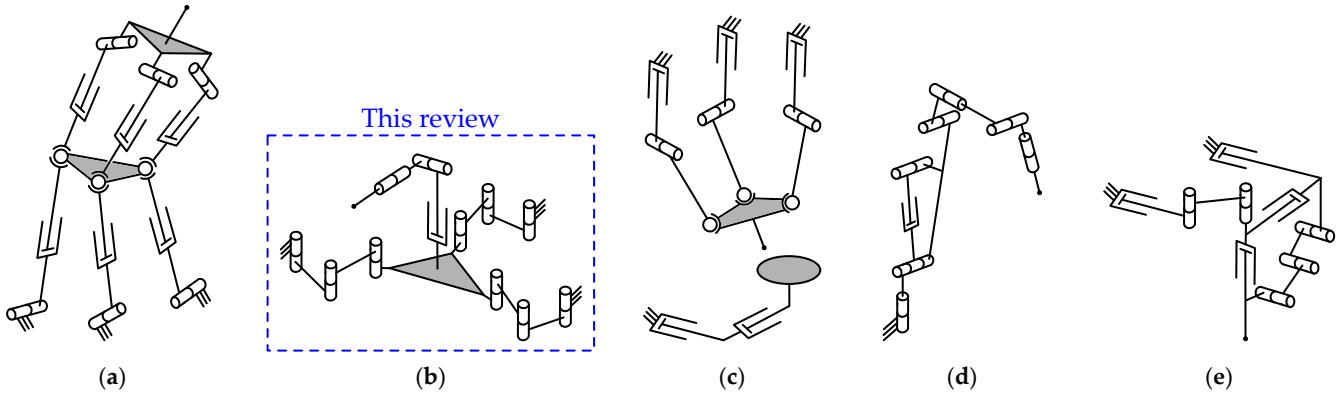

Figure 1. Architectures of robotic manipulators referred to as "parallel–serial" or "hybrid": (**a**) parallel–parallel [17]; (**b**) parallel–serial (connected) [18]; (**c**) parallel–serial (independent) [21]; (**d**) quasi-serial [22]; (**e**) interconnected [23].

The architectures above can be mixed as well. For example, there are parallel–serial systems of the third type where one module is a manipulator of the second type [24]. Furthermore, a manipulator can be placed on a mobile platform, which is used to position it in space and increase its operating range [25]. Some manipulators also include two parallel modules connected by a serial kinematic chain [26]. All these architectures are examples of parallel–serial manipulators, also called "hybrid" manipulators in the literature.

This review focuses on parallel–serial manipulators of the second type. In these systems, a parallel part is not necessarily a multi-DOF parallel mechanism—it can be represented by a simple closed-loop mechanism with one [27] or two [28] DOFs (Figure 2a,b). A serial part can also be a 1-DOF one-joint mechanism [29] (Figure 2c). The reasons that

we consider this type of parallel–serial manipulators among the others and perform this review are the following:

1. Parallel–parallel and interconnected manipulators (the first and fifth types in the classification above) are rarely used in practice because of their complex design.
2. Development and analysis of parallel–serial manipulators with independent modules (the third type) are usually performed separately for each module, and there are many studies devoted to parallel and serial manipulators, including some recent reviews [11,30].
3. Quasi-serial manipulators (the fourth type) are often treated as well-studied serial manipulators, and a review of these systems has also been performed recently [31].
4. There were no recent reviews of parallel–serial manipulators of the second type, while these manipulators are becoming more popular and widespread in practice nowadays.

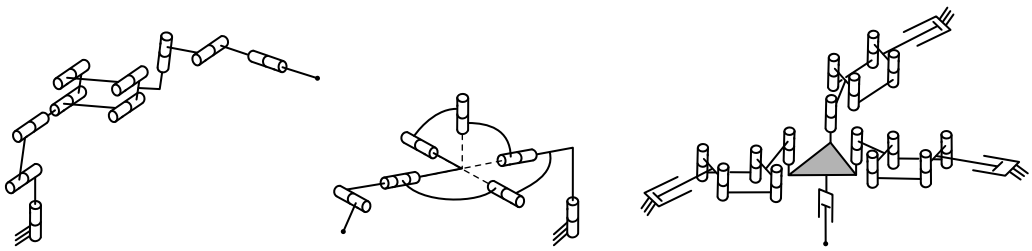

(**a**) (**b**) (**c**)

Figure 2. Examples of parallel–serial manipulators with trivial parallel and serial parts: (**a**) parallel part is a 1-DOF parallelogram linkage [27]; (**b**) parallel part is a 2-DOF single-loop spherical linkage [28]; (**c**) serial part is a 1-DOF one-joint translational mechanism [29].

From now on, we use the terms "parallel–serial" or "hybrid" to name parallel–serial manipulators of the second type. There are numerous works devoted to these manipulators; in particular, many studies focus on the development and analysis of parallel mechanisms used in hybrid mechanical systems. The current review does not aim to cover all the existing articles or find a paper where a parallel–serial manipulator was presented for the first time. Instead, it aims to analyze the papers that can be easily found and accessed by other scholars and readers. Given the above, the considered papers were selected based on the following inclusion and exclusion criteria:

1. The papers discuss parallel–serial manipulators of the second type and not the other types.
2. The papers primarily focus on parallel–serial manipulators and not on the parallel manipulator.
3. Patents and theses are not included in this review.

We selected two familiar databases, Scopus and Google Scholar, to search for the relevant papers that met the criteria above. The search was a multi-step process performed as follows:

1. First, we used Scopus to search for papers that considered parallel–serial or hybrid manipulators, robots, and mechanisms. For this purpose, we defined the following search request: TITLE-ABS-KEY((hybrid OR (parallel W/0 seri*)) W/0 (manip* OR robot* OR mechan*)). The results were then limited to the engineering field. At that moment, we had 2512 articles (17 September 2024). After excluding inappropriate publications according to the criteria above, we selected 280 papers.
2. Next, we examined the references in the selected publications using the same criteria and repeated this process for each new paper. After this step, we obtained 368 papers.
3. Finally, we checked the citations of each selected work in Google Scholar and defined the following search request for each set of citations: (hybrid OR (parallel-seri*)). After that, we repeated this procedure for each newly obtained paper. As a result, we obtained 510 papers, which were included and analyzed in this review.

Figure 3 shows the distribution of selected papers by year, starting from 1988 and ending in 2025. We see the number of studies in the last decade is more than in all the previous years, and it continues to increase each year. The decrease in the paper number in 2024 is probably because not all papers published this year have been indexed in Scopus and Google Scholar at the moment of writing this review. Nonetheless, these results verify the growing interest in parallel–serial manipulators.

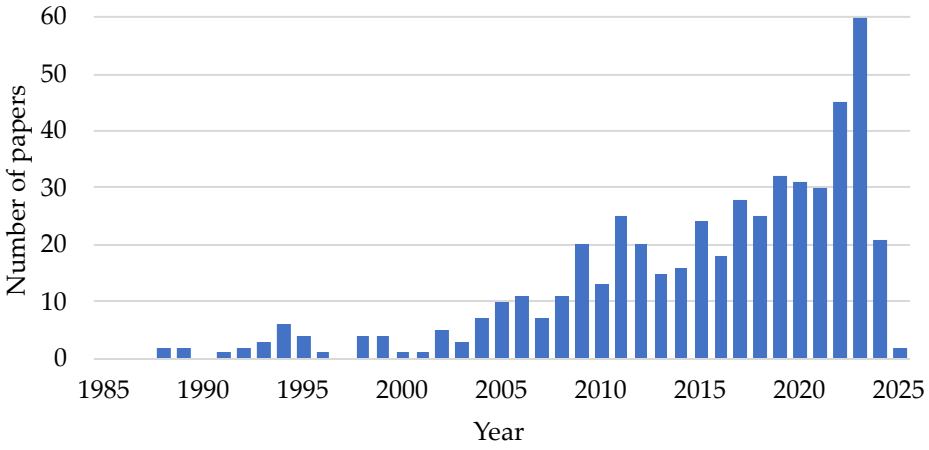

Figure 3. Distribution of selected papers by year.

Figure 4 illustrates the distribution of selected papers by manipulator application, ignoring works where the application is not specified. Machining dominates all the other applications put together. In the next section, we explore these applications in more detail and consider the architectures of proposed parallel–serial manipulators.

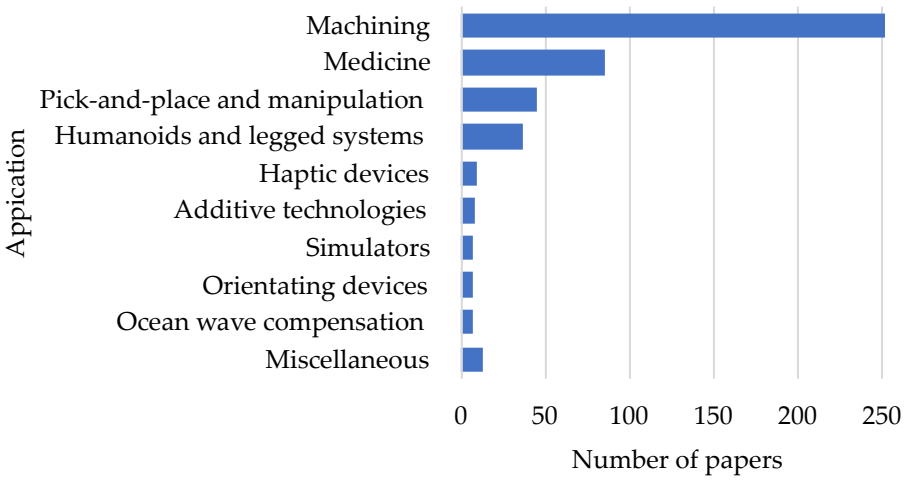

Figure 4. Distribution of selected papers by application.

3. Applications and Architectures

This section looks at the applications of parallel–serial manipulators presented in Figure 4 and examines the architectures of these mechanical systems. In addition, the section mentions the problems solved by scholars when they designed and analyzed these manipulators. The methods scholars have used to handle these problems are discussed in Section 4. The kinematic schemes of manipulators presented in this section aim to illustrate the relative arrangement of the joints rather than the structural design. The latter can be found in the corresponding articles cited in the text.

In this paper, we use the following abbreviations for joints: R for revolute, P for prismatic, Pa for parallelogram, Pa* for spatial parallelogram, H for helical, C for cylindrical, U for universal, and S for spherical joints. The underline indicates the actuated joints of the

parallel part; the number before a letter indicates the number of corresponding branches of the parallel part. The parallel part is enclosed in parentheses. We also use the term "branch" to name a kinematic chain of the parallel mechanism within the parallel–serial manipulator. For example, notation (1-UP/3-UPS)RRR means the manipulator has a parallel part attached to the base with one unactuated UP branch and three UPS branches with actuated prismatic joints. The parallel part is followed by an RRR serial chain, where all the joints are, of course, actuated.

3.1. Machining

Figure 4 shows that machining is the most popular application of parallel–serial manipulators. This is because parallel–serial manipulators combine the benefits of parallel and serial architectures, providing high rigidity, motion accuracy, and workspace, which are critical for machining operations. These operations are not limited to milling or drilling but include grinding, polishing, welding, and sheet forming.

The literature review reveals that existing parallel–serial machining manipulators differ mainly in their underlying parallel mechanisms. Therefore, we found it convenient to classify the manipulators according to this mechanism. The rest of the subsection illustrates this classification and covers various architectures of hybrid machining robots.

3.1.1. Manipulators Based on the Tricept Parallel Mechanism

Manipulators in this family are based on a 3-DOF parallel mechanism called Tricept and patented by Neumann [32]. This mechanism has one UP branch, which defines the motion type of the output link, and three UPS branches, which include actuators. Based on this scheme, scholars have proposed different parallel–serial manipulators considered next.

Tetrabot (tetrahedral robot) [33] was probably the first ever parallel–serial manipulator, which was used for assembly operations. In this robot, the output link of the Tricept parallel mechanism is augmented with an RRR serial spherical wrist (Figure 5a). This 6-DOF kinematics has become suitable for other applications as well. For example, Choi and Lee [34] considered using this parallel–serial manipulator for propeller grinding and developed its physical prototype. In the prototype, the serial wrist was designed as a geared mechanism. The authors analyzed the kinematics, dynamics, and position/velocity control of this manipulator in their paper [35]. Zhao et al. [36] designed another prototype of such a parallel–serial manipulator and applied it to polishing operations. In their later works, the authors focused on kinematic calibration [37], stiffness [38] and repeatability [39] analysis, and different control strategies [40,41] of this robot.

While 6-DOF manipulators can reach any desired end-effector posture, most machining operations only need five DOFs to position and align the tool. In this regard, most Tricept-based parallel–serial robots are equipped with a 2-DOF RR serial wrist (Figure 5b). The obtained (1-UP/3-UPS)RR architecture is the one that is actually called Tricept in most cases. Parallel–serial manipulators with this architecture have been the subject of numerous articles and successfully applied in practice [42]. For example, among the pioneering studies are the works of Siciliano [43,44], who analyzed the inverse and direct kinematics of this robot but focused mainly on the 3-DOF parallel part. Milutinović et al. [45] continued these studies and considered the kinematics of the serial wrist, while Eastwood and Webb [46] used these kinematic models and discussed how thermal deformations affect the positioning accuracy of the robot. Besides conventional milling and drilling operations, the Tricept parallel–serial manipulator has been used for incremental sheet forming [47,48], friction stir welding [49,50], and optical polishing [51,52]. Most recent applications include processing large optical mirrors [53–55].

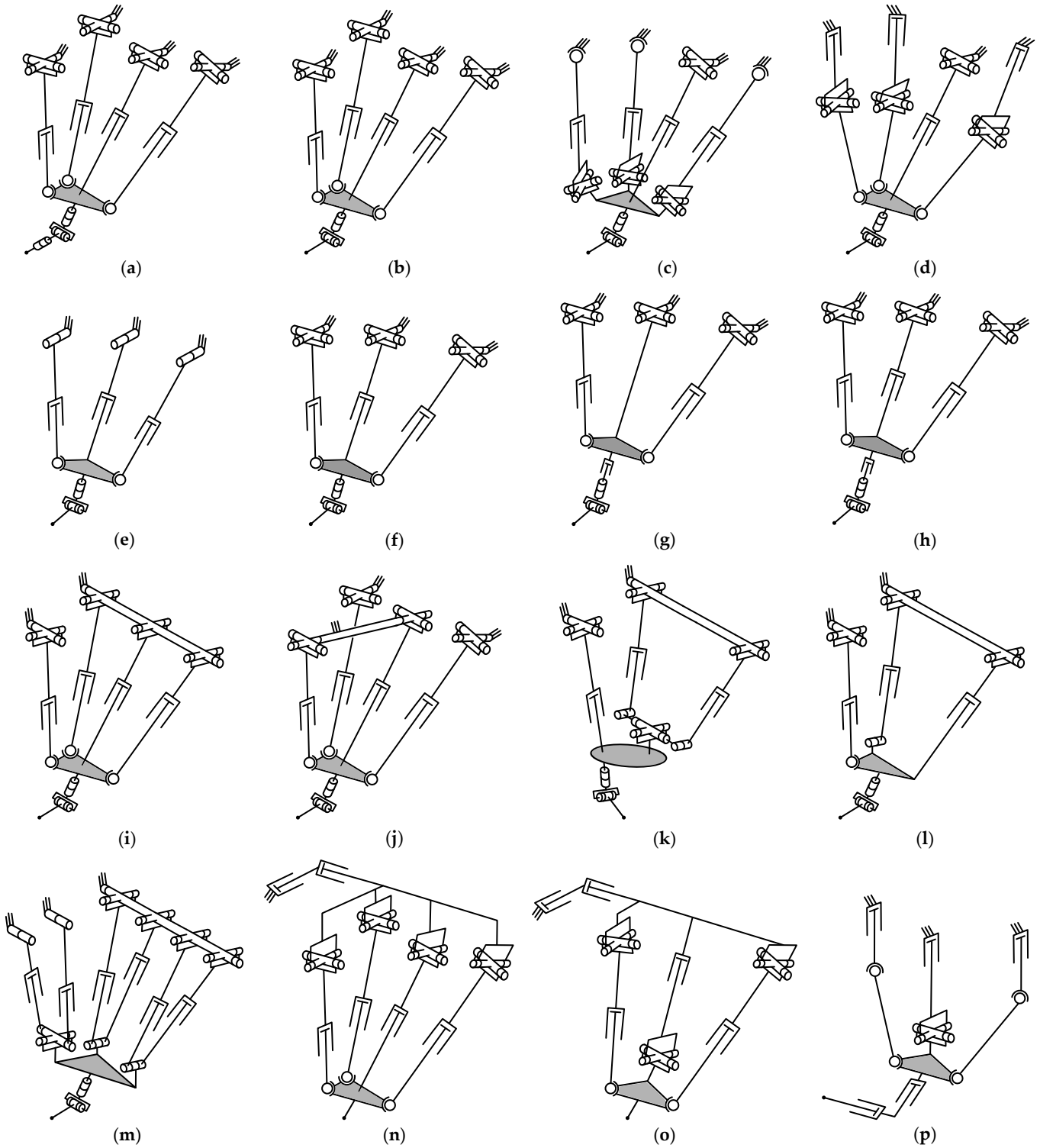

Figure 5. Parallel–serial machining manipulators of the Tricept family: (**a**) (1-UP/3-UPS)RRR (Tetrabot) [33]; (**b**) (1-UP/3-UPS)RR (Tricept) [43]; (**c**) (1-UP/3-SPU)RR [56]; (**d**) (1-UP/3-PUS)RR (Georg V) [57]; (**e**) (1-RP/2-RPS)RR (Bicept) [58]; (**f**) (1-UP/2-UPS)RR (TriVariant) [59]; (**g**) (1-U/2-UPS)PRR (TriVariant B) [60]; (**h**) (1-UP/3-UPS)PRR (Tricept IV) [61]; (**i**) (R(1-RP/2-RPS)/1-UPS)RR (TriMule) [62]; (**j**) (R(1-RP/1-RPS)/2-UPS)RR (Trifree) [63]; (**k**) (R(2-RPR)U/1-UP)RR [64]; (**l**) (R(1-RP/1-RPR)/1-UPS)RR [65]; (**m**) (R(4-RPR)/(2-RPR)R)RR [66]; (**n**) PP(1-UP/3-UPS) [67]; (**o**) PP(1-PU/2-UPS) [68]; (**p**) (1-PU/2-PSS)PP [69].

The actuated branches of the Tricept manipulator have a UPS architecture where the universal joint is located at the base. An SPU branch with the spherical joint placed at the base is a natural kinematic equivalent of this architecture, and other scholars have also considered Tricept manipulators with these branches (Figure 5c). Thus, Kim et al. [56] developed such a (1-UP/3-SPU)RR parallel–serial manipulator, analyzed its kinematics [70] and dynamics [71,72], and performed a kinematic calibration of the physical prototype [56]. Another kinematically equivalent design was proposed by Tönshoff et al. [57], who developed a Georg V manipulator with three PUS branches, featuring actuated prismatic joints at the base (Figure 5d).

Inspired by the successful design of Tricept, scholars proposed different Tricept-based architectures of parallel–serial manipulators. For example, Li et al. [58] considered a 4-DOF (1-RP/2-RPS)RR robot called Bicept (Figure 5e). This robot includes a 2-DOF planar Tricept-like parallel mechanism where spherical joints are used to compensate for misalignment and can be replaced with revolute joints. The robot stiffness and performance were examined in papers [73,74], but all the analysis was conducted for the planar parallel mechanism.

Huang et al. [59] introduced a TriVariant manipulator (Figure 5f), where one UPS was removed and the drive was displaced to the UP branch, which became the UP actuated branch. This manipulator has been the subject of many studies, which considered its kinematics [59,75,76], dynamics [77], stiffness analysis [78], dimensional synthesis [79], and calibration [80]. Most of these studies, however, focused on the 3-DOF parallel part. The TriVariant manipulator was later modified into TriVariant B [60], where the actuated prismatic joint was moved to the serial chain, so the robot architecture became (1-U/2-UPS)PRR (Figure 5g). The authors analyzed its kinematics [60], dynamics [81], and stiffness [82], with a major focus on the 2-DOF parallel mechanism.

Based on the Tricept and TriVariant B designs, Sun et al. [61] proposed a novel parallel–serial manipulator, Tricept IV, with the (1-UP/3-UPS)PRR architecture (Figure 5h). In this manipulator, the prismatic joints in the UP branch and the PRR serial chain are coaxial, which results in kinematic redundancy and increases the manipulator workspace. The authors evaluated the stiffness of this robot [61,83], performed its dimensional synthesis [84], and also considered the robot application for friction stir welding [85].

In the Tricept-based parallel–serial manipulators discussed so far, the parallel mechanism had three or four branches attached to the base. Scholars soon discovered how to simplify and lighten the design by combining the base joints of these branches [62]. This idea led to the development of the TriMule robot [62,86]—one of the most studied parallel–serial manipulators at the moment. In this robot, the universal joints of the UP branch and two UPS branches share a yoke that rotates relative to the base (Figure 5i). We can notate the TriMule architecture as (R(1-RP/2-RPS)/1-UPS)RR and see it has only two joints placed on the base, simplifying the robot design. The TriMule manipulator has become the subject of many papers devoted to its kinematics [87,88], dynamics and gravity compensation [89–93], stiffness [94–97], performance evaluation [98,99], optimal design [100], path planning [101–104], feed rate scheduling [105–107], calibration [108–116], and control [117–121]. Diverse applications of the TriMule robot include helical milling [122], collaborative mirror milling of large thin-walled parts [14,123–126], grinding [127], friction stir welding [128–133], and trimming unidirectional carbon fiber-reinforced polymers [134]. Apart from these, the TriMule robot was mounted on a mobile platform and applied for large-scale machining of aerospace components [135,136]. There also exists a 6-DOF TriMule design with a 3-DOF RRR spherical wrist, as in Tetrabot [137].

The TriMule success inspired scholars to develop other similar parallel–serial manipulators. For example, Wang et al. [63] proposed a Trifree robot with an (R(1-RP/1-RPS)/2-UPS)RR architecture (Figure 5j), where the universal joints of two branches had a common yoke. The authors analyzed the kinematics and dynamics of this robot in their works [138,139]. Li et al. [64] presented an (R(2-RPR)U/1-UP)RR manipulator (Figure 5k), whose parallel mechanism had only three branches, and performed dimensional synthesis of this mechanism. Another design with three branches was introduced by Dong et

al. [65], who used an asymmetrical (R(1-RP/1-RPR)/1-UPS)RR architecture (Figure 5l). Finally, Liu et al. [66] considered a super redundantly actuated (R(4-RPR)/(2-RPR)R)RR manipulator, whose parallel mechanism had three DOFs and six drives (Figure 5m). To our knowledge, all these novel manipulators exist only as computer models; no physical prototypes have been created.

All previous parallel–serial manipulators were equipped with a 2- or 3-DOF spherical wrist. There also exist Tricept-based architectures without this wrist but with a PP serial kinematic chain. Thus, Luo et al. [67] proposed a PP(1-UP/3-UPS) robot with a parallel mechanism placed on the PP moving frame (Figure 5n). A similar design with a 1-PU/2-UPS parallel mechanism was introduced by Shan et al. [68], who placed this mechanism on the XY moving table and used it as a spindle posture alignment device (Figure 5o). One more design was devised in paper [69], where the PP serial kinematic chain was placed on the platform of the 1-PU/2-PSS parallel mechanism (Figure 5p). This manipulator is intended to process machine components with complex and/or longitudinal shapes, and studies [140,141] analyzed its kinematics, including workspace and singularities. All these listed manipulators, however, are only available as computer models.

3.1.2. Manipulators Based on the Sprint Z3 Parallel Mechanism

The parallel–serial manipulators discussed in this subsection rely on the Sprint Z3 parallel machine tool patented by Wahl [142] (the kinematic scheme of this mechanism traces back to Hunt's paper [143]). Unlike Tricept, this parallel mechanism does not have a passive branch but includes three symmetrically arranged PRS branches. Each branch imposes one constraint, leaving the output link with two rotational and one translational DOFs. Numerous papers have studied this parallel mechanism [11], but we focus on parallel–serial manipulators based on its kinematics.

The first example is the Ecospeed machine center [144], which includes this 3-PRS parallel mechanism mounted on a 2-DOF PP serial chain (Figure 6a). San et al. analyzed the kinematics and error sources of this parallel–serial manipulator in their recent work [145]. Other scholars also considered a 4-DOF P(3-PRS) architecture, which was used with a 1-DOF moving table. Multiple studies examined the error sensitivity [146,147], stiffness analysis [148], calibration [149–152], and control [153–155] of this robot. Huang et al. [24] developed a similar manipulator where the revolute joints were replaced with parallelogram joints (Figure 6b). The authors considered the dynamics [156], calibration [157,158], and control [159] of the manipulator, focusing on its 3-DOF parallel part. The actuated parallelogram joints were used in an RRRP(3-PaRS) manipulator [160] (Figure 6c) based on a 4-DOF SCARA-type serial chain and a 3-DOF CaPaMan (Cassino Parallel Manipulator). The authors made a prototype of this manipulator for wood drilling and considered its position and force control. A SCARA-type serial chain was also used in a (3-PSP)RRRP manipulator [161], attached to the moving platform of the parallel mechanism (Figure 6d). This 7-DOF manipulator was designed for welding operations inside a steam generator, and the authors analyzed the robot workspace and control in the cited paper.

The architectures mentioned above included actuated prismatic or parallelogram joints near the base of the parallel mechanisms. There were also manipulators where these joints are placed in the middle of the branches. For example, Wang et al. [162] developed a 6-DOF PPP(3-RPS) robot (Figure 6e) for marine propeller processing and addressed its kinematic calibration in paper [163]. A similar parallel mechanism was used in a P(3-RPS)R manipulator (Figure 6f) designed for blade machining and polishing [164]. The authors applied this manipulator with a 1-DOF moving platform and performed its calibration in work [165]. Li et al. [166] "inverted" the branches of the parallel mechanism and introduced a (3-SPR)RR architecture (Figure 6g). The authors analyzed the performance [167] and stiffness [168,169] of this manipulator and discussed its calibration [170], with the main focus on the parallel part. Li et al. [171] proposed a robot with one RPS and two SPR branches (Figure 6h) and examined its kinematics and performance. This manipulator was

designed for friction stir welding and was supposed to operate with a 1-DOF moving table, but as far as we know, there is no physical prototype of this robot.

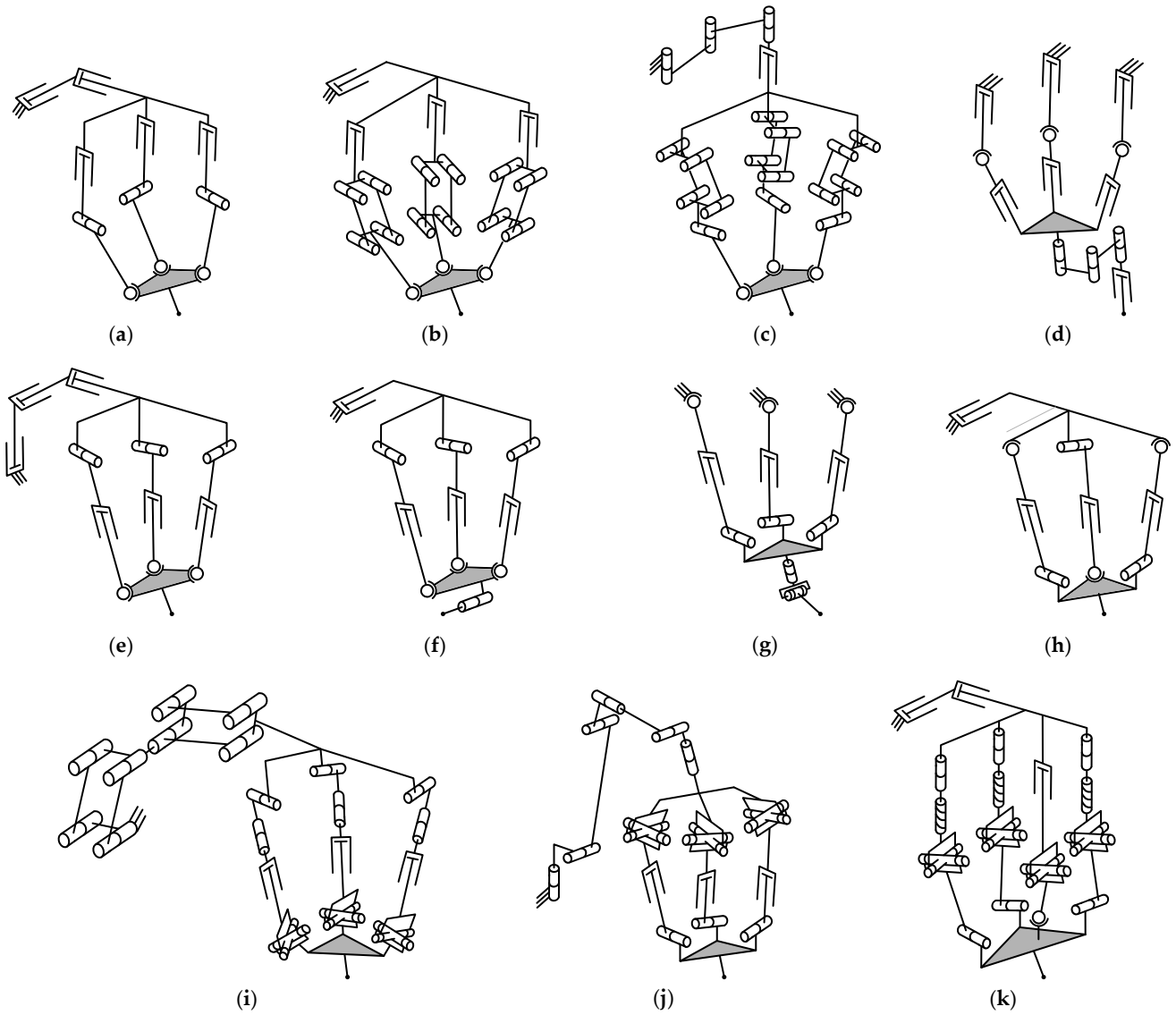

Figure 6. Parallel–serial machining manipulators of the Sprint Z3 family: (**a**) PP(3-PRS) (Ecospeed) [144]; (**b**) P(3-PPaS) [24]; (**c**) RRRP(3-PaRS) [160]; (**d**) (3-PSP)RRRP [161]; (**e**) PPP(3-RPS) [162]; (**f**) P(3-RPS)R [164]; (**g**) (3-SPR)RR [166]; (**h**) P(1-RPS/2-SPR) [171]; (**i**) PaPa(3-RCU) [25]; (**j**) RRRRRR(3-UPR) [172]; (**k**) PP(1-PUS/3-RHUR) [173].

There also exist several architectures where a parallel mechanism has a universal joint in its branches. For example, Chong et al. [25] introduced a PaPa(3-RCU) manipulator (Figure 6i) aimed at polishing wind turbine blades. Here, C means passive revolute and actuated prismatic joints with collinear axes. The 2-DOF PaPa serial chain had a complex actuation scheme, omitted in the figure, and was placed on a mobile platform to increase the robot workspace. The authors performed the elasto-geometrical calibration of this robot [174] and considered its control strategies [175]. Another polishing robot was designed by Xu et al. [172] and included a 3-DOF 3-UPR parallel mechanism attached to a 6-DOF serial manipulator (Figure 6j). Unlike the previous architectures discussed in this subsection, the parallel mechanism is overconstrained. The authors studied the robot dynamics and control and performed its dimensional synthesis in the cited paper, focusing on the parallel part. Finally, we mention a PP(1-PUS/3-RHUR) manipulator (Figure 6k) proposed by Tian et al. [173]. The parallel mechanism of the manipulator includes a PUS

branch to increase the large-stroke stiffness of this mechanism. The authors analyzed kinematics and performed a multi-objective design optimization of this robot, which currently exists only as a computer model.

3.1.3. Manipulators Based on the Exechon Parallel Mechanism

Manipulators discussed in the two previous subsections were based on 3-DOF non-overconstrained parallel mechanisms. Scholars also considered the use of overconstrained parallel mechanisms in parallel–serial manipulators. One of the most notable manipulators in this family is the 5-DOF Exechon robot proposed by Neumann [176]. It includes a 3-DOF overconstrained parallel mechanism with one SPR central branch and two UPR lateral branches, where the base axes of the universal joints are collinear (Figure 7a). The output link of the parallel mechanism is equipped with an RR spherical wrist. This manipulator has been successfully applied in industry [177], including optical [178] and large-scale [179–181] machining. Numerous articles performed its mobility [182], kinematic [183–185], and stiffness [186–189] analyses, as well as calibration [190]. Some scholars studied Exechon manipulators with offsets in the base joints [191,192] and both the base and the wrist joints [193–196]. Sagar et al. [197] also considered a 7-DOF kinematically redundant design with a 4-DOF serial chain developed for placing fixture heads along sheet metal (Figure 7b).

Inspired by the Exechon success, scholars proposed different modifications of its design. For example, Li et al. [198] inverted the central branch of the parallel mechanism and considered the (1-RPS/2-UPR)RR architecture (Figure 7c). In their study, the authors performed a multi-objective dimensional synthesis of this robot. Tengfei et al. [199] inverted the lateral chains and developed a (1-RPS/2-RPU)RR parallel–serial manipulator called Exe-Variant (Figure 7d). Paper [200] evaluated its workspace and performance. The authors also considered a variation of this design where this parallel mechanism was placed on a PR serial chain [201] (Figure 7e), whose revolute joint represented a carriage moving along a circular rail. This architecture provides a large workspace essential for machining aeronautic components, as the authors discussed in their paper. Jin et al. [202] proposed a PP(1-SPR/2-RPU) parallel–serial robot for similar applications (Figure 7f). However, as we know, all the manipulators discussed in this paragraph exist only as computer models.

The aforementioned manipulators were developed by inverting the central and/or lateral branches of the 3-DOF parallel mechanism. Other scholars also modified the structure of these branches. For example, Xu et al. [203] introduced a 4-DOF manipulator with the UPR central branch (Figure 7g). This manipulator, operating with a 1-DOF moving table, has been the subject of multiple studies that have focused on its kinematics [204], dynamics [205], stiffness [206], optimal design [207,208], and calibration [209]. Zhang et al. [210] changed the structure of all branches and proposed a PP(1-PRPS/2-PRU) manipulator with redundant actuation (Figure 7h). The authors analyzed the mobility and workspace of this robot, focusing on its parallel part. Another original design with one SP and two UPU branches and an RR spherical wrist was introduced in work [211] (Figure 7i). This manipulator has also become the subject of many studies devoted to its kinematics [212,213], dynamics [214–216], stiffness [217–219], and calibration [220]. Finally, Xu et al. [221] developed an RP(1-RRS/2-RRU) inner-cavity machining robot without prismatic joints in the parallel mechanism (Figure 7j). The authors studied the robot kinematics and dynamics, performed its dimensional synthesis, and designed a 3D-printed prototype.

There are also Exechon-inspired parallel–serial manipulators whose parallel mechanism has four branches. Thus, Yue et al. [222] proposed a (1-SPR/1-SPR/2-UPU)RR architecture with one passive branch (Figure 7k). In their work, the authors analyzed the mobility and kinematics of this robot and performed its dimensional optimization. Zhang et al. [223] presented a PP(2-RPU/2-SPR) redundantly actuated manipulator (Figure 7l) and considered its kinematics [223], dynamics [224], stiffness analysis [225], and optimal design [226]. The authors focused mainly on the 3-DOF parallel mechanism and developed a physical prototype only for this mechanism.

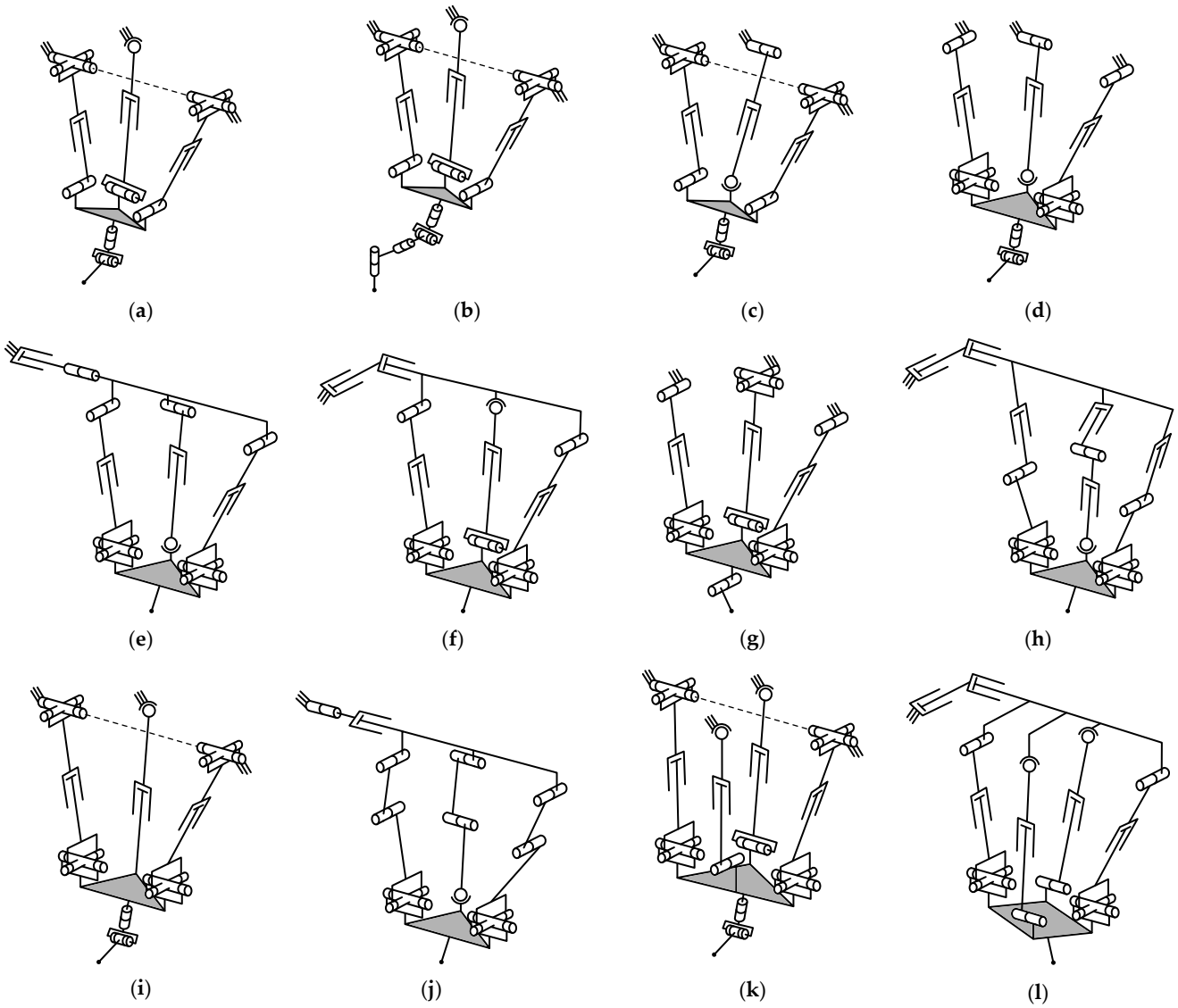

Figure 7. Parallel–serial machining manipulators of the Exechon family: (**a**) (1-SPR/2-UPR)RR (Exechon) [176]; (**b**) (1-SPR/2-UPR)RRRR [197]; (**c**) (1-RPS/2-UPR)RR [198]; (**d**) (1-RPS/2-RPU)RR (Exe-Variant) [199]; (**e**) PR(1-RPS/2-RPU) [201]; (**f**) PP(1-SPR/2-RPU) [202]; (**g**) (1-UPR/2-RPU)R [203]; (**h**) PP(1-PRPS/2-PRU) [210]; (**i**) (1-SP/2-UPU)RR [211]; (**j**) RP(1-RRS/2-RRU) [221]; (**k**) (1-SPR/1-SPR/2-UPU)RR [222]; (**l**) PP(2-RPU/2-SPR) [223].

3.1.4. Manipulators Based on Planar Parallel Mechanisms

This subsection covers parallel–serial machining manipulators based on parallel mechanisms whose end-effector performs planar motion. We can classify these manipulators into two groups, as discussed next.

The first group includes manipulators with 2-DOF parallel mechanisms. For example, Li et al. [227] proposed a 3-DOF (1-PR/1-PRR)P architecture (Figure 8a). The authors analyzed the kinematics of this hybrid robot and developed its prototype. Ma et al. [228] introduced a 5-DOF P(1-RP/1-RPR)RR manipulator with an RR spherical wrist (Figure 8b). Unlike the previous design, the prismatic actuators of the parallel mechanism were connected to its base by revolute joints. A similar architecture was considered by Wang et al. [229] who used a 1-RR/1-RRR parallel mechanism as a parallel module (Figure 8c). The authors applied this robot for machining large casting parts and discussed simulations and experiments in paper [230]. Uchiyama et al. [231] designed a (1-PR/1-PRP)PRR manipulator for robotized deburring operations (Figure 8d). The authors studied the kinematics of this robot and proposed a continuous path control algorithm, which was successfully applied

in practice. Another 5-DOF manipulator with an identical PRR serial chain was developed by Guo et al. [232]. Unlike the architectures above, the 2-DOF planar parallel mechanism had one PR passive branch and two PRP branches with prismatic actuators at the base (Figure 8e). In their later works, the authors analyzed workspace [233], dynamics [234,235], and control [236] of this robot.

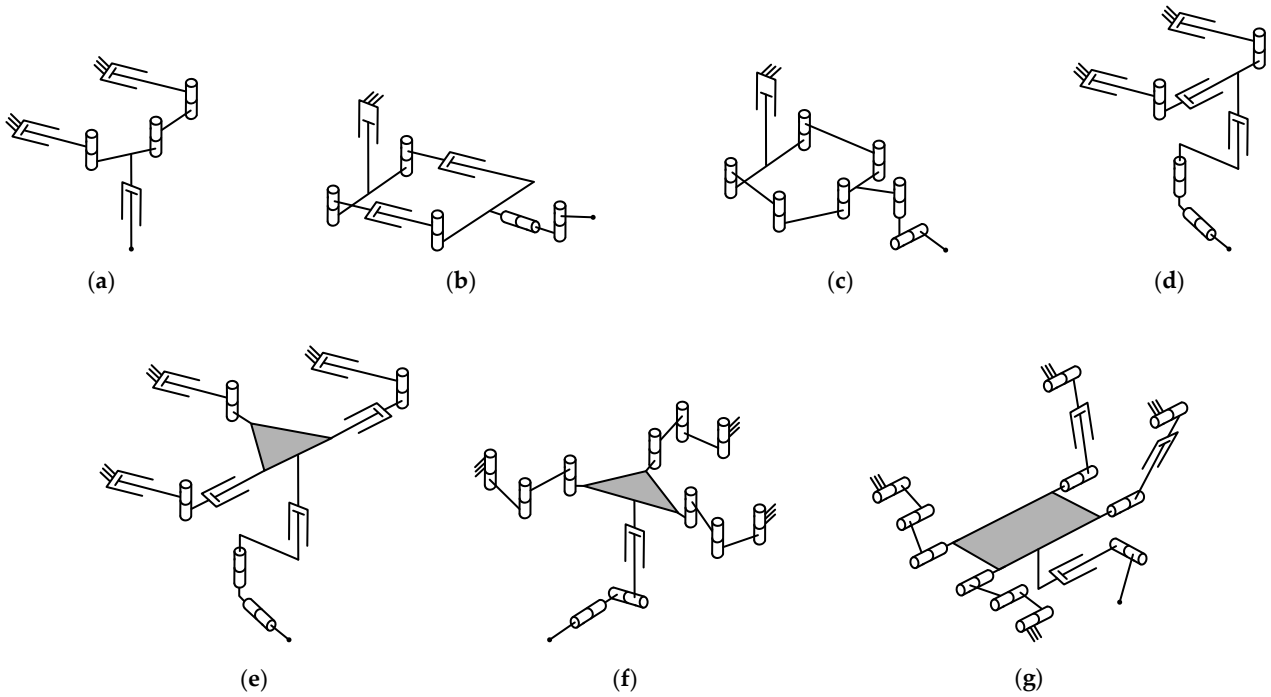

Figure 8. Parallel–serial machining manipulators based on planar parallel mechanisms: (**a**) (1-PR/1-PRR)P [227]; (**b**) P(1-RP/1-RPR)RR [228]; (**c**) P(1-RR/1-RRR)RR [229]; (**d**) (1-PR/1-PRP)PRR [231]; (**e**) (1-PR/2-PRP)PRR [232]; (**f**) (3-RRR)PRR [237]; (**g**) (2-RPR/2-RRR)PR [69].

The second group includes manipulators with 3-DOF parallel mechanisms, and there are just a couple of architectures within this group. The first is a (3-RRR)PRR manipulator developed by Yang et al. [237] for deburring operations (Figure 8f). The authors created a robot prototype with a modular design, and its kinematic analysis can be found in studies [18,238]. Finally, paper [69] introduced a (2-RPR/2-RRR)PR redundantly actuated manipulator for processing elongated objects (Figure 8g). At the moment, this manipulator exists only as a computer model, and its kinematics has been analyzed recently in works [239,240].

3.1.5. Manipulators Based on the Delta Parallel Mechanism

The Delta mechanism, proposed by Clavel [241], has become one of the most successful parallel architectures. The output link of this mechanism has three translational DOFs provided by parallelogram joints in its branches. However, there are just a few examples of Delta-based parallel–serial manipulators applied for machining, possibly because of their lower rigidity compared to other architectures discussed in the previous subsections.

The first example is the JDYP51 polishing machine tool [242] based on the Delta mechanism with prismatic actuators (Figure 9a). The output link of the parallel mechanism is equipped with an RR spherical wrist. Paper [243] analyzed manipulator stiffness, and the authors of [244] optimized the polishing process performed with this robot. Xu et al. [245] introduced another polishing manipulator based on the Delta mechanism. Unlike the previous design, the branches of this mechanism use spatial parallelogram joints with spherical joints (Figure 9b). A 1-DOF serial chain connects to the moving platform by a revolute joint, actuated by an auxiliary RUPU branch, which is omitted in the figure for clarity. This 4-DOF parallel–serial manipulator moves the processed object, while the

polishing tool is placed on an independent 2-DOF serial mechanism. In the later works, the authors considered path planning [246], dynamics [247,248], stiffness [249], optimal design [250], calibration [251], and control [252] of this robot, focusing on the parallel part.

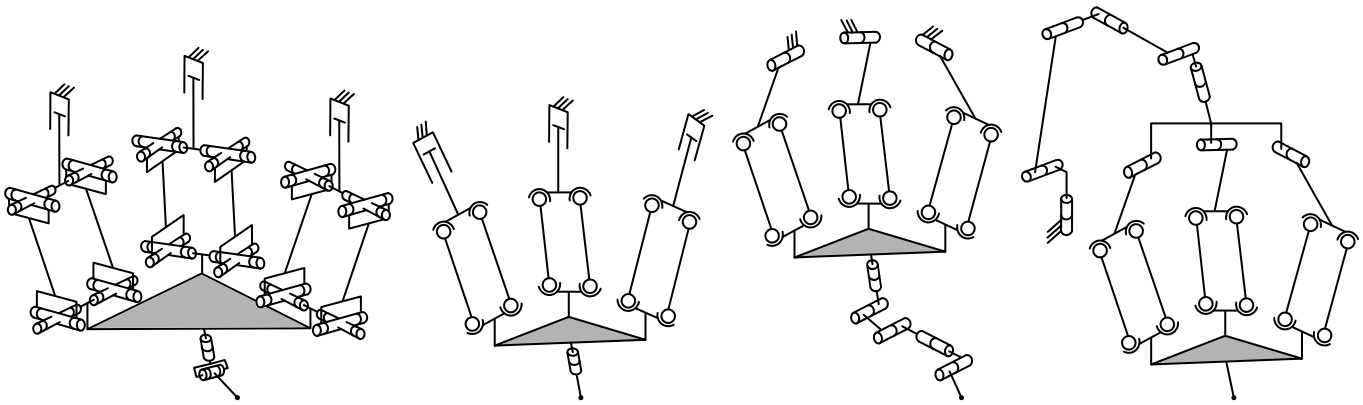

(**a**) (**b**) (**c**) (**d**)

Figure 9. Parallel–serial machining manipulators based on the Delta parallel mechanism: (**a**) (3-PRPaR)RR (JDYP51) [242]; (**b**) (3-PPa*)R [245]; (**c**) (3-RPa*)RRRRR [253]; (**d**) RRRRRR(3-RPa*) [254].

Other examples of Delta-based manipulators include kinematically redundant architectures, which, to our knowledge, exist only as computer models. Thus, Mohammadipanah and Zohoor [253] proposed an 8-DOF hybrid robot with an RRRRR serial chain (Figure 9c). The authors considered its application for arc welding and analyzed the kinematics and dynamics of this manipulator. Nguyen et al. [254] studied a 9-DOF macro-mini milling robot where the Delta mechanism was attached to the end-effector of the 6-DOF Kawasaki RS030N industrial manipulator (Figure 9d). The main focus of the authors' work was on the compliance analysis and error compensation of this robot.

3.1.6. Manipulators Based on the Gough–Stewart Platform

The 6-DOF Gough [255] or Gough–Stewart [256] platform is another successful parallel mechanism used in numerous applications [257]. This mechanism has six UPS branches that provide its output link with high stiffness and positioning accuracy. However, we found just a few examples of parallel–serial machining manipulators based on the Gough–Stewart platform. The reason is that these manipulators have kinematically redundant architectures with more than six DOFs, which are rarely needed for machining purposes.

On the other hand, such redundancy can increase the workspace of the parallel mechanism. Thus, Wu et al. [258] developed a 10-DOF parallel–serial manipulator called IWR (Intersector Welding Robot), where the Gough–Stewart platform was mounted on a PPRR serial chain (Figure 10a). This robot was designed for assembly operations in the vacuum vessel of the ITER (International Thermonuclear Experimental Reactor). There are multiple studies devoted to stiffness analysis [259–261], calibration [262–266], and control [267–270] of this robot. In works [271,272], the authors also considered a 7-DOF prototype of this manipulator with a 1-DOF serial chain (Figure 10b). Finally, we can mention study [273], whose authors installed the Gough–Stewart platform on the end-effector of a 6-DOF UR5e robotic arm (Figure 10c). This parallel–serial manipulator was applied to position a touch probe.

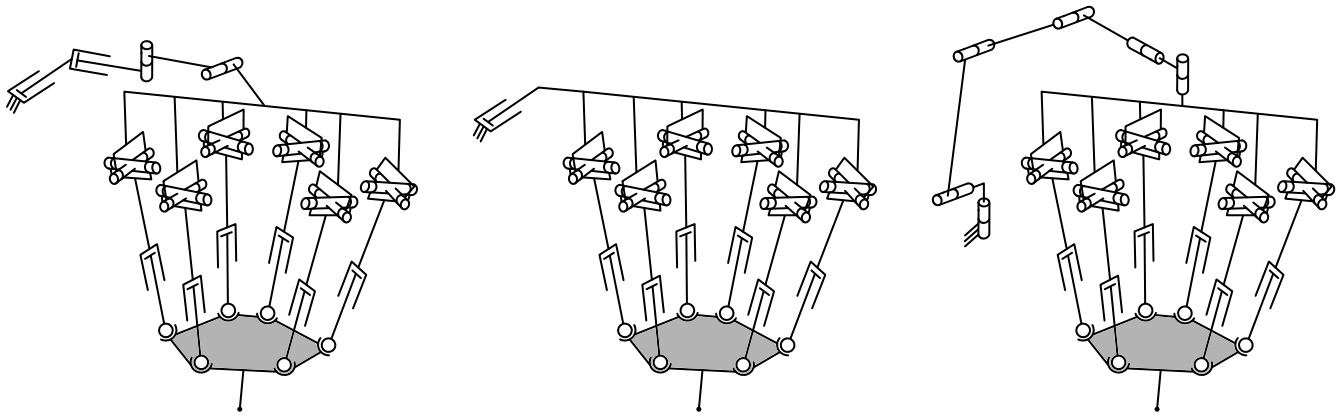

(**a**) (**b**) (**c**)

Figure 10. Parallel–serial machining manipulators based on the Gough–Stewart platform: (**a**) PPRR(6-UPS) (IWR) [258]; (**b**) P(6-UPS) [271]; (**c**) RRRRRR(6-UPS) [273].

3.1.7. Other Manipulators

This subsection covers parallel–serial manipulators, which we cannot put in any of the previous groups. It is interesting that there are just a few manipulators in this family, and we found only two architectures with working prototypes used in practice.

The first example is the 6-DOF RNT (Robot of a New Type) developed by Mianowski et al. [274] for milling and polishing large objects. This robot features a 2-DOF 1-RR/2-UPS parallel mechanism placed on the rotating base, and the output link of this mechanism is equipped with an RRR spherical wrist (Figure 11a). The authors considered the design, control, and applications of RNT in their later studies [275,276]. The second example is the 7-DOF CraftsRobot [277], which was also applied for processing large-scale objects. The robot includes a 5-DOF 1-UCR/4-UCU parallel mechanism attached to the PaPa serial chain with the same architecture as in the previously discussed PaPa(3-RCU) manipulator [25] (Figure 11b). Similar to that work, the parallel–serial manipulator was installed on the moving platform, which increased its workspace. In recent works, scholars have considered the stiffness [278], optimal design [279], and error compensation [280] of this hybrid robot.

Other manipulators considered below exist only as computer models. There are several architectures based on 4-DOF parallel mechanisms. For example, Lu et al. [281] introduced a PP(1-PRU/3-PUS) manipulator and analyzed the workspace and dynamics of its parallel part (Figure 11c). Another design was considered by Tian et al. [282], where one PUS branch was replaced with the second PRU branch (Figure 11d). The authors performed the mobility analysis of this robot and found that it had no singular configurations. Li et al. [283] studied a similar P(2-RPU/2-UPS) architecture where prismatic actuators of the parallel mechanism were displaced to the middle of its branches (Figure 11e). In their paper, the authors considered the kinematics and dynamics of this parallel–serial manipulator. Finally, Tian et al. [284] modified their previous design and proposed a robot where all the universal joints of the parallel mechanism were placed on the base (Figure 11f). The authors studied the robot kinematics and performed its dimensional synthesis.

To conclude this subsection, we mention two manipulators based on 3-DOF parallel mechanisms. The first one is a 5-DOF manipulator with a 3-PUU translational parallel mechanism considered by Wang et al. [285] (Figure 11g). The manipulator was intended for polishing, and the authors optimized the polishing process in their study. The second example is a (3-UPU)RRR hybrid machining robot introduced by Dou et al. [286] (Figure 11h). In their work, the authors performed a comprehensive stiffness analysis of this manipulator.

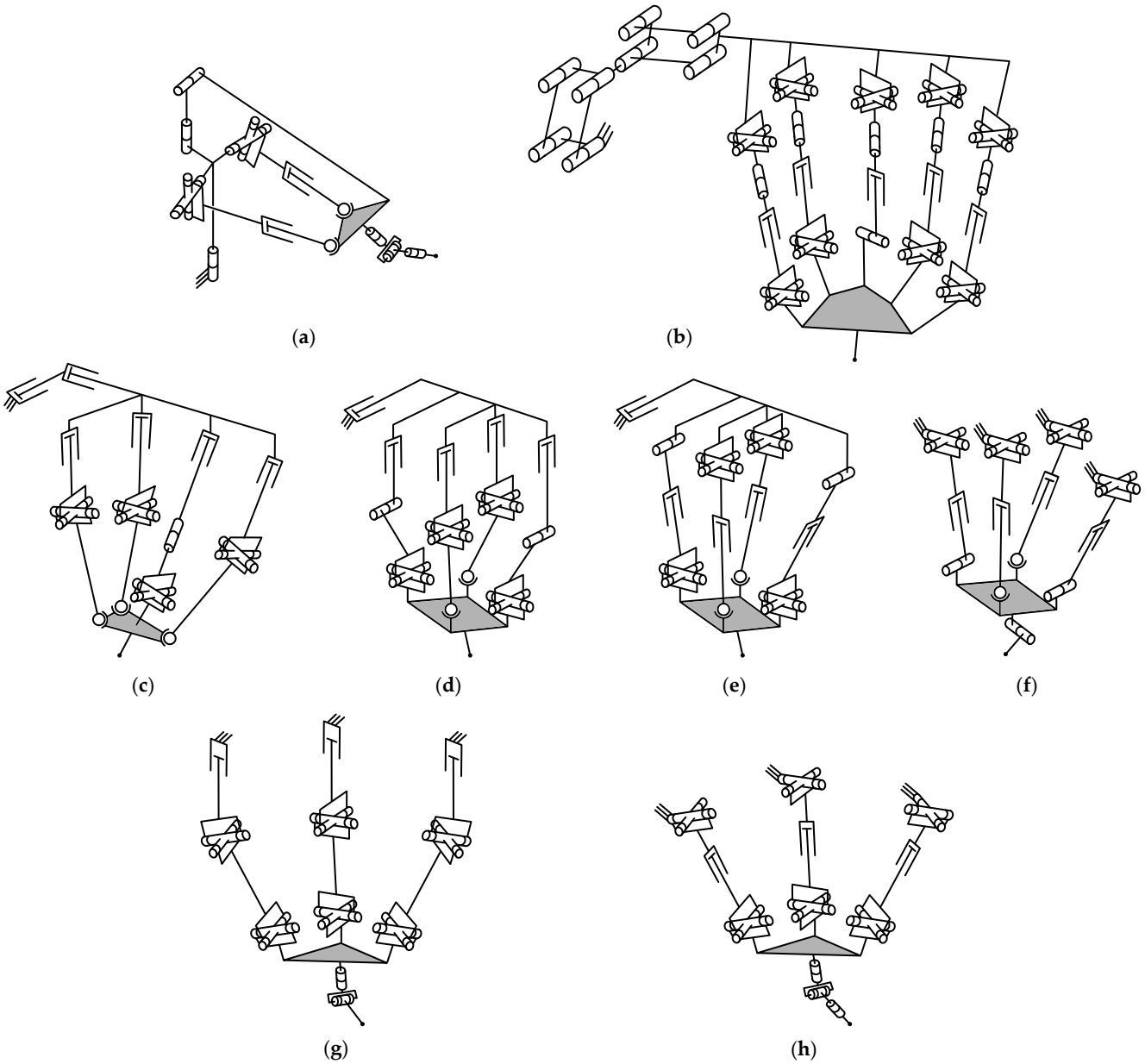

Figure 11. Parallel–serial machining manipulators based on other parallel mechanisms: (**a**) R(1-RR/2-UPS)RRR (RNT) [274]; (**b**) PaPa(1-UCR/4-UCU) (CraftsRobot) [277]; (**c**) PP(1-PRU/3-PUS) [281]; (**d**) P(2-PRU/2-PUS) [282]; (**e**) P(2-RPU/2-UPS) [283]; (**f**) (2-UPR/2-UPS)R [284]; (**g**) (3-PUU)RR [285]; (**h**) (3-UPU)RRR [286].

3.2. Medicine

Medicine is the second most popular sphere where parallel–serial manipulators find their use (Figure 4). Unlike the previous subsection, where we classified machining manipulators by the underlying parallel mechanism, we found it more convenient to classify medicine hybrid robots by application. The rest of this subsection considers these applications and corresponding parallel–serial manipulators in more detail.

3.2.1. Manipulators for Minimally Invasive Surgery

Minimally invasive surgery implies performing operations with a single incision point of the instrument. Scholars have developed various parallel–serial manipulators to position the instrument in such a way. One of the most famous and well-studied robots is PARAMIS, proposed by Plitea et al. [287]. This 5-DOF manipulator includes a 2-DOF planar parallel

mechanism placed on the revolute base and equipped with an RR serial chain (Figure 12a). There are many papers devoted to kinematics [288–290], dynamics [291], control [292], and simulations [293,294] of this robot, while study [295] considered a modified design of the RR serial chain. Based on PARAMIS, Pisla et al. introduced PARASURG 5M-1 [296] and 5M-2 [297] manipulators with a 1-PR/1-PRR parallel mechanism (Figures 12b,c). The difference between the 5M-1 and 5M-2 architectures is in the joint arrangement of the RR serial chain. The authors analyzed the kinematics [298] and dynamics [299,300] of both architectures, while Stoica et al. [301–303] and Szilaghyi et al. [304,305] considered the actuation of the RR chain using auxiliary kinematic chains. The 5M-2 design became the basis for another robot, PARASURG 9M [306], where the serial chain was equipped with a 4-DOF instrument. It includes a 3-DOF miniature spherical parallel mechanism and a prismatic joint—Figure 12d shows a simplified representation of the PARASURG 9M manipulator. In later works, scholars analyzed the mobility [307], kinematics [308,309], and control architecture [310,311] of this robot. A similar 1-PR/1-PRR planar parallel mechanism was also used in two 5-DOF parallel–serial manipulators, proposed by Peng et al. [312] and Li et al. [313] for spine surgery (Figure 12e,f). The architectures of the manipulators differ only by the joint order in the 3-DOF serial chain. In their studies, the authors focused on the kinematics, optimal design, and control of these two robots.

The design of several parallel–serial manipulators provides its end-effector with a fixed incision point called a remote center of motion (RCM). One way to obtain an RCM is to use a spherical mechanism. Thus, Degirmenci et al. [314] introduced a 6-DOF PPP(1-RR/1-RRR)R manipulator for microsurgery, which included a 2-DOF parallel spherical mechanism (Figure 12g). In their study, the authors analyzed the robot performance and developed its physical prototype. Tucan et al. [315] presented a similar 5-DOF manipulator where the spherical mechanism had a circular rail (kinematically equivalent to a revolute joint, as shown in Figure 12h). The authors considered the kinematic modeling of this robot. Circular rails were also used for intermediate revolute joints in a 4-DOF (1-RR/1-RRR)PR manipulator proposed by Cao et al. [316] (Figure 12i). In their paper, the authors performed a dimensional synthesis of this robot but focused mainly on the 2-DOF parallel part. Li et al. [317] introduced another 4-DOF robot with an original 1-RRPR/1-RRRR 2-DOF parallel mechanism and a similar PR serial chain (Figure 12j). The authors' study was devoted to the kinematic analysis and performance evaluation of this mechanism. Finally, we mention a 6-DOF (1-PPRR/1-PPRRP)PR manipulator devised by Yang et al. [318] for intraocular surgery (Figure 12k). The 4-DOF parallel mechanism in this manipulator is actuated by piezoelectric drives. The authors developed a physical prototype of the robot and considered its control system in studies [319,320].

Most parallel mechanisms in the hybrid manipulators above have two DOFs and two branches. Scholars also proposed several architectures where the parallel part has three DOFs and three or more branches. For example, Tanev [321] introduced a 4-DOF (1-RRR/2-SPU)P manipulator with a spherical branch, which provides the RCM (Figure 12l). Subsequent works of the author focused on its stiffness [322] and singularities [323]. The RRR spherical chain was also used to provide the RCM in the parallel–serial manipulator considered by Phan et al. [324]. This chain was attached by an additional revolute joint to the 3-DOF Delta-type mechanism with linear drives (Figure 12m). The Delta mechanism also served as the basis for a 6-DOF hybrid manipulator with an RRP serial chain, proposed by Hong et al. [325] for neurosurgery (Figure 12n). However, to our knowledge, these three manipulators exist only as computer models. The final examples mentioned here are two hybrid robots developed for needle guidance. The first one is a PP(3-PRS) manipulator introduced by Chung et al. [326] (Figure 12o). The end-effector of this robot is equipped with a force-torque sensor and a handle for manual positioning during operations. The second example is an RRR(1-S/3-PSS) manipulator designed by Puglisi et al. [327] and based on a 3-DOF spherical parallel mechanism (Figure 12p). In their study, the authors analyzed the kinematics and performance of this mechanism and developed its physical prototype.

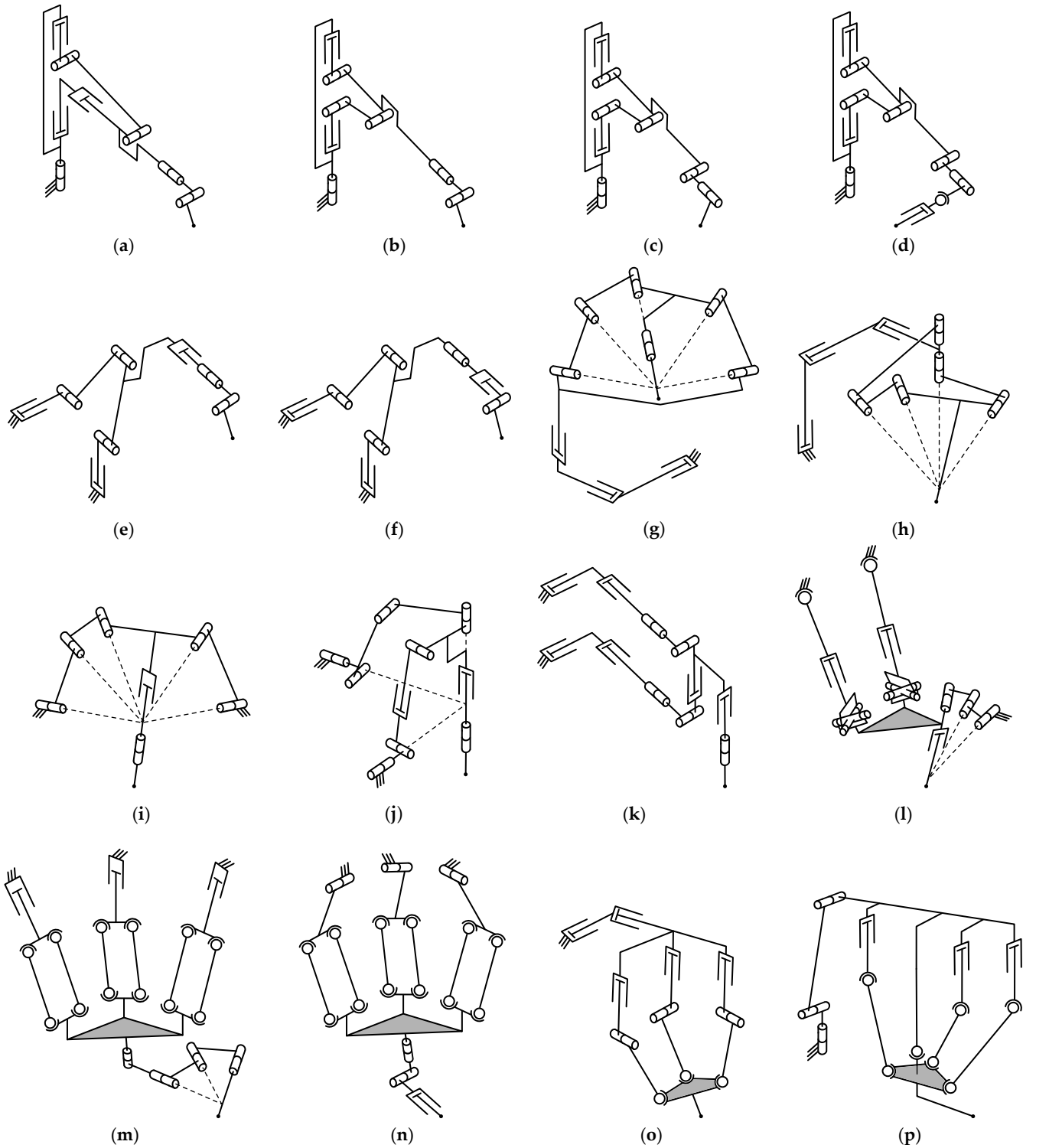

Figure 12. Parallel–serial manipulators for minimally invasive surgery: (**a**) R(1-PP/1-PRR)RR (PARAMIS) [287]; (**b**) R(1-PR/1-PRR)RR (PARASURG 5M-1) [296]; (**c**) R(1-PR/1-PRR)RR (PARASURG 5M-2) [297]; (**d**) R(1-PR/1-PRR)RRSP (PARASURG 9M) [306]; (**e**) (1-PR/1-PRR)PRR [312]; (**f**) (1-PR/1-PRR)RPR [313]; (**g**) PPP(1-RR/1-RRR)R [314]; (**h**) PPP(1-RR/1-RRR) [315]; (**i**) (1-RR/1-RRR)PR [316]; (**j**) (1-RRPR/1-RRRR)PR [317]; (**k**) (1-PPRR/1-PPRRP)PR [318]; (**l**) (1-RRR/2-SPU)P [321]; (**m**) (3-PPa*)RRRR [324]; (**n**) (3-RPa*)RRP [325]; (**o**) PP(3-PRS) [326]; (**p**) RRR(1-S/3-PSS) [327].

3.2.2. Manipulators for Non-Minimally Invasive Surgery

Some parallel–serial manipulators developed for surgical operations do not have the RCM and are not intended for minimally invasive operations. For example, Ceccarelli et al. [328] proposed CaHyMan (Cassino Hybrid Manipulator) based on the 3-DOF 3-PaRS CaPaMan mentioned in Section 3.1.2. Here, the moving platform of CaPaMan is equipped with an RP serial chain (Figure 13a). The authors evaluated the stiffness of this manipulator and performed experiments in their subsequent studies [329,330]. Other CaPaMan-based parallel–serial surgical robots feature architectures with seven [331,332] and nine [333,334] DOFs, where the parallel mechanism is attached to 4-DOF SCARA and 6-DOF PUMA serial manipulators (Figure 13b,c).

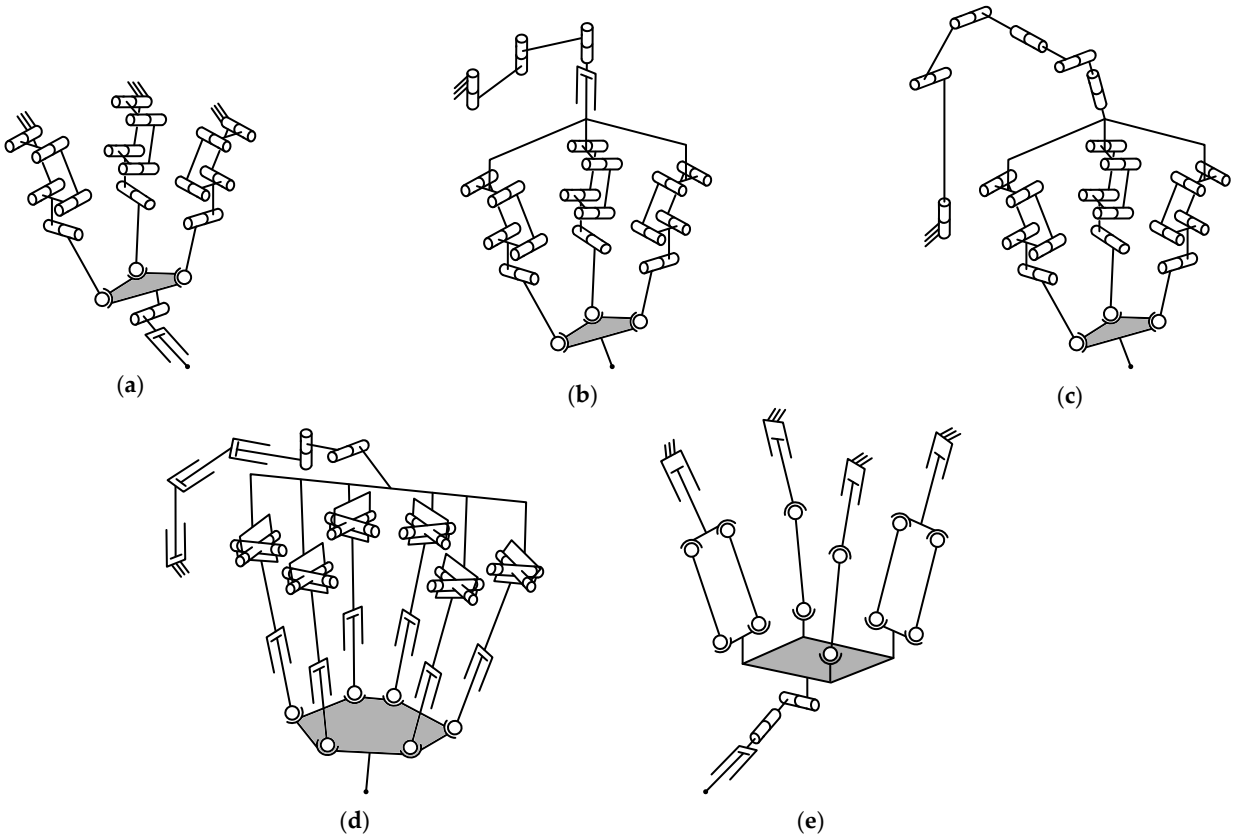

Figure 13. Parallel–serial manipulators for non-minimally invasive surgery: (**a**) (3-PaRS)RP (CaHyMan) [328]; (**b**) RRRP(3-PaRS) [331]; (**c**) RRRRRR(3-PaRS) [333]; (**d**) PPRRR(6-UPS) [335]; (**e**) (2-PSS/2-PPa*)RRP (Cheope) [336].

Feng et al. [335] introduced another surgical hybrid robot. This robot, designed for dental implant surgery, includes a 6-DOF Gough–Stewart platform attached to a PPPRR serial chain (Figure 13d). In their later works, the authors focused on the robot accuracy analysis [15,337] and calibration [338]. The last example is a Cheope manipulator designed by Tosi et al. [336]. It relies on a 4-DOF reconfigurable modular parallel mechanism with an RRP serial chain (Figure 13e). The authors considered various branch arrangements of this robot and analyzed its kinematics.

3.2.3. Manipulators for Fracture Reduction

Fracture reduction involves realigning broken bones, and scholars have developed various hybrid robotic systems for this purpose. The first group of manipulators is based on the 6-DOF Gough–Stewart platform. Raabe et al. [339] considered using this platform, attached to the linear guide, for the reduction in intra-articular joint fractures (Figure 14a). That idea was advanced by Dagnino et al. [340], who replaced the linear guide with a

4-DOF PPRR serial chain (Figure 14b). In papers [341,342], this system was applied to the reduction in complex knee fractures. In their other works [343,344], the authors considered a Gough–Stewart platform attached to the 6-DOF UR10 serial robot (Figure 14c). The latter is used for coarse positioning, while the platform serves for precise movements.

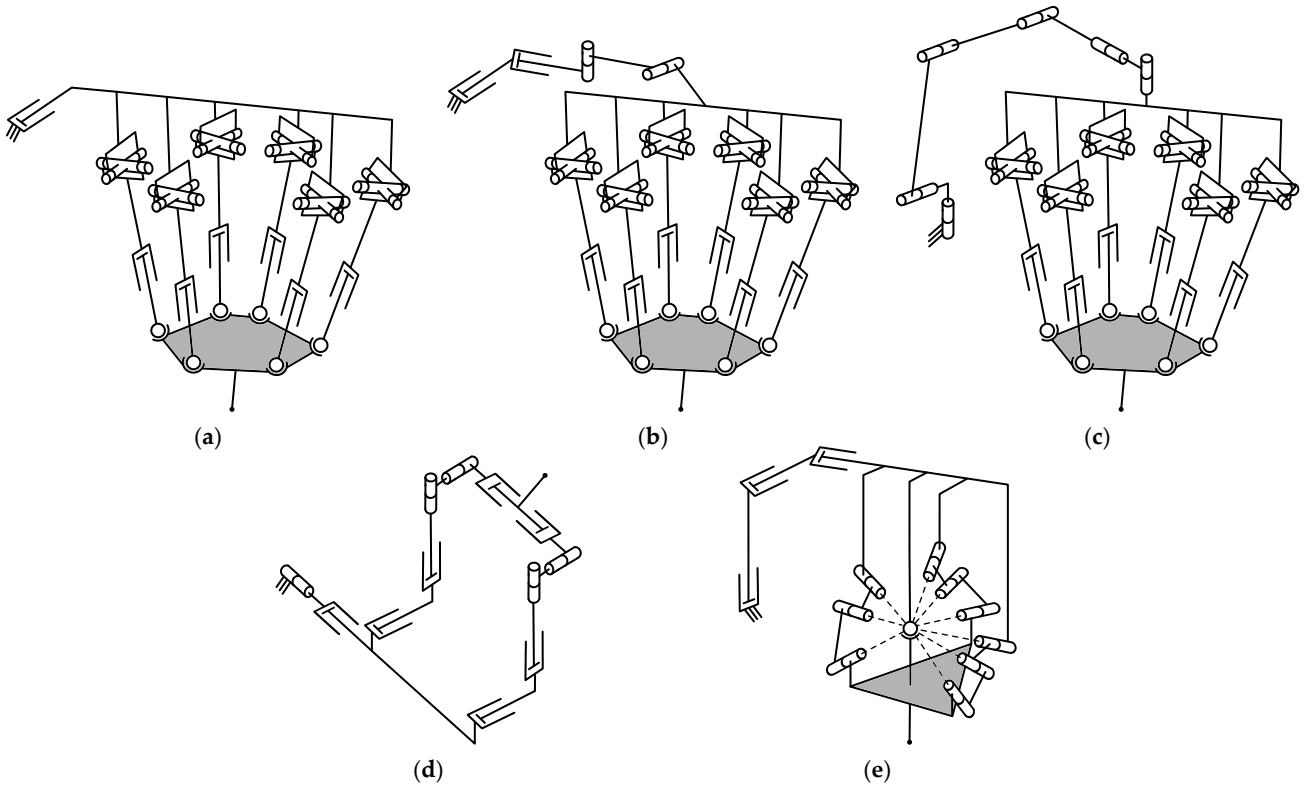

Figure 14. Parallel–serial manipulators for fracture reduction: (**a**) P(6-UPS) [339]; (**b**) PPRR(6-UPS) [340]; (**c**) RRRRRR(6-UPS) [343]; (**d**) RP(2-PPRRP) [345]; (**e**) PPP(1-S/3-RRR) [346].

Other examples of fracture reduction hybrid robots do not utilize the Gough–Stewart mechanism. Ye et al. [345] introduced a 6-DOF manipulator with a 4-DOF 2-PPRRP parallel mechanism attached to an RP serial chain (Figure 14d). The revolute joint of this chain is actuated by an extra RPR branch, whereas the end-effector includes an auxiliary aligning mechanism. This manipulator was designed for fracture reduction in the femur shaft, and subsequent studies examined its kinematics [347,348] and control [349–351]. The second example is a 6-DOF manipulator proposed by Cai et al. [346] for pelvic fracture reduction and based on a 3-DOF 1-S/3-RRR spherical parallel mechanism (Figure 14e). The authors focused on the kinematics and dynamics of this mechanism and presented its prototype.

3.2.4. Manipulators for Rehabilitation

Rehabilitation manipulators help patients restore the movements of their limbs. The literature review reveals several parallel–serial robots designed for these purposes: they all were developed for the rehabilitation of lower limbs. For example, Shi et al. [352] proposed a 4-DOF manipulator based on a 2-DOF 1-U/1-UPU/1-UPS parallel mechanism (Figure 15a). The authors analyzed the mobility and kinematics of this robot in their study. Zhang et al. [353] developed a hybrid manipulator with a similar parallel mechanism and two serial chains, one for each leg of the patient (Figure 15b). In studies [354–356], the authors considered the robot kinematics and control and performed diverse experiments with its prototype. Among other examples are two 4-DOF ankle rehabilitation manipulators proposed by Li et al. [357] and Qu et al. [358]. Both manipulators have similar architectures: they include a 3-DOF parallel mechanism with a PU branch placed on the rotary platform; the only difference is in the two other branches (Figure 15c,d). The final example is a 3-DOF

manipulator designed by Mohanta et al. [359]. It is based on a 2-DOF 1-PR/1-PRP planar parallel mechanism that moves along a linear guide (Figure 15e). The authors' studies focused on the robot kinematics, dynamics, and control [360].

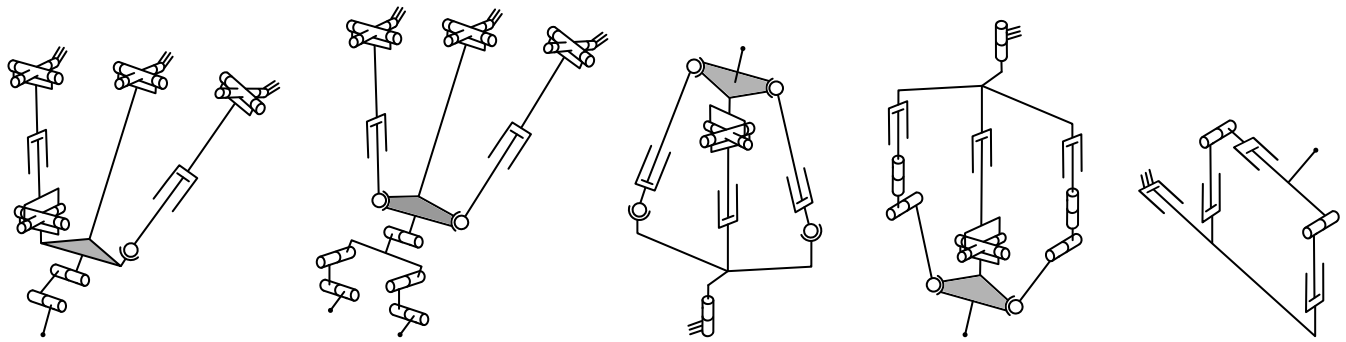

(**a**) (**b**) (**c**) (**d**) (**e**)

Figure 15. Parallel–serial manipulators for rehabilitation: (**a**) (1-U/1-UPU/1-UPS)RR [352]; (**b**) (1-U/2-UPS)RRR [353]; (**c**) R(1-PU/2-SPS) [357]; (**d**) R(1-PU/2-CRS) [358]; (**e**) P(1-PR/1-PRP) [359].

3.2.5. Other Manipulators

This subsection covers parallel–serial manipulators whose applications do not fit the categories discussed earlier. The first example is a robotic prosthetic arm designed by Wang et al. [361]. This manipulator includes a 2-DOF spherical parallel mechanism with two prismatic actuators and an RRR serial chain (Figure 16a). The authors' study was devoted to the kinematic analysis of this robot. Larbi et al. [362] developed CochleRob, a 5-DOF parallel–serial robot for intracochlear navigation. The manipulator is based on a 3-DOF Delta robot placed on an RR spherical serial chain (Figure 16b). In papers [362,363], the authors studied the kinematics, dynamics, and different control strategies of CochleRob. Kucuk and Gungor [364] introduced a 9-DOF hybrid manipulator based on another familiar parallel mechanism—the Gough–Stewart platform, which was attached to a SCARA-type serial chain (Figure 16c). The authors focused on robot kinematic analysis but did not specify its medical application. One more kinematically redundant manipulator was presented by Singh et al. [27]. The parallel part of this 7-DOF manipulator represents a simple 1-DOF parallelogram linkage placed between two RRR serial chains (Figure 16d). The robot was applied as a haptic device for robot-assisted surgery, and the authors performed its kinematic analysis [365–367] and gravity balancing [368]. The final example is another medical assistive manipulator introduced in paper [69]. It includes a 2-DOF 1-PR/1-PRR planar parallel mechanism equipped with a PPR serial chain (Figure 16e). Works [369,370] performed a kinematic analysis of this robot, but its physical prototype has not been designed so far.

3.3. Pick-and-Place and Manipulation

Serial robots have been used widely for pick-and-place operations and object manipulation. However, because of their serial architecture, these robots have a limited payload. Scholars have addressed this issue by combining serial kinematic chains with parallel mechanisms, making a trade-off between payload and workspace dimensions, which are critical for pick-and-place tasks.

The subsequent paragraphs present various parallel–serial manipulators designed for pick-and-place operations. To make the presentation more concise, we classified the manipulators into two groups: non-kinematically redundant architectures with six or fewer DOFs and kinematically redundant architectures with seven or more DOFs.

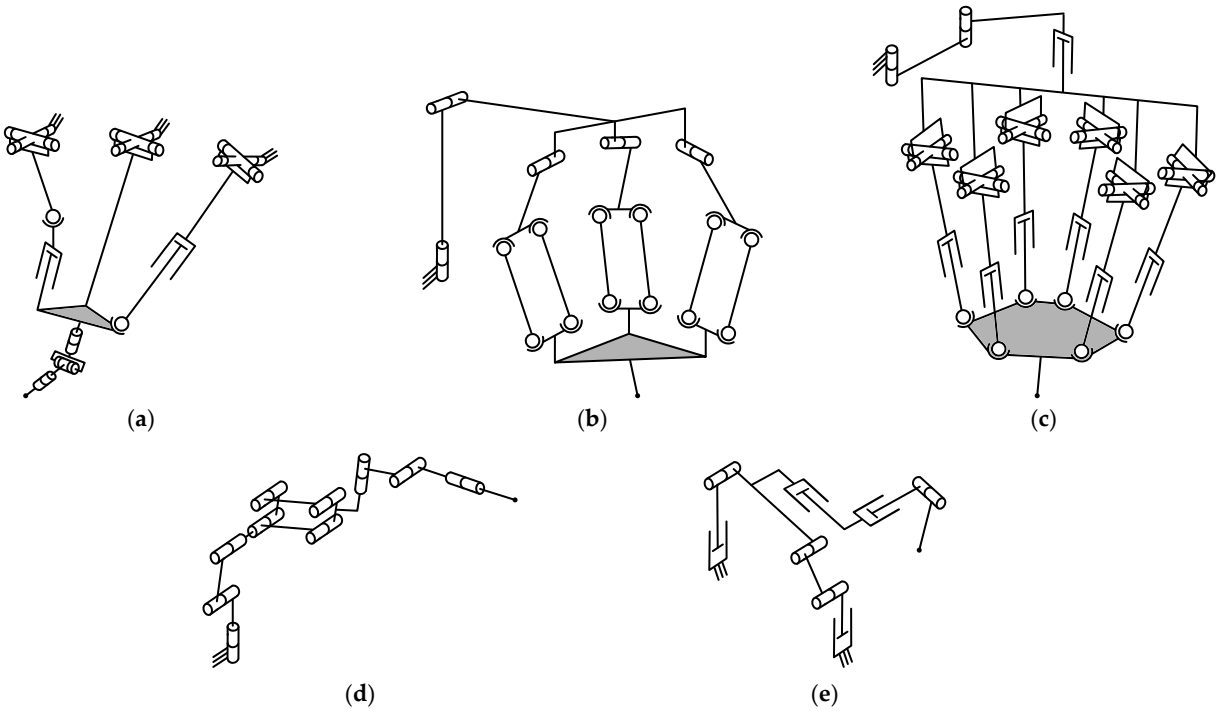

Figure 16. Parallel–serial manipulators for other medicine applications: (**a**) (1-U/1-UPS/1-USP)RRR [361]; (**b**) RR(3-RPa*) (CochleRob) [362]; (**c**) RRP(6-UPS) [364]; (**d**) RRR(1-Pa)RRR [27]; (**e**) (1-PR/1-PRR)PPR [69].

3.3.1. Non-Kinematically Redundant Manipulators

The Delta robot is often applied for quick pick-and-place operations, and scholars have proposed various parallel–serial manipulators based on its architecture. For example, Liu et al. [371] equipped a Delta robot with an RRR non-spherical wrist (Figure 17a), studied its kinematics, and performed rapid pick-and-place experiments. Wu et al. [372] designed a similar manipulator with a 2-DOF RR wrist and analyzed its kinematics and dynamics [373,374], while Deng et al. [375] considered its application for labeling end-faces of round steels. Papers [376–378] presented similar 5-DOF manipulators based on a Delta-type robot with prismatic actuators (Figure 17b). Qiong et al. [379] studied a 4-DOF strawberry picking manipulator, with a Delta robot mounted on a linear guide (Figure 17c).

Huang et al. [380] introduced a Diamond mechanism—a planar equivalent of a Delta manipulator (Figure 17d). This 2-DOF translational mechanism was also placed on a linear guide and applied for quality inspection of rechargeable batteries. The authors performed the optimal design of this manipulator [380] and estimated the maximum required torques of its actuators [381]. Zou et al. [29] proposed a 4-DOF pick-and-place manipulator based on another planar parallel mechanism with parallelogram joints (Figure 17e). In their study, the authors considered the kinematic performance and dimensional synthesis of the manipulator, focusing on its parallel part. A 3-DOF planar parallel mechanism was also used in a 6-DOF manipulator presented by Moosavian et al. [382]. This mechanism was placed on a mobile platform and equipped with an RRR planar serial chain (Figure 17f). In paper [383], the authors studied the dynamics and posture stability of the entire mechanical system. Shen et al. [384] also considered the dynamic balance of another 6-DOF hybrid manipulator designed for tea picking. The parallel mechanism of this manipulator was a trivial planar four-bar linkage attached to a PPPRR serial chain (Figure 17g).

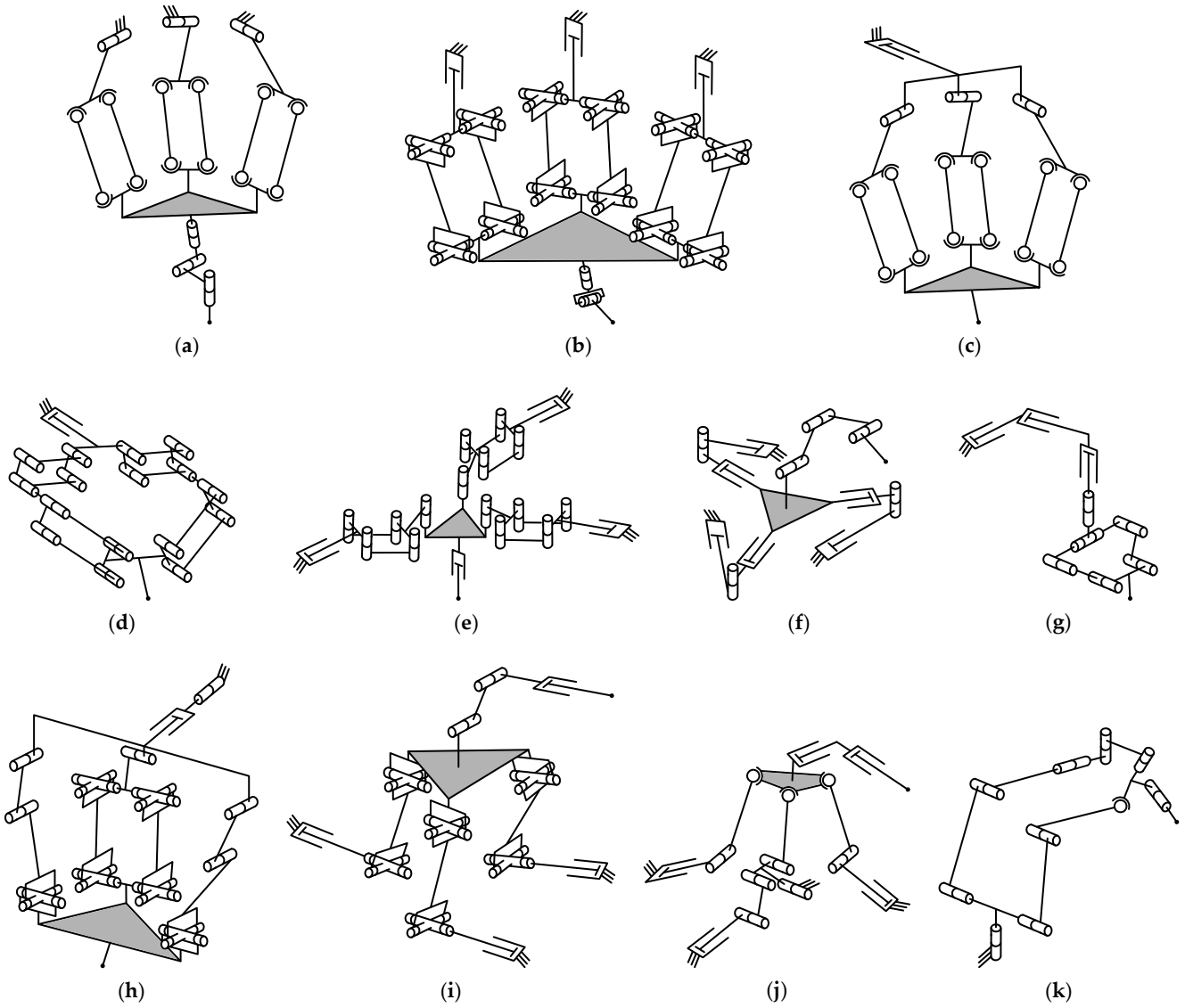

Figure 17. Non-kinematically redundant pick-and-place parallel–serial manipulators: (**a**) (3-RPa*)RRR [371]; (**b**) (3-PRPaR)RR [376]; (**c**) P(3-RPa*) [379]; (**d**) P(2-PaPa) [380]; (**e**) (3-PPaR)P [29]; (**f**) (3-PRP)RRR [382]; (**g**) PPPRR(1-RR/1-RR) [384]; (**h**) RP(1-RRPaR/2-RRU) [385]; (**i**) (3-CRRR)RRP [386]; (**j**) ((1-R/1-PRR)/2-PRS)PP [387]; (**k**) R(1-RRUR/1-RRS)R [388].

Some hybrid pick-and-place manipulators rely on parallel mechanisms with more complex architectures. Lv et al. [385] developed a 5-DOF robot based on a 1-RRPaR/2-RRU parallel mechanism (Figure 17h). The authors' studies were devoted to the robot kinematic and dynamic analysis [389]. Moosavian et al. [386] added an RRP serial chain to a 3-CRRR translational parallel mechanism and obtained a 6-DOF hybrid manipulator (Figure 17i). Like the other authors' manipulator discussed in the preceding paragraph, it was placed on a mobile platform. In their later work [390], the authors analyzed the robot dynamics, while paper [391] considered a design with an RR serial chain. Lian et al. [387] introduced a 5-DOF hybrid robot for assembling in a cabin. The robot relies on a 3-DOF parallel mechanism, which includes a slider-crank linkage in one of its branches (Figure 17j). The authors optimized the robot design and explored other branch architectures in a subsequent paper [392]. The final example is a 6-DOF parallel–serial manipulator called H6A (Hybrid 6-Axis) and proposed by Golla et al. [388]. The robot includes a 4-DOF 1-RRUR/1-RRS placed on a rotary platform and equipped with a rotating end-effector (Figure 17k). The authors' study was devoted to the kinematic analysis of this manipulator.

3.3.2. Kinematically Redundant Manipulators

The first example of kinematically redundant hybrid manipulators is ARTISAN—one of the oldest parallel–serial manipulators proposed by Waldron et al. [393]. It included a 3-DOF 3-RPS parallel mechanism attached to a 7-DOF kinematic chain with a spherical wrist (Figure 18a). The authors considered the kinematics of this wrist and the parallel mechanism, and paper [394] presented a robot prototype. Choi et al. [395] developed a 7-DOF hybrid manipulator with the same parallel mechanism and a PRRR serial chain (Figure 18b). The parallel part and one joint of the serial chain had pneumatic actuators, and the robot was designed to help a human worker attach heavy ceramic tiles to a wall. Elsamanty et al. [19] installed a 3-DOF 3-RRS parallel mechanism to the end-effector of a 6-DOF KUKA KR6 R900 industrial robot (Figure 18c). This was implemented to enrich the movement flexibility and expand the workspace of the serial part, as the authors discussed in their work [396]. A similar 3-RSR mechanism was used by Liang et al. [397], who combined this mechanism with a SCARA-type serial chain (Figure 18d). The authors developed a computer model of this robot and considered its kinematics. Goubej and Švejda [398] introduced AGEBOT, a parallel–serial manipulator for operations in aggressive environments. It relies on a 3-DOF spherical parallel mechanism attached to a PRRR serial chain (Figure 18e). The authors studied the robot kinematics [399] and control [400] and designed its prototype. Another 7-DOF architecture was considered in paper [401]. This anthropomorphic hydraulically actuated manipulator includes a 2-DOF (1-R/1-RPR)R/1-SPU parallel mechanism, forming a spherical wrist together with the distal revolute joint (Figure 18f). In this mechanism, the RPR branch was attached to the yoke of the universal joint instead of the moving platform, making a local closed loop. The authors' work was devoted to the robot mobility and kinematic analysis, and its prototype was also created.

The parallel mechanism in the kinematically redundant manipulators above was placed near the robot end-effector. There are also examples where it was located near the base. Thus, Cheng [402] introduced UPSarm, a 10-DOF parallel–serial manipulator. It included a 2-DOF planar parallel mechanism and a serial chain with several co-axial prismatic joints (Figure 18g). The spherical wrist also had a parallel architecture, and the first revolute joint of the serial chain was driven by an auxiliary slider-crank mechanism. In their later studies, the author and his colleagues considered robot kinematics [403,404] and collision-free motion planning [405,406]. Wang et al. [407] proposed a 7-DOF hybrid manipulator for satellite on-orbit service and capturing malfunctioned satellites. This manipulator relies on a 3-DOF 1-UP/2-UPS parallel mechanism and a 4-DOF RRRR serial chain (Figure 18h). The authors focused on the kinematics [408], dynamics and control [16], and calibration [409] of this robot.

Finally, we mention two manipulators based on the Gough–Stewart platform. The first example is a 9-DOF robot presented in paper [410] (Figure 18i). It was placed on a mobile platform, and the authors considered the kinematics and tip-over stability of this mechanical system. Kim et al. [411] developed another hybrid manipulator based on the Gough–Stewart platform for harvesting heavy fruits. Here, this platform was installed on a rotary platform and equipped with a rotating end-effector (Figure 18j). The authors focused on robot control and designed its prototype.

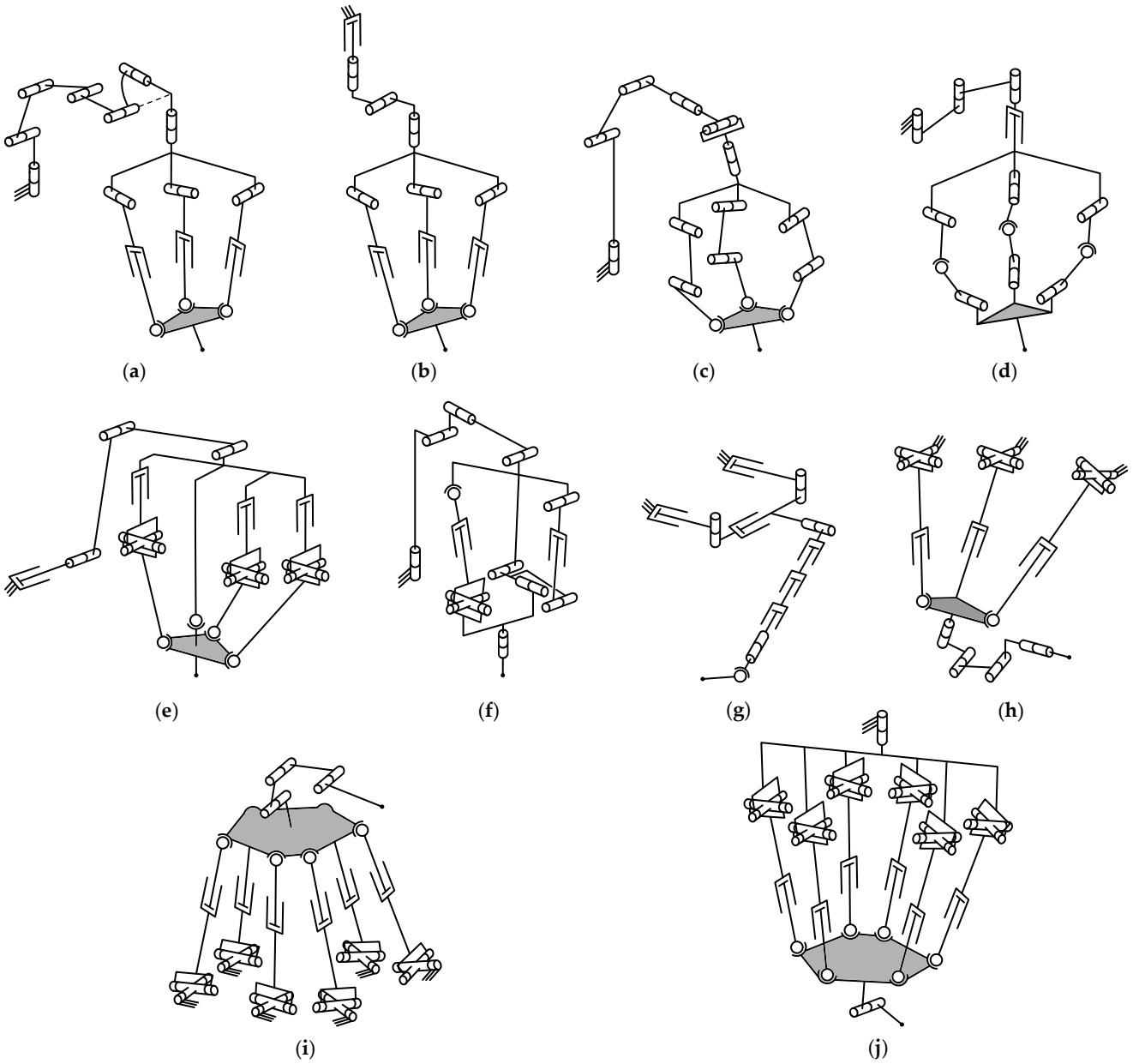

Figure 18. Kinematically redundant pick-and-place parallel–serial manipulators: (**a**) RRRRRRR(3-RPS) (ARTISAN) [393]; (**b**) PRRR(3-RPS) [395]; (**c**) RRRRRR(3-RRS) [19]; (**d**) RRRP(3-RSR) [397]; (**e**) PRRR(1-S/3-PUS) (AGEBOT) [398]; (**f**) RRRR((1-R/1-RPR)R/1-SPU)R [401]; (**g**) (1-PR/1-PRP)RPPPRS (UPSarm) [402]; (**h**) (1-UP/2-UPS)RRRR [407]; (**i**) (6-UPS)RRR [410]; (**j**) R(6-UPS)R [411].

3.4. Humanoids and Legged Systems

Humanoids and other walking robotic systems often include parallel–serial manipulators that form their arms, wrists, legs, and other components [31]. The literature review has shown that most of these manipulators rely on spherical parallel mechanisms with two or three DOFs. For example, Wang et al. [412] considered a 3-DOF leg design for a wheel-leg hybrid rescue robot based on a 2-DOF 1-U/2-UPS parallel mechanism (Figure 19a). The authors analyzed the manipulator kinematics [412] and dynamics [413]. In studies [414,415], Niu et al. examined the same manipulator used for another wheel-leg robot and developed its prototype. So et al. [416] considered a similar leg mechanism with another joint arrangement of the 1-DOF serial chain (Figure 19b). Besides that, the universal joint in the U branch was actuated in the authors' prototype, which served as a hip module of a biped robot. Zhang et al. [417] designed a parallel–serial torso for humanoid robots

with a similar architecture, where the end-effector spherical joints were replaced with the universal ones (Figure 19c).

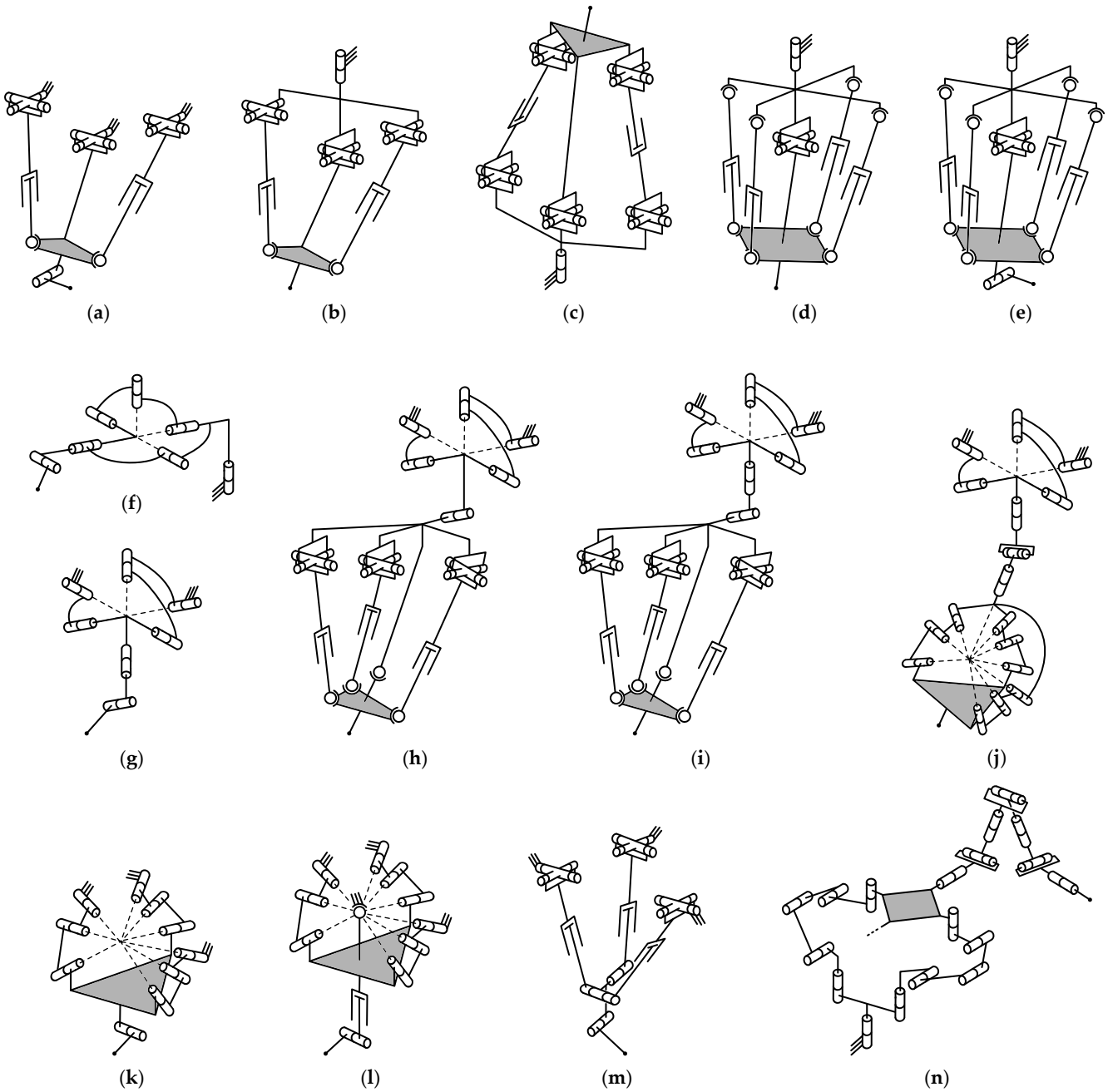

Figure 19. Parallel–serial manipulators used for humanoids and legged systems: (**a**) (1-U/2-UPS)R [412]; (**b**) R(1-U/2-UPS) [416]; (**c**) R(1-U/2-UPU) [417]; (**d**) R(1-U/4-SPS) (HYDROïD) [418]; (**e**) R(1-U/4-SPS)R [419]; (**f**) R(1-RR/1-RRR)R [28]; (**g**) (1-RR/1-RRR)RR [420]; (**h**) (1-RR/1-RRR)R(1-S/3-UPS) [421]; (**i**) (1-RR/1-RRR)RR(1-S/3-UPS) [422]; (**j**) (1-RR/1-RRR)RRR(3-RRR) [26]; (**k**) (3-RRR)R [423]; (**l**) (1-S/3-RRR)PR [424]; (**m**) (3-UPR)R [425]; (**n**) (2-RRRRR)RRRRRRR (Reconbot) [426].

Inspired by the leg mechanism above, Alfayad et al. [427] developed a hip module with a similar hybrid architecture for another humanoid robot called HYDROïD. The only difference was in the parallel mechanism: the authors replaced UPS branches with kinematically equivalent SPS branches. This was the beginning of a series of works in which the authors considered various modifications of this parallel–serial architecture. Thus, in papers [428,429], the authors added offsets to the end-effector joints and applied the mani-

pulator as a shoulder module. Another modification included two auxiliary SPS branches and cable transmission [418] (Figure 19d). The authors used it for the ankle and wrist of the HYDROïD robot and studied its controller architecture in paper [430]. Abdellatif et al. [419,431] considered a similar ankle mechanism with a toe revolute joint (Figure 19e).

2-DOF spherical parallel mechanisms in the discussed manipulators included a U branch. Scholars have also used a closed-loop five-bar spherical linkage (with a 1-RR/1-RRR architecture) to generate the same spherical motion. For example, Li et al. [28] proposed a 4-DOF hybrid humanoid manipulator for on-orbit servicing that includes such a mechanism (Figure 19f). In their other works, the authors considered the robot kinematics [432], dynamics [433], and control [434] and designed its prototype. Paper [420] introduced another 4-DOF hybrid humanoid arm with the 1-RR/1-RRR spherical mechanism and an RR serial chain (Figure 19g) and analyzed its kinematics and dynamics. Subsequent studies proposed various modifications of this architecture. In the first one [421], the authors replaced the last revolute joint in the serial chain with a 1-S/3-UPS spherical parallel mechanism (Figure 19h). The authors' paper was devoted to the kinematic and dynamic analysis of this manipulator. In the second modification [422], the authors turned that revolute joint back and derived a 7-DOF kinematically redundant architecture (Figure 19i). Its kinematics, dynamics, and optimal trajectory planning were considered in papers [435,436]. Sun et al. [26] proposed a similar humanoid robotic arm. The authors added a third revolute joint to the serial chain and replaced the 1-S/3-UPS spherical mechanism with a 3-RRR one (Figure 19j). Papers [437,438] considered the dimensional synthesis of this 8-DOF manipulator.

The 3-RRR spherical parallel mechanism was also used as a parallel part of other hybrid manipulators. Thus, Gao et al. [423,439] applied it in a 4-DOF robotic leg of a quadruped robot (Figure 19k). Feller and Siemers [424] designed an innovative robotic leg for a three-legged mechanism, where the parallel mechanism included an additional S branch (Figure 19l). The serial chain of this leg had a passive spring-loaded prismatic joint. Papers [440–442] considered the manipulator design, kinematics, and performance.

Finally, we mention two architectures not based on spherical parallel mechanisms. The first one is a parallel–serial arm of the LARMbot humanoid robot [425]. It includes a 3-DOF parallel mechanism with three UPR branches (Figure 19m). Fort et al. [443–445] thoroughly discussed the manipulator design, and Ceccarelli [446] considered its various applications. The second example is Reconbot, a reconfigurable hybrid robot proposed by Ding et al. [426]. This robot relies on a reconfigurable parallel mechanism with two RRRRR branches whose output link is equipped with two 7-DOF kinematically redundant serial chains (Figure 19n, where one chain is omitted for clarity). The manipulator was placed on a mobile platform and used for rescue operations. In their paper, the authors analyzed robot mobility and showed the parallel mechanism could have from zero to five DOFs.

3.5. Haptic Devices

Haptic devices provide the force-feedback interface between a user and a virtual or remotely operated environment. Scholars have proposed diverse haptic devices [447], and some of them have parallel–serial architectures. For example, Li et al. [448] developed HFFD-6 (Hybrid Force Feedback Device with Six DOFs) based on the Delta mechanism (Figure 20a). The manipulator end-effector attaches to the moving platform of this mechanism with a 3-DOF RRR spherical serial chain. A similar device with a 4-DOF RRRR spherical chain was considered in paper [449], and Hao et al. [450] added a 1-DOF gripper to the haptic end-effector. Bilgincan and Dede [451] used another 3-DOF translational parallel mechanism with parallelogram joints and constructed a 6-DOF haptic manipulator, which also included the RRR spherical serial chain (Figure 20b). In paper [452], the authors analyzed the manipulator dynamics. The last example is a 6-DOF parallel–serial haptic device proposed by Tang and Payandeh [453]. It is based on a 3-RRR spherical parallel mechanism and an RRR non-spherical serial chain (Figure 20c). The authors' works were devoted to kinematic analysis [454] and experimental studies [455,456] of this haptic device.

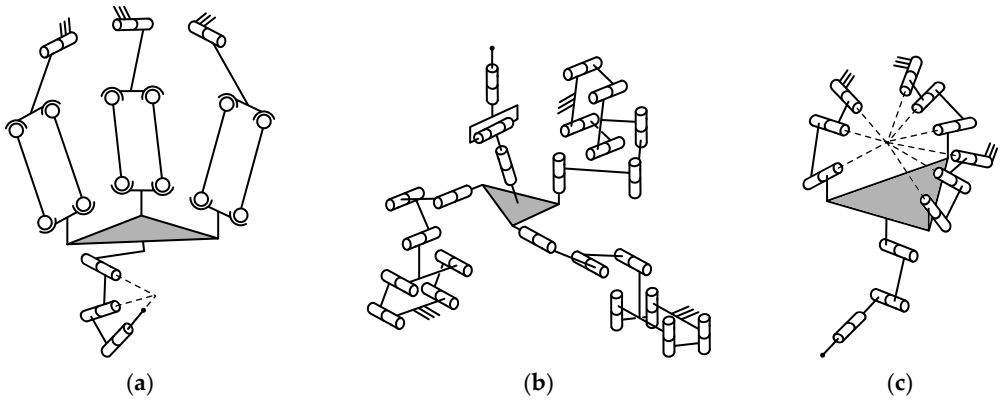

Figure 20. Haptic devices based on parallel–serial manipulators: (**a**) (3-RPa*)RRR (HFFD-6) [448]; (**b**) (3-PaRRR)RRR [451]; (**c**) (3-RRR)RRR [453].

3.6. Additive Technologies

Robotic systems for additive technologies, such as 3D printing, rarely need more than three translational DOFs to position the end-effector. However, scholars have added rotational DOFs to make the end-effector more versatile. Thus, Lu and Li [457] proposed a 6-DOF 3D printing manipulator with a 3-PUU translational parallel mechanism and an RRR serial chain (Figure 21a). In papers [458,459], the authors analyzed manipulator dynamics, focusing on its parallel part. Zhou et al. [460] presented another hybrid architecture for 3D printing. It included a 3-CPaRR translational parallel mechanism with decoupled kinematics and an RR spherical wrist (Figure 21b). In a later work [461], the authors modified the robot design: they removed one revolute joint from each branch of the parallel mechanism and considered a non-spherical RR serial chain (Figure 21c). Paper [462] studied the effect of joint clearance on robot performance. Antonov et al. [463] designed a prototype of a 5-DOF parallel–serial manipulator for selective laser sintering. The manipulator featured a 4-RPR redundantly actuated planar parallel mechanism installed on a linear guide and equipped with a rotating end-effector (Figure 21d). A recent paper [464] performed stiffness analysis and dimensional synthesis of this manipulator.

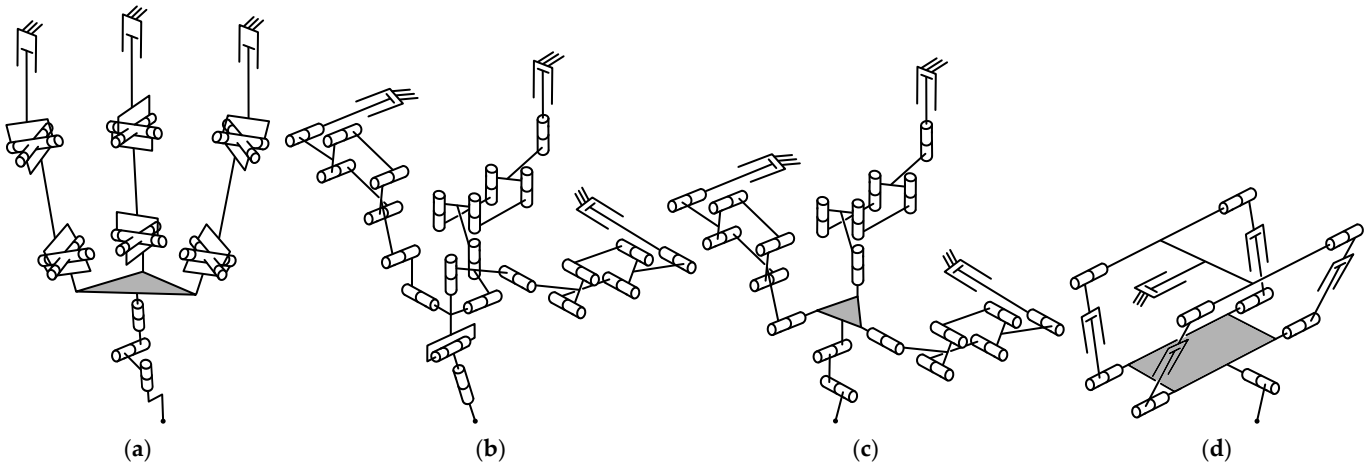

Figure 21. Parallel–serial manipulators for additive technologies: (**a**) (3-PUU)RRR [457]; (**b**) (3-CPaRR)RR [460]; (**c**) (3-CPaR)RR [461]; (**d**) P(4-RPR)R [463].

3.7. Simulators

There are many simulators based on the Gough–Stewart platform, and scholars have also developed parallel–serial simulators using this mechanism. For example, Cong et al. [465] installed a rotating end-effector on this platform (Figure 22a). The authors' study was devoted to the kinematic analysis and simulations of the robot, with the main focus on the parallel part. Wang et al. [466] placed the Gough–Stewart platform on a 3-DOF RRR

spherical turn-table and applied it as a flight simulator (Figure 22b). The authors considered robot kinematics in paper [467] and used kinematic redundancy to avoid singularities.

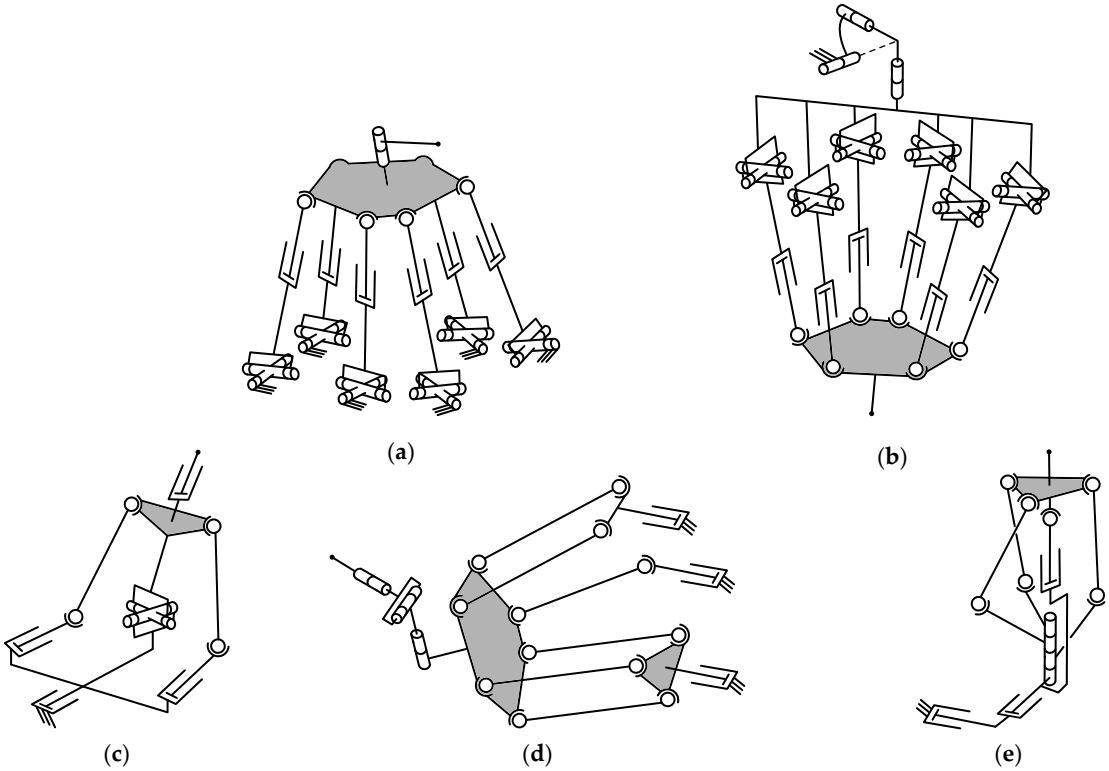

Figure 22. Parallel–serial manipulators applied as simulators: (**a**) (6-UPS)R [465]; (**b**) RRR(6-UPS) [466]; (**c**) P(1-U/2-PSS)P [468]; (**d**) (1-PSS/2-PPa*)RRR [469]; (**e**) PP(1-PS/3-RSS) [470].

Among other examples is a 4-DOF urban bus driving simulator proposed by Jaberi et al. [468]. It is based on a 2-DOF 1-U/2-PSS parallel mechanism mounted on a linear guide (Figure 22c). In their study, the authors analyzed kinematics and evaluated the mechanism performance. Qazani et al. [469] designed a 6-DOF hybrid simulator based on a 3-DOF Gantry-Tau translational mechanism and an RRR spherical wrist (Figure 22d). Paper [471] considered various control strategies of this robot. Another 6-DOF simulator was developed by Nabavi and Enferadi [470]. It included a 4-DOF 1-PS/3-RSS parallel mechanism with co-axial revolute joints installed on a 2-DOF XY moving table (Figure 22e). The authors' research was focused on manipulator dynamic analysis.

3.8. Orienting Devices

This subsection considers parallel–serial manipulators applied as positioning or orienting devices. The first example is a 3-DOF hybrid robot proposed by Gao et al. [472]. It is based on a 2-DOF five-bar spherical mechanism whose output link is equipped with a rotating end-effector (Figure 23a). The authors focused on the dynamic analysis of this robot in their paper. Xu et al. [473] developed another rotary platform based on a 2-DOF spherical parallel mechanism. This redundantly actuated mechanism has one passive U branch and three UPS branches (Figure 23b). The rotating joint of the serial chain was actuated by an auxiliary branch, and the authors considered the robot design and calibration in study [474]. Zhang et al. [475] proposed a hybrid antenna device based on a 3-DOF 3-RRRRR parallel mechanism with symmetrically arranged branches (Figure 23c). In their later works, the authors focused on the robot dynamics [476] and dimensional synthesis [477]. The last example in this subsection is a 6-DOF positioning stage studied by Wang and Chen [20]. It includes a 3-PPS parallel mechanism installed on a 2-DOF moving table (Figure 23d). The authors designed a robot prototype and considered its calibration procedure.

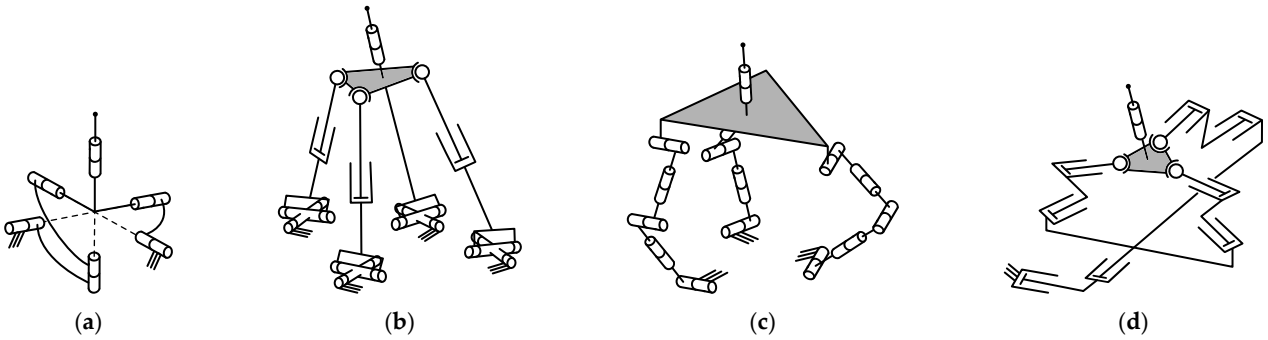

(**a**) (**b**) (**c**) (**d**)

Figure 23. Parallel–serial manipulators applied as orienting devices: (**a**) (1-RR/1-RRR)R [472]; (**b**) (1-U/3-UPS)R [473]; (**c**) (3-RRRRR)R [475]; (**d**) PP(3-PPS)R [20].

3.9. Ocean Wave Compensation

Manipulators presented in this subsection are installed on ships and developed to compensate for ocean waves. For example, Wang et al. [478] considered a manipulator composed of a 6-DOF Gough–Stewart platform and an RRP serial chain (Figure 24a). The manipulator end-effector represents a telescopic gangway used for service operations [479]. The authors studied kinematics and motion planning for this mechanical system in works [480–482]. Niu et al. [483] proposed a similar manipulator where the Gough–Stewart platform was replaced with a 3-DOF 1-UP/3-UPU parallel mechanism (Figure 24b). In that paper, the authors considered the kinematics and dynamics of this robot. The final example is a 6-DOF hybrid platform developed by Tang et al. [484]. It relies on a similar 3-DOF parallel mechanism but includes a PPR serial chain (Figure 24c). The authors designed a robot prototype and analyzed its mobility and kinematics.

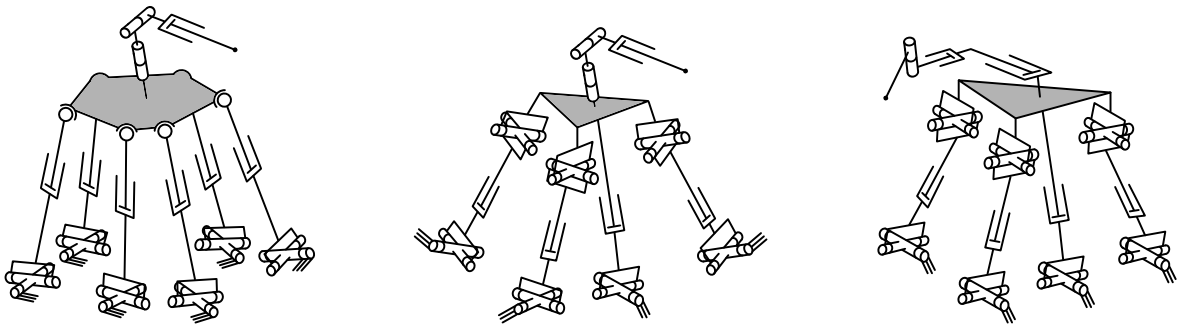

(**a**) (**b**) (**c**)

Figure 24. Parallel–serial manipulators for ocean wave compensation: (**a**) (6-UPS)RRP [478]; (**b**) (1-UP/3-UPU)RRP [483]; (**c**) (1-UP/3-UPU)PPR [484].

3.10. Other Applications

This subsection discusses parallel–serial manipulators used in other applications not mentioned earlier. Thus, Wu et al. [485] proposed a 5-DOF spray-painting robot based on a 3-DOF planar parallel mechanism with two branches (Figure 25a). In paper [486], the authors analyzed the robot kinematics and dynamics and performed its dimensional synthesis, focusing on the parallel part. Wang et al. [487] considered another 5-DOF painting robot, which included a 1-U/2-SPU parallel mechanism and an RRR serial chain (Figure 25b), and studied its kinematics. Karim et al. [488] designed a 7-DOF PP(3-RPS)RR parallel–serial manipulator for high-power, high-repetition laser operations (Figure 25c). The authors developed a prototype of this device, and their later studies were devoted to its accuracy analysis [489,490] and control system [491]. An original pole-climbing parallel–serial robot was proposed by Vossoughi et al. [492]. This 4-DOF system included a 3-RPR planar parallel mechanism attached to a rotary base (Figure 25d). In later works, the authors focused on the dynamics [493], dimensional synthesis [494], design [495], and various

applications [496] of the robot. Yan et al. [497] considered another exotic parallel–serial manipulator used for robotic dancing. It was based on a 4-DOF parallel mechanism attached to an RR serial chain (Figure 25e). In their study, the authors considered the robot kinematics and developed its prototype.

Finally, we mention a few studies devoted to the theoretical analysis of some parallel–serial manipulators, without mentioning specific applications or developing physical prototypes. Chablat et al. [498,499] considered singularities and isoconditioning loci of a 3-DOF manipulator, which included a 2-DOF planar five-bar linkage (Figure 25f). Huang et al. [500] and Lee and Kim [501] studied the instantaneous kinematics of 6-DOF parallel–serial manipulators based on a 3-RPS parallel mechanism and an RRR serial chain (Figure 25g). The authors also performed a similar analysis for a hybrid manipulator with an RRP serial chain [502] (Figure 25h). Chen [503] considered the dynamics of a 9-DOF manipulator based on the Gough–Stewart platform equipped with an RRR serial chain (Figure 25i). Cha et al. [504] analyzed another kinematically redundant robot with the same parallel mechanism attached to a PPP serial chain (Figure 25j). The authors' study was devoted to the robot kinematics and redundancy resolution.

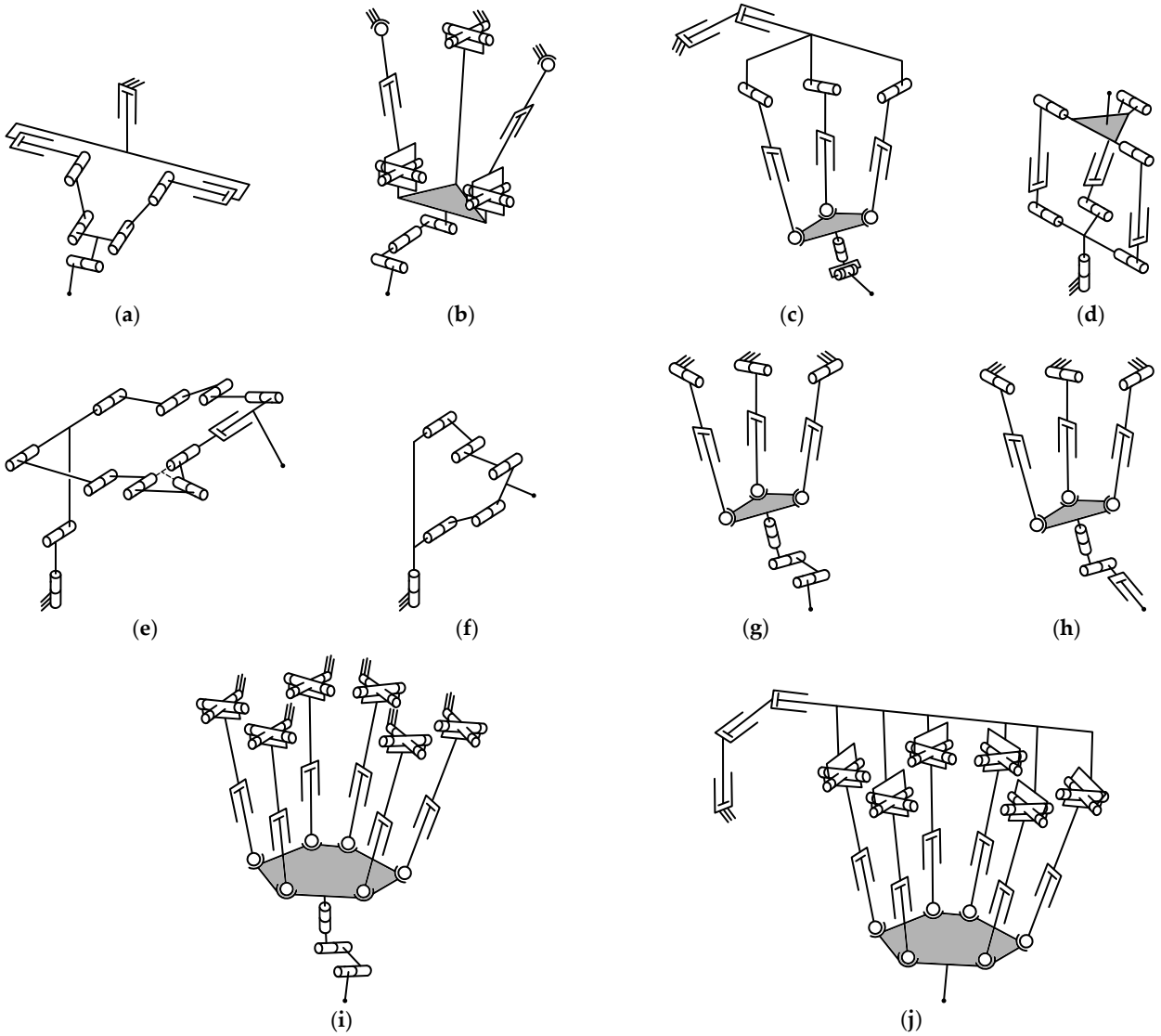

Figure 25. Other parallel–serial manipulators for miscellaneous applications: (**a**) P(1-PRR/1-PRR)R [485]; (**b**) (1-U/2-SPU)RRR [487]; (**c**) PP(3-RPS)RR [488]; (**d**) R(3-RPR) [492]; (**e**) RR(1-RRRR/1-RRRRRP) [497]; (**f**) R(1-RR/1-RRR) [498]; (**g**) (3-RPS)RRR [500]; (**h**) (3-RPS)RRP [502]; (**i**) (6-UPS)RRR [503]; (**j**) PPP(6-UPS) [504].

4. Design and Analysis

The previous section presented many architectures of parallel–serial manipulators. The current section discusses what methods scholars used when they developed and analyzed these manipulators. We consider various techniques for their type synthesis, mobility, kinematic, and dynamic analysis, optimal design, control, and calibration.

4.1. Type Synthesis

The first step in developing a manipulator is selecting its kinematic scheme—this process is known as type synthesis. There are different approaches for solving the type synthesis problem, classified and thoroughly discussed in works [505,506]. Here, we focus on the methods applied to synthesize parallel–serial manipulators.

Chakarov and Parushev [507] were among the first to tackle this problem by using mobility formulae and Assur groups with linear actuators. The authors took a primary serial chain and located these groups between its links. After that, the drives in the serial chain were replaced with the linear actuators in Assur groups, resulting in quasi-serial manipulators discussed in Section 2 (Figure 1d). Campos et al. [508] followed a similar approach based on Assur groups and synthesized symmetrical manipulators from a 0-DOF primary mechanism.

The synthesis approaches above considered only the number of DOFs, ignoring the output link motion type. Other studies examined the nature of these DOFs as well. Thus, Zeng and Fang [509,510] developed a generalized method based on group theory and represented mechanisms as logical matrices, aiming to automate the type synthesis procedure. This method was advanced in works [23,511], where the authors introduced several novel manipulators. However, the major focus of these studies was on interconnected mechanisms. We can also mention the work of Shen et al. [512], who applied the so-called position and orientation characteristics sets (POC sets) to synthesize parallel–serial manipulators with three to five DOFs, which was the development of the authors' previous study [513]. Many novel manipulators were obtained by considering various combinations of parallel mechanisms and serial kinematic chains.

The mentioned studies proposed systematic techniques to synthesize parallel–serial manipulators with a different number of DOFs and different motion types. Other works focused on the type synthesis of mechanisms with a specific number of DOFs and specific motion types. For example, Qin et al. [514,515] used the so-called generalized function sets to design 5-DOF parallel–serial manipulators with three translational and two rotational DOFs (3T2R motion type), where parallel mechanisms had three or four DOFs. Following this approach, the authors created over three hundred different mechanisms. The same method was used by the authors in works [516–518] to synthesize 3R2T parallel–serial manipulators. He et al. [408] followed this approach when designing a 7-DOF (1-U$\underline{P}$/2-U$\underline{P}$S)RRRR hybrid manipulator.

Most other synthesis approaches of parallel–serial manipulators rely on the (instantaneous) screw theory or Grassmann line geometry. Thus, Xie et al. [519] applied the latter for the type synthesis of parallel mechanisms with one translational and two rotational DOFs (1T2R motion type), which constituted a parallel part of 5-DOF hybrid manipulators. Chong et al. [25] used a similar method to develop a 3-R$\underline{C}$U mechanism within another 5-DOF parallel–serial manipulator. Screw theory was applied for the type synthesis of TriMule [62,86], (1-U/3-U$\underline{P}$S)R [473] and R(1-$\underline{P}$U/2-$\underline{C}$RS) [358] manipulators, and hybrid manipulators based on planar parallel mechanisms [520]; most of these studies focused on the synthesis of parallel mechanisms. Zhang et al. [521] also combined the methods of instantaneous and finite screw theory to generate novel manipulators for space operations. Finally, we mention paper [522], whose authors synthesized 5-DOF hybrid manipulators with a 3-DOF parallel mechanism by replacing a fragment of the primary serial chain.

4.2. Mobility Analysis

Mobility analysis is closely related to the type synthesis, and it aims to compute the number of DOFs of the manipulator end-effector and verify that it has the desired motion type. For parallel–serial manipulators, the mobility analysis is usually performed separately for serial and parallel parts using traditional approaches, and then the results are combined. Most of these approaches rely either on mobility formulae or screw theory, as exemplified below.

Thus, Zanganeh and Angeles [523] introduced a generalized approach suitable for a wide class of hybrid manipulators using mobility formulae and graph representations of the mechanisms. The formulae were also applied for mobility analysis of different parallel–serial manipulators with five to nine DOFs [140,228,298,307,353,497] considered in Section 3. The major limitation of this method is that it does not reveal the motion type of the manipulator and may yield incorrect results for overconstrained mechanisms.

Screw theory resolves this problem and has become a standard tool for the mobility analysis of parallel and parallel–serial manipulators. For example, scholars used this approach to analyze the mobility of different manipulators with four [171,357,475], five [202,222,283], and six [484] DOFs. Other authors also combined screw theory with mobility formulae, which were used to validate the results. This is probably the most popular technique for mobility analysis, successfully applied to parallel–serial manipulators with three [412,414,415], four [352], five [66,210,223,282,284,354,385,460], six [318], seven [401], and eight [26] DOFs or a reconfigurable design [426], which were discussed in Section 3.

Other methods of mobility analysis included a combination of screw theory and Grassmann–Cayley algebra [182] and the use of POC equations [377].

4.3. Position Analysis

Position analysis aims to solve two fundamental problems: the forward (or direct) kinematic problem and the inverse one. In forward kinematics, we have to describe the motion of all links of the manipulator (in particular, of its end-effector) in terms of the input motion of the actuators. The inverse kinematics considers the opposite problem and aims to express the motion of the links required for the specified trajectory of the manipulator end-effector. Both problems form the foundation for the entire kinematic and subsequent dynamic analysis of the manipulator, as well as its performance evaluation, calibration, and control.

Solving forward kinematics for serial manipulators is straightforward, while inverse kinematics is usually more challenging. The opposite is true for parallel robots: their inverse kinematics has a simple closed-form solution most times, while forward kinematics is often solved numerically. In this regard, position analysis of parallel–serial manipulators becomes challenging in both forward and inverse directions. Next, we consider how scholars have addressed the position analysis of various hybrid robots. This analysis is performed in most papers cited in Section 3, so this subsection only discusses several representative examples and general techniques and ignores works that focus only on the kinematics of the parallel or serial part.

The first step in position analysis is deriving equations that relate actuator displacements to the end-effector configuration. One way to solve this problem is to replace the parallel mechanism with an equivalent virtual serial chain, perform the analysis for this chain, and then return to the parallel mechanism. Shukla and Paul proposed this method in their work [524] and used the Denavit–Hartenberg (D-H) approach to establish coordinate frames and obtain the desired equations. The D-H approach was used to derive equations for different parallel–serial manipulators with four [28], five [487], six [453,454,497], and seven [253,397] DOFs. Singh et al. [27,365,366] also suggested an improved D-H notation and analyzed a 7-DOF manipulator with that method. As an alternative to the D-H approach, some scholars derived the equations using the product-of-exponentials (POE) formula. This method does not need to introduce intermediate reference frames, and it was applied to parallel–serial manipulators with four [475,476], five [239,369], eight [26], or

ten [266] DOFs. In works [237,238,484], the authors also used the POE formula to model the kinematics of the serial chain within the whole manipulator. However, because most parallel–serial manipulators include lower-mobility parallel and serial mechanisms with simple architectures, scholars prefer geometrical (vector) methods [34,35,60,81,317,502] to obtain the kinematic equations.

After deriving the equations, the next step is to use them to solve a forward or an inverse kinematic problem. Since inverse kinematics is crucial for robot control and practical applications, scholars have mainly focused on solving this problem when analyzing parallel–serial manipulators. Most non-kinematically redundant manipulators used in practice and considered in Section 3 admit a closed-form solution to this problem; for example, manipulators with three [227,412,414,415,431], four [203,352,420], five [87,93,139,222,282,284,412], and six [421] DOFs. Sometimes, a solution to the inverse kinematics can be found independently for serial and parallel parts [45,161,211,278,371,398,399,471], simplifying the kinematic analysis.

For some parallel–serial manipulators, the inverse kinematic problem does not have a closed-form solution. For example, Waldron et al. [393] solved the inverse kinematics for the 6-DOF part of the 10-DOF ARTISAN manipulator with numerical methods. López-Custodio et al. [192,196] also applied numerical techniques to solve this problem for the Exechon-based parallel–serial manipulator with offset joints. One should also mention study [432], whose authors used a fuzzy logic compensator to enhance online computations of the inverse kinematics for a 4-DOF manipulator.

Unlike manipulators with three to six DOFs discussed so far, the inverse kinematics of kinematically redundant parallel–serial manipulators admits an infinite number of solutions. A standard way that scholars used to overcome this issue is fixing the redundant DOFs and then tackling inverse kinematics using familiar approaches. For example, Wang et al. [407] and He et al. [408] fixed one actuator in the serial chain of the 7-DOF robot and solved the inverse problem by combining analytical and numerical methods. A similar technique was applied to another 7-DOF parallel–serial manipulator in study [435]. Cheng [403] resolved the kinematic redundancy of the 10-DOF UPSarm manipulator using specific rules and selected the joints to be fixed depending on the robot application. Unlike these works, whose authors fixed an actuator of the serial chain, Cheng et al. [401] specified one Cartesian coordinate of the joint center to resolve the redundancy of a 7-DOF hybrid robot. Kucuk and Gungor [364] analyzed a 9-DOF manipulator based on a 6-DOF Gough–Stewart platform and assumed that the position vector of this platform was known; after that, the authors computed a closed-form solution to the inverse kinematic problem. There also exist other approaches for resolving kinematic redundancy. Thus, an original approach was proposed by Wang et al. [478,481], who solved the inverse kinematics of a similar 9-DOF parallel–serial manipulator using a fuzzy algorithm. Cha et al. [504] considered another 9-DOF manipulator based on the Gough–Stewart platform and solved its inverse kinematics with an optimization procedure, which aimed to minimize the motion of the serial mechanism for the specified trajectory.

Position analysis in the papers cited above focused mainly on inverse kinematics. Other studies also considered both inverse and forward kinematics. Since many parallel–serial manipulators include lower-mobility parallel mechanisms with two or three DOFs, a solution to the forward kinematics can often be found in a closed form or reduced to a univariate polynomial equation using elimination techniques. These methods were successfully applied to different hybrid manipulators with three [360], four [29,171,245,321,425,493], five [140,228,235,303,313,315,328,361,363,374], and six [345,348,388] DOFs. However, applying the methods above can be challenging or computationally ineffective, so other scholars used numerical techniques to solve forward kinematics. These techniques included a standard Newton's iterative method [34,88,162,165,195,448], an optimization approach [358], and methods based on neural networks [184,185,223].

4.4. Instantaneous Kinematic Analysis

The main goal of the instantaneous kinematic analysis is to derive Jacobian matrices that relate speeds in the actuated joints of the manipulator to its end-effector velocities. This analysis forms the basis for subsequent singularity determination and performance optimization, where cost functions are often based on these matrices [525]. Scholars have followed several approaches to analyze the instantaneous kinematics of parallel–serial manipulators, and here, we present several illustrative examples. As in the previous subsection, we ignore studies that focus just on the parallel or serial part of the whole manipulator.

The most straightforward method is to differentiate kinematic equations obtained in position analysis. For example, this technique was applied to hybrid manipulators with three [360,415], four [171], five [298,313,375,460], and six [348] DOFs. The listed studies show this method is straightforward, but symbolic differentiation of the kinematic equations can be cumbersome. Another drawback of this method is that the Jacobian matrices obtained this way do not give a clear geometrical interpretation to singular configurations and can also catch the so-called representation singularities, which are not true kinematic singularities of a robot [526].

The second approach for instantaneous kinematics is to write vector equations for the linear and angular velocities of the end-effector. Sklar and Tesar [527] were probably the first to propose a concise procedure for parallel–serial manipulators. Chung et al. [528] modified this method and suggested replacing a parallel mechanism with a virtual joint. Most other studies are less generalized and consider specific architectures with three [499], four [420,493], five [283,361], six [393,484], or seven [435] DOFs. There are also examples where the vector approach is combined with the differentiation approach considered above [93,216,238,371,413,482,529]. To summarize, the vector method results in more compact expressions than the differentiation approach. The obtained relations usually include cross- and dot-products of vector variables, providing a clear geometrical interpretation of singularities. The main drawback of this technique is that there is no unique way to eliminate speeds in unactuated joints.

The third method, which avoids the limitations of the previous ones, relies on the screw theory, and there are several systematic approaches based on this concept. Thus, Etemadi-Zanganeh and Angeles [530,531] introduced a procedure suitable for general hybrid manipulators and used the screw-system annihilator to exclude speeds in unactuated joints. Monsarrat and Gosselin [532] developed another systematic method applicable to robots with flexible links. Sun et al. [533] proposed an approach based on replacing a parallel part with an equivalent serial chain. However, these approaches either ignored motion constraints or suggested using pseudo-inverted Jacobian matrices, which could be less intuitive for understanding. To overcome these issues, Antonov and Fomin [370] have recently proposed another screw-theory-based method suitable for a wide class of non-kinematically redundant parallel–serial manipulators, which generalized the authors' previous works [141,240]. Most other studies focused on manipulators with specific architectures: for example, on parallel–serial robots with three [418], four [432], five [138,173,282,284], and six [18,35,501,502] DOFs. In paper [182], screw theory was combined with Grassmann–Cayley algebra.

4.5. Singularity Analysis

Singularities represent configurations of the manipulator where its end-effector loses DOFs or acquires uncontrollable motions. Determining singular configurations relates directly to the instantaneous kinematic analysis discussed in the previous subsection, and numerous papers considered this topic [13]. Here, we focus on studies devoted to the singularities of parallel–serial manipulators.

The methods scholars used to analyze singular configurations match the methods of the instantaneous kinematic analysis that we considered above. The first approach is to equate a determinant of Jacobian matrices to zero and find a scalar condition indicating a singularity. This method was applied to different parallel–serial manipulators with

three [418,427], four [171,423], five [284,295,298,303,312], and six DOFs [388]. In some works, this method was used only for the parallel part of the hybrid robot; for example, for 2-DOF parallel mechanisms [317,401,468].

The second way to determine singular configurations is to find geometrical conditions when the determinant is zero. Liu et al. [60] and Tosi et al. [336] followed this technique but considered only the parallel part of their hybrid robots. In contrast, Laryushkin et al. [141] determined the singularities of the whole manipulator and constructed Jacobian matrices using screw theory.

Screw theory generalizes the geometrical method, and it allows detecting singular configurations with no need to compute the determinants. Scholars applied screw theory to analyze the singularities of parallel–serial manipulators with four [316], six [327,484], and eight [26] DOFs. Grassmann line geometry, as a special case of screw theory, was also used to tackle this problem [282], while Tanev [323] combined screw theory techniques with geometric algebra. Most of these works, however, focused just on the parallel mechanisms.

Finally, we mention the works of Wang et al. [466,467], who studied how to avoid singularities using kinematic redundancy.

4.6. Workspace Analysis

The workspace of a manipulator represents the set of postures achievable by its end-effector. The workspace shape and dimensions are determined by the manipulator geometrical parameters, joint constraints, link interference, and singular configurations. For robots with three or greater DOFs, there are different types of workspaces depending on the considered orientations [257]. This subsection covers the methods scholars have used to analyze the workspaces of parallel–serial manipulators.

The conventional and probably most popular approach is a discretization method based on inverse kinematics. In the first step, the entire motion space of the manipulator end-effector is sampled into discrete points. Next, for each point, we use inverse kinematics and check whether we meet all the joint constraints and other restrictions. As we saw in Section 4.3, the inverse kinematic problem of most developed parallel–serial manipulators has a closed-form solution, so it becomes quite simple to implement this method. Scholars applied it for workspace analysis of various hybrid robots with three [412], four [29,171,476], five [45,199,201,210,211,213,284,295,303,328,385], six [281,327,346,421,484], and seven [336] DOFs.

As discussed in Section 4.3, some architectures of parallel–serial manipulators admit a closed-form solution to the forward kinematic problem, which can help determine the workspace. Unlike the previous method, we sample the set of actuator displacements and then use forward kinematics to find the end-effector posture. Scholars followed this approach to obtain the workspace of manipulators with four [317,425], five [140,223,232,298,312], seven [161], and nine [396] DOFs. In paper [393], the authors used a numerical solution to the forward kinematic problem. Other numerical techniques applied to workspace analysis of parallel–serial robots included interval analysis [197,468] and a chord method [463].

A geometrical method represents another way to construct the robot workspace. The idea behind this method is to analyze geometrical objects (surfaces and volumes), corresponding to the sets of possible locations of the manipulator links, and then find their intersections or unions. Compared to the discretization techniques, the geometrical method provides a more accurate workspace boundary, but it is more challenging to implement for manipulators with three or more DOFs. There are just a few examples of its application, where it was used for parallel mechanisms with two [73] and three [249,486,492] DOFs, which constituted the part of hybrid manipulators.

4.7. Dynamic Analysis

Dynamic analysis of a manipulator aims to derive equations of motion that relate its kinematic parameters (positions, velocities, and accelerations of the links) and dynamic

parameters (internal and external forces and torques). These equations serve multiple purposes. Foremost, they allow computing the motor torques required to realize a specified end-effector motion. This analysis is the foundation for selecting the appropriate motors for the manipulator.

Scholars have applied different techniques to analyze the dynamics of parallel–serial manipulators. The earliest attempts to tackle this problem included the work of Sklar and Tesar [527], who proposed an approach based on so-called influence coefficients. This generalized approach, suitable for a wide class of hybrid manipulators, was refined in later studies [528,534,535]. However, to our knowledge, it was not applied to the manipulators discussed in Section 3, and scholars preferred using other techniques.

The first one relies on Newton–Euler equations, written for each manipulator link. The major challenge here is solving the composed system of equations, which includes many joint reactions we are usually not interested in. Unlike serial robots, where this method leads to efficient recursive dynamic computations, implementing it to hybrid manipulators becomes problematic because of the closed-loop nature of parallel mechanisms. There are just a few examples where Newton–Euler equations were used to model dynamics of parallel–serial manipulators with four [420,493], five [389], six [35], seven [16,435], and nine [503] DOFs.

The second approach is based on Lagrange's equations. In this method, we compute the kinetic and potential energies of the links and their derivatives, without considering joint reactions (except for friction forces). Finding these derivatives often leads to cumbersome calculations, which is the major limitation of Lagrange's equations. Thus, this approach was used in few papers that studied the dynamics of parallel–serial manipulators with three [359], five [374,461], six [346], and seven [395] DOFs.

The virtual work principle is another tool to derive equations of motion. Compared with the Newton–Euler and Lagrangian methods, it ignores internal joint reactions and does not require composing and differentiating energy functions. These advantages have made the virtual work principle the most popular technique for analyzing the dynamics of parallel–serial manipulators. Zhang et al. [529] have recently presented a generalized formulation of this method for these robots. Its application can be found in numerous papers that considered different hybrid manipulators with three [413,486], four [155,156,205,247,248,433], five [77,81,93,178,216,221,224,283,291,300,301], six [281,458,483], and nine [172] DOFs. Most of these works, however, focused on the dynamics of the parallel mechanism or considered a serial chain attached to its moving platform as a lumped mass.

Some scholars also combined the methods listed above during dynamic analysis. There are examples of combining Newton–Euler equations with Lagrangian approach [234,253,383], and Lagrangian approach with the virtual work principle [421,452,472]. The less widespread methods of dynamic analysis were based on screw theory [138,476] and Gibbs–Appell equations [470].

4.8. Performance Evaluation

This subsection considers the methods scholars have used to evaluate the performance of the developed parallel–serial manipulators. Most methods rely on computing different metrics (performance indices), whose definitions are not presented here but can be found in relevant papers [536,537]. To make the presentation more concise, we classify these methods and metrics into three groups (kinematic, static, and dynamic), as discussed next.

4.8.1. Kinematic Performance

Metrics of kinematic performance reflect how drive errors affect the positioning accuracy of the manipulator end-effector and how close the considered configuration is to singularity. A conventional approach here is to compute the condition number (or its inverse, also known as the conditioning index) of the Jacobian matrix, and it was applied by scholars in numerous studies [314,317,358,457,486,498] to estimate manipulator dex-

terity. A similar method is to compute and evaluate the singular values of the Jacobian matrix [60,138].

Input and output transmission indices represent other common metrics used to evaluate the kinematic performance. Transmission indices are based on screw theory and generally applied to parallel manipulators. Researchers used these metrics to evaluate the performance of 3-DOF parallel mechanisms in hybrid manipulators with four [171] and five [25,166,167,214,219] DOFs.

Some scholars also introduced their own original metrics to analyze the kinematic performance of specific parallel–serial manipulators. Thus, Jaberi et al. [468] and Wang et al. [146,147] proposed different sensitivity indices, which were applied to the parallel part of the considered hybrid robots. Zou et al. [29] introduced the so-called level index to evaluate translational and rotational manipulability. Lee and Kim [538] estimated the manipulability and resistivity of a planar parallel–serial manipulator by constructing the corresponding ellipsoids.

4.8.2. Static Performance

The static performance evaluation of a manipulator relates directly to its stiffness analysis. This analysis considers the deformations and displacements of the manipulator links under external loads, which is crucial for high-precision operations. Section 3.1 shows that the stiffness analysis of parallel–serial manipulators is the subject of many studies. Here, we mention typical techniques applied by scholars.

The first and probably most popular method is the analytical approach. The idea behind this method is to derive stiffness/compliance matrices of the links using elastic or beam models and then combine these matrices to obtain the resulting stiffness matrix of the whole manipulator. This matrix maps the applied load to the end-effector deformations and allows estimating the robot stiffness. The more detailed the considered models, the more accurate the obtained results, but the computation complexity increases as well. In search of a trade-off between model accuracy and complexity, scholars proposed different analytical approaches and applied them to various parallel–serial manipulators with three [415], four [249,322], five [92,97,129,188,196,200,201,206,213,225,329], six [61,85,286], seven [278], nine [254], and ten [260] DOFs.

The second, semi-analytical method aims to overcome the drawbacks of the preceding approach. In this method, the compliance matrices of the links are determined using computer-aided design. It offers more accurate and less computationally expensive results than elastic models. On the other hand, we have to recompute these compliance matrices if the link geometry changes, which is the main limitation of the semi-analytical approach. Nevertheless, variations of this method were successfully applied to stiffness analysis of parallel–serial manipulators with four [74], five [82,168,169], and six [38] DOFs; in particular, to the analysis of the 5-DOF TriMule robot [89,90,94–96].

Finally, finite element analysis (FEA) can also be used to evaluate the manipulator stiffness. Most works cited above used FEA to verify the results of analytical and semi-analytical methods. Papers [73,78,208,218,219] also illustrate the application of FEA to different parallel–serial manipulators.

4.8.3. Dynamic Performance

Similar to the metrics of kinematic performance that rely on Jacobian matrices, the metrics of dynamic performance are generally based on the manipulator mass matrix. Thus, scholars analyzed the so-called dynamic dexterity of parallel–serial manipulators by computing the condition number or singular values of the mass matrix [77,100,221,421,459,485]. Kong et al. [178] calculated the trace of this matrix and introduced the joint reflected inertia coefficient to evaluate the dynamic performance of a 5-DOF manipulator. A similar study was performed by Wang et al. [159], who analyzed the variations of components of the mass matrix and the gravity vector over the workspace. The authors of [98] defined an original performance index based on the gravity-center position and applied it to the analysis of

the TriMule robot. Finally, we mention studies [215,216] whose authors used dynamic equations to estimate the maximum driving forces.

4.9. Dimensional Synthesis

Dimensional synthesis, also known as optimal design, aims to determine the dimensions of the manipulator links, which are appropriate for a specific application. These dimensions are usually computed with an optimization procedure that tries to maximize or minimize some objective function [525].

Maximizing the volume of the manipulator workspace is probably the simplest formulation of the dimensional synthesis problem, which was considered in works [172,222,284]. Most other studies have defined the objective function using performance metrics discussed in the previous subsection. One conventional method here is to maximize the global conditioning index that reflects the kinematic performance of a manipulator. Scholars followed this approach to optimize the dimensions of hybrid robots with four [316,423] and five [60,64,79,181,312] DOFs. The authors of [58,73,84,449] also considered modified (weighed) variants of the conditioning index.

Transmission indices have also been used as objective functions in the dimensional synthesis problem. For example, Sun et al. [438] maximized these indices and optimized the geometry of an 8-DOF humanoid robotic arm. He et al. [279] studied the hierarchical optimization of a 5-DOF manipulator: first, the authors used transmission indices to evaluate the kinematic performance and optimized dimensional parameters; after that, the authors optimized structural parameters of the links to improve the stiffness performance. The stiffness criterion was also considered by Tang et al. [200]. The authors introduced a local dexterity index, which reflected both the dexterity and stiffness of the robot with no need to allocate weighting factors.

The studies mentioned above optimized the dimensions of the links by maximizing or minimizing a single performance metric. In other works, the authors performed a multi-objective optimization of robot geometry. For example, the authors of [67,70,494] combined workspace and dexterity criteria, while Xu et al. [474] considered the maximum workspace and load-bearing capacity. Zou et al. [29] solved the optimal design problem for a 4-DOF pick-and-place robot by maximizing the workspace volume and manipulability indices. Zhang et al. [207,208] optimized the geometry of another 4-DOF manipulator by considering different transmission indices, while Dong et al. [65] performed dimensional synthesis of TriMule by maximizing these indices and the ratio of the workspace volume to the robot footprint. In paper [91], the authors also considered this ratio and the lateral stiffness of the manipulator.

The stiffness criterion has often been combined with other performance metrics when solving the optimal design problem. Thus, Xu et al. [250] considered a weighed sum of the global stiffness index and workspace volume as an objective function. Li et al. [198] also included a comprehensive kinematic index based on the condition number. Paper [375] performed a similar analysis that combined a stiffness index with the condition number of the Jacobian matrix. Among other kinematic and static metrics considered with a stiffness index are transmission indices [173] and the total mass of a manipulator [387,392].

Dynamic performance indices have also been used together with other metrics in the dimensional synthesis of parallel–serial manipulators. For example, Li et al. [271] combined a dynamic dexterity index with a stiffness index, while Zhao et al. [100] considered these metrics and a global kinematic index. The authors of [221,486] optimized dynamic performance with workspace dimensions and other kinematic metrics. Finally, we mention the work of Zhang et al. [226], who performed a multi-objective optimization considering a workspace evaluation index, a transmission index, a stiffness index, a dexterity index, an energy efficiency index, and an inertia coupling index.

4.10. Control

The manipulator control system aims to reduce the error between the specified and actual trajectories of the end-effector. Scholars have proposed different techniques to solve this problem [539,540]. One of the most widely applied methods is to use P, PI, PD, or PID (proportional–integral–derivative) controllers to track the error of the actuators. Thus, Chen et al. [161] applied a PD controller for a 7-DOF manipulator, while Liu et al. [120] considered a cascade control scheme with P and PI controllers and feedforward speed compensation for TriMule. In paper [112], the authors modified this approach by collecting data from externally mounted encoder systems. Similar control schemes were used in studies [118,159]. Wang et al. [153–155] also applied cascade control with feedforward compensation to another hybrid machine tool, while Goubej and Švejda [400] proposed a cascade PID control for 7-DOF AGEBOT. Mohatna et al. [359] applied conventional PID controllers for a 3-DOF rehabilitation robot. Alfayad et al. [418] also implemented a PID controller but computed feedback signals using the end-effector motion and inverse kinematic models. Another example is the work of Qazani et al. [469], who combined PID and neural network controllers for the 6-DOF hybrid robot.

Feedback linearization (also known as inverse dynamics control or computed torque control) is another familiar control strategy that aims to compensate for the non-linear dynamics of a manipulator. Cheng [403] used this method and a PID controller to control the 10-DOF UPSarm manipulator. Wu et al. [268] applied similar techniques combined with a feedforward controller to suppress the chattering of 10-DOF IWR. Feedback linearization was also used together with a PID controller [363] and LQR [362] (linear quadratic regulator) to control 6-DOF CochleRob.

Sliding mode control represents one more method of non-linear control, which was applied to parallel–serial robots. Qin et al. [433,434] implemented it to control a 4-DOF humanoid manipulator, and Yang et al. [117] implemented sliding mode control for 5-DOF TriMule. Vasanthakumar et al. [360] combined this method with a non-linear disturbance observer. A similar technique was applied by Dong et al. [55], who developed an active disturbance rejection controller with an extended state observer and non-linear state error feedback and applied it to a polishing robot.

The end-effector of many parallel–serial manipulators touches a processed object, and it is often necessary to control the contact force. Thus, hybrid force/position control was applied to manipulators with six [393], seven [160], and ten [340] DOFs. Impedance (admittance) control is another well-known method of force control, which renders a viscoelastic contact model. Wang et al. [407] and He et al. [16] used this technique in a capturing experiment with a 7-DOF hybrid manipulator. In studies [172,175,252], the authors implemented different impedance controllers for polishing robots, while papers [320,335,355] used these control schemes in medical applications.

Fuzzy logic controllers have also been used in the control schemes of parallel–serial manipulators. The applications of these controllers include harvesting [411], fracture reduction [350], and motion simulators [471]. In papers [40,269], the authors used fuzzy logic to tune the gains of PID controllers. Finally, Li et al. [313] proposed a fuzzy variable admittance controller for a 5-DOF spine surgery robot.

4.11. Calibration

Geometrical and inertial parameters of a physical manipulator can differ from its mathematical model and their nominal values. This difference affects the motion accuracy of the manipulator end-effector, and the calibration aims to evaluate the real values of the parameters and compensate for the errors [541,542].

The literature review of parallel–serial robots has shown that scholars focused mainly on their kinematic calibration, i.e., on identifying geometrical parameters. Most proposed calibration techniques rely on the following concepts. First, the error model is derived, typically at the position level (using forward kinematics) or velocity level (using Jacobian matrices). Next, the end-effector configuration is estimated using external measurement

systems. Finally, an optimization procedure (e.g., the least squares method) updates the values of geometrical parameters until the measured data match the error model.

We found it convenient to classify the existing calibration studies by the applied measurement equipment. One of the most popular techniques for measuring the end-effector posture is to use a laser tracker. Pan et al. [170] applied it for the home position calibration of a 5-DOF machining robot. Zhao et al. [36,37] calibrated a 6-DOF polishing robot and derived the error model using screw theory and the POE formula. The latter was also used by Ye et al. [220,543], who performed a laser tracker calibration of a 5-DOF overconstrained hybrid manipulator and proposed a residual index for the optimization of measurement configurations [544]. He et al. [409] used a laser tracker and the concept of a kinematic equivalent limb to calibrate a 7-DOF manipulator for capturing space objects. Chen et al. [174] considered another kinematically redundant robot and established its error model separately for serial and parallel parts. The authors then identified geometrical parameters with a regularized least squares method. The same technique was applied by Tian et al. [108], who calibrated the TriMule robot and derived its error model using screw theory. There are other studies where scholars performed a laser tracker calibration of TriMule and used neural networks [111,113,137], an extended Kalman filter [115], and a linearized error model of the equivalent system [116]. Wang et al. [263,264] used a laser tracker and an MCMC (Markov Chain Monte Carlo) parameter identification method to calibrate 10-DOF IWR. In their other works, the authors used differential evolution when solving the optimization problem [265] and established the error model with the POE formula [266]. Finally, we mention the work of Moser et al. [545], who proposed a unified calibration approach for serial, parallel, and hybrid robots. The authors exemplified their method with a laser tracker calibration of a 7-DOF manipulator based on the Gough–Stewart platform.

Double ball-bar is another familiar measurement tool used for kinematic calibration. However, for some reason, scholars have rarely applied it to parallel–serial manipulators. Few examples include the calibration of Tricept [56], TriVariant [80], and Exechon [190] hybrid machine tools.

Coordinate measuring machines (CCMs) have also been applied to calibrate parallel–serial manipulators. Thus, Wang and Chen [20] attached a tooling ball to the end-effector of a 6-DOF hybrid positioning stage and used a CCM for its kinematic calibration. Nagao et al. [193,194] calibrated an Exechon-like robot with an articulated arm CCM. Another calibration technique with multiple dial indicators was performed by Huang et al. [24,157], who identified the parameters of a hybrid machine tool based on the Sprint Z3 architecture. The computations were based on a regularization approach, which was later developed into a modified singular value decomposition method [158]. Li et al. [149–152] continued these studies and used the concept of a virtual tool center point position constraint.

One more approach to kinematic calibration is to place a sensor on the end-effector itself. For example, Xu et al. [474] installed a three-axis gyroscope on the 3-DOF hybrid rotary platform and calibrated its parameters with the damped least squares method. Fan et al. [165] used a laser displacement sensor attached to the moving platform of a polishing robot. The authors then solved the optimization calibration problem with a genetic algorithm. Finally, Fu et al. [109,110] calibrated TriMule using a 3D-vision sensor placed on its end-effector. In a recent paper [114], the authors proposed an original self-calibration technique based on these vision measurements.

5. Discussion

Two previous sections presented diverse architectures and applications of parallel–serial manipulators and discussed various methods of their synthesis and analysis. The current section recaps the results of the performed review and mentions perspective directions for forthcoming studies.

5.1. Applications and Architectures

Figure 26 illustrates the distribution of the papers considered in Section 3 by year and application. We see machining applications of parallel–serial manipulators not only dominate the other ones but continue attracting scholars—the number of papers in this field increases with each year. Analysis of the last decade also shows the growth of studies devoted to humanoid robots and legged systems. At the same time, some novel applications of parallel–serial manipulators have appeared, including additive technologies and ocean wave compensation.

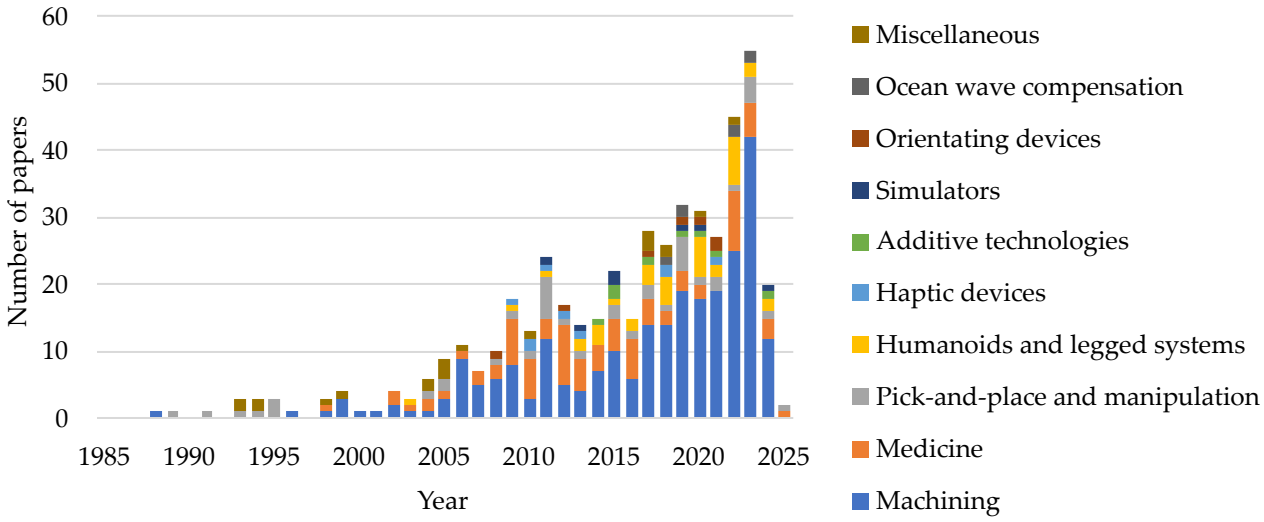

Figure 26. Distribution of applications of parallel–serial manipulators by year.

Table 1 lists the amount of architectures presented in Section 3 in Figures 5–25 and the applications where these architectures have been applied. To make the presentation more concise, we classified the manipulators by the motion type of their parallel part and the number of DOFs of the entire manipulator. Notation mTnR in the first column means the moving platform of the parallel mechanism has m translational and n rotational DOFs. In this table, 1T1R and 2T1R refer to 2- and 3-DOF planar motion; 2R and 3R refer to 2- and 3-DOF spherical motion; 1T2R combines various architectures, including hybrid manipulators based on Tricept, Sprint Z3, Exechon, and other parallel mechanisms whose moving platform has one translational and two rotational DOFs. Abbreviations used in the table cells are explained under the table. For example, the intersection of the "3T" row and the "4" column contains the "1MA" and "1PP" entries. It means there are two 4-DOF hybrid architectures based on 3-DOF translational parallel mechanisms: one for machining and the other for pick-and-place operations. This table ignores two manipulators considered in Section 3: (1) a 6-DOF manipulator with an R(1-RRUR/1-RRS)R architecture [388] (Figure 17k) where the motion type of the 4-DOF parallel mechanism does not meet any type in the first column; (2) a reconfigurable manipulator with a (2-RRRRR)RRRRRRR architecture [426] (Figure 19n) where the parallel mechanism can have from zero to five DOFs.

The table shows that 5-DOF parallel–serial manipulators dominate hybrid robots with other numbers of DOFs. This is reasonable because machining, which usually requires five DOFs, is the most widely considered application of parallel–serial manipulators. We also observe that most manipulators are based on 3-DOF parallel mechanisms. Such mechanisms prevail among other lower-DOF parallel mechanisms and often have a simple and symmetrical design, motivating their use in hybrid manipulators. Parallel mechanisms with two DOFs are the second most popular option. Scholars prefer planar mechanisms (1T1R and 2T) for machining and medicine robots and spherical mechanisms (2R) for medicine robots, humanoids, and legged systems.

Table 1. Amount of architectures of parallel–serial manipulators and their applications *.

Parallel Part Motion Type	Number of DOFs of a Parallel–Serial Manipulator										Total
	3	**4**	**5**	**6**	**7**	**8**	**9**	**10**	**11**	**12**	
1T	–	–	–	–	1ME	–	–	–	–	–	1
1R	–	–	–	1PP	–	–	–	–	–	–	1
1T1R	1MA 1ME 1MS	1MA	4MA 5ME	–	–	–	1ME	1PP	–	–	15
2T	–	1PP	1ME	–	–	–	–	–	–	–	2
2R	4HL 2OD	3ME 3HL 1SM	1MA 3ME 1MS	1MA 1ME 1HL	1PP 1HL	1HL	–	–	–	–	24
1T2R	–	3MA 2ME 1HL 1OD	27MA 2ME 1PP	4MA 1OD 2OW 2MS	3MA 1ME 3PP 1MS	–	1MA 1ME 1PP	1PP	–	–	58
2T1R	–	1PP 1MS	1MA 1PP 1AT 1MS	1MA 1PP	–	–	–	–	–	–	8
3T	–	1MA 1PP	2MA 1ME 1PP 2AT	1ME 2PP 2HD 1AT 1SM	1ME	1MA	1MA	–	–	–	18
3R	1ME	1HL	1HL	2ME 1HD	1PP	–	–	–	–	–	7
1T3R	–	–	–	–	1MA 1SM	–	–	–	–	–	2
2T2R	–	–	3MA	2ME 1MS	–	–	–	–	–	–	6
3T1R	–	–	–	–	1ME	–	–	–	–	–	1
3T2R	–	–	–	–	1MA	–	–	–	–	–	1
3T3R	–	–	–	–	1MA 1ME 1SM	1PP	1ME 1PP 1SM 1OW 2MS	1MA 1ME	1ME	1MA 1ME	15
Total	10	21	59	31	18	3	11	4	1	3	159

* Applications: MA—machining, ME—medicine, PP—pick-and-place, HL—humanoids and legged systems, HD—haptic devices, AT—additive technologies, SM—simulators, OD—orienting devices, OW—ocean wave compensation, MS—miscellaneous.

5.2. Design and Analysis

Figure 27 shows what has been the subject of scholars' studies devoted to parallel–serial manipulators throughout the years. We analyzed the papers considered in Section 4 and grouped closely related topics. In the figure, "kinematics" includes position, velocity, singularity, and workspace analysis, while "optimal design" includes performance evaluation and dimensional synthesis. We also combined type synthesis and mobility, as they often come together.

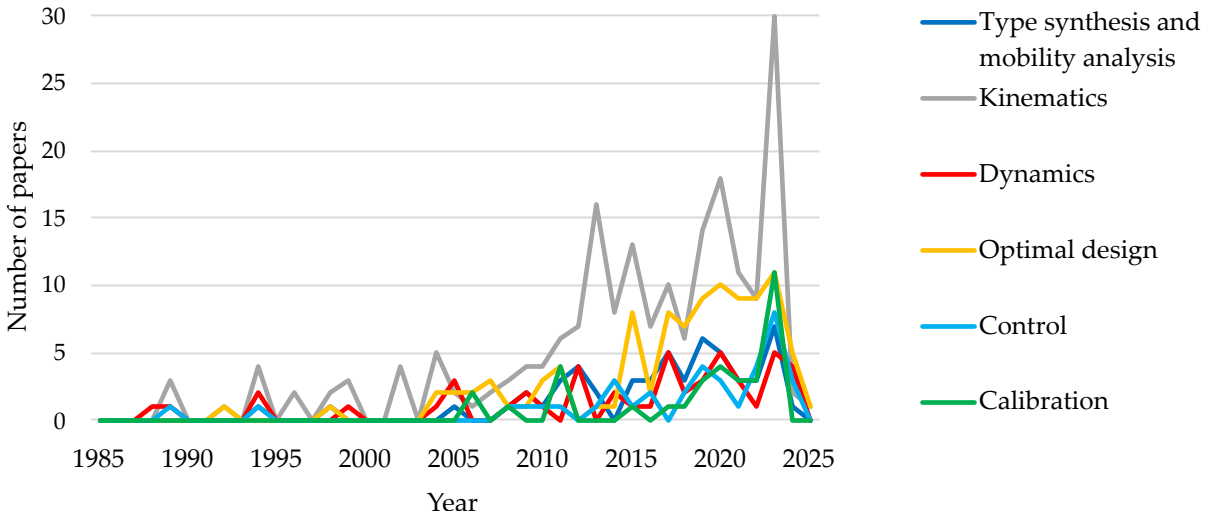

Figure 27. Distribution of research topics of parallel–serial manipulators by year.

As expected, kinematics dominates other research topics because it represents the foundation for all subsequent stages of design and analysis. At the same time, we observe the growing number of papers devoted to optimal design, calibration, and control. These topics relate directly to the practical applications of parallel–serial manipulators, indicating their widespread use in the last decade. The number of papers devoted to the type synthesis and mobility analysis is growing, too. We can explain it by the fact that screw theory and group theory, the two most powerful methods used to solve these problems [506], have become standard tools in mechanism and machine theory and robotics. This allows scholars to obtain appropriate architectures of hybrid robots in the first step of their development.

5.3. Perspectives

The review showed that the number of studies devoted to parallel–serial manipulators is growing, and these manipulators have become more popular in recent years. In this regard, we believe they will continue attracting scholars. Below are some research topics that seem promising for future investigations:

- *New applications of parallel–serial manipulators.* Although machining remains the most popular application of hybrid robots, some novel applications have appeared in the last decade, such as ocean wave engineering, additive technologies, or medicine operations considered in this review. We believe parallel–serial manipulators will find other applications in the near future as well.
- *New architectures of parallel–serial manipulators.* The diversity of architectures presented in this review indicates that scholars continue developing new manipulators in search of the best design. At the same time, most hybrid robots rely on parallel mechanisms with two or three DOFs and typical motion types, while 6-DOF parallel mechanisms in kinematically redundant systems are represented just by the Gough–Stewart platform. It looks attractive and promising to study hybrid robots where parallel mechanisms have four or five DOFs, non-typical motion types, and reconfigurable design.
- *Comprehensive methods of design and analysis.* Despite a large number of studies devoted to parallel–serial manipulators, many works focus on the design and analysis of only the parallel part. In particular, papers devoted to type synthesis, singularity analysis, performance evaluation, and dimensional synthesis of hybrid robots usually concentrate on the parallel mechanism and ignore the serial chain. Developing integrated methods that will analyze the full parallel–serial architecture also appears promising for future studies.

6. Conclusions

This review justified the broad dissemination of parallel–serial (hybrid) manipulators in diverse applications, including machining, medicine, and pick-and-place operations, as well as more exotic applications like ocean wave compensation, additive technologies, and climbing robotic systems. We used Scopus and Google Scholar databases and analyzed 510 papers devoted to hybrid robots. The paper presented 161 architectures of these robots and discussed the methods of their type synthesis, mobility, kinematic, and dynamic analysis, optimal design, control, and calibration. As research interest in parallel–serial manipulators continues to grow, we believe there will be new achievements in this field and new architectures and applications of these robotic systems.

Funding: This research was supported by Russian Science Foundation (RSF) under grant No. 22-79-10304, https://rscf.ru/en/project/22-79-10304/ (accessed on 10 November 2024).

Data Availability Statement: The presented data are available on request from the author.

Conflicts of Interest: The author declares that he has no conflicts of interest.

References

1. Ye, W.; Tang, T.; Li, Q. Robotized manufacturing equipment: A review from the perspective of mechanism topology. *Sci. China Technol. Sci.* **2023**, *66*, 1683–1697. [CrossRef]
2. 500 Peters, B.S.; Armijo, P.R.; Krause, C.; Choudhury, S.A.; Oleynikov, D. Review of emerging surgical robotic technology. *Surg. Endosc.* **2018**, *32*, 1636–1655. [CrossRef]
3. Gonzalez-Aguirre, J.A.; Osorio-Oliveros, R.; Rodríguez-Hernández, K.L.; Lizárraga-Iturralde, J.; Morales Menendez, R.; Ramírez-Mendoza, R.A.; Ramírez-Moreno, M.A.; Lozoya-Santos, J.J. Service robots: Trends and technology. *Appl. Sci.* **2021**, *11*, 10702. [CrossRef]
4. Flores-Abad, A.; Ma, O.; Pham, K.; Ulrich, S. A review of space robotics technologies for on-orbit servicing. *Prog. Aerosp. Sci.* **2014**, *68*, 1–26. [CrossRef]
5. Sivčev, S.; Coleman, J.; Omerdić, E.; Dooly, G.; Toal, D. Underwater manipulators: A review. *Ocean Eng.* **2018**, *163*, 431–450. [CrossRef]
6. Ceccarelli, M. *Fundamentals of Mechanics of Robotic Manipulation*, 2nd ed.; Springer: Cham, Switzerland, 2022. [CrossRef]
7. Bi, Z.M.; Lin, Y.; Zhang, W.J. The general architecture of adaptive robotic systems for manufacturing applications. *Robot. Comput. Integr. Manuf.* **2010**, *26*, 461–470. [CrossRef]
8. Karupusamy, S.; Maruthachalam, S.; Veerasamy, B. Kinematic modeling and performance analysis of a 5-DoF robot for welding applications. *Machines* **2024**, *12*, 378. [CrossRef]
9. Borrell, J.; Perez-Vidal, C.; Segura, J.V. Optimization of the pick-and-place sequence of a bimanual collaborative robot in an industrial production line. *Int. J. Adv. Manuf. Technol.* **2024**, *130*, 4221–4234. [CrossRef]
10. Zhu, Z.; Hu, H. Robot learning from demonstration in robotic assembly: A survey. *Robotics* **2018**, *7*, 17. [CrossRef]
11. Russo, M.; Zhang, D.; Liu, X.J.; Xie, Z. A review of parallel kinematic machine tools: Design, modeling, and applications. *Int. J. Mach. Tools Manuf.* **2024**, *196*, 104118. [CrossRef]
12. Huang, X.; Rendon-Morales, E.; Aviles-Espinosa, R. ROMI: Design and experimental evaluation of a linear Delta robotic system for high-precision applications. *Machines* **2023**, *11*, 1072. [CrossRef]
13. Müller, A.; Zlatanov, D. (Eds.) *Singular Configurations of Mechanisms and Manipulators*; Springer: Cham, Switzerland, 2019. [CrossRef]
14. Liu, Q.; Liu, H.; Xiao, J.; Tian, W.; Ma, Y.; Li, B. Open-architecture of CNC system and mirror milling technology for a 5-axis hybrid robot. *Robot. Comput. Integr. Manuf.* **2023**, *81*, 102504. [CrossRef]
15. Tao, B.; Feng, Y.; Fan, X.; Lan, K.; Zhuang, M.; Wang, S.; Wang, F.; Chen, X.; Wu, Y. The accuracy of a novel image-guided hybrid robotic system for dental implant placement: An in vitro study. *Int. J. Med. Rob. Comput. Assist. Surg.* **2023**, *19*, e2452. [CrossRef]
16. He, J.; Zheng, H.; Gao, F.; Zhang, H. Dynamics and control of a 7-DOF hybrid manipulator for capturing a non-cooperative target in space. *Mech. Mach. Theory* **2019**, *140*, 83–103. [CrossRef]
17. Nayak, A.; Caro, S.; Wenger, P. Kinematic analysis of the 3-RPS-3-SPR series–parallel manipulator. *Robotica* **2019**, *37*, 1240–1266. [CrossRef]
18. Gallardo-Alvarado, J. Unified infinitesimal kinematics of a 3-RRR/PRR six-degree-of-freedom parallel-serial manipulator. *Meccanica* **2023**, *58*, 795–811. [CrossRef]
19. Elsamanty, M.; Faidallah, E.M.; Hossameldin, Y.H.; Abd Rabbo, S.M.; Maged, S.A. Design, simulation, and kinematics of 9-DOF serial-parallel hybrid manipulator robot. In Proceedings of the 2021 3rd Novel Intelligent and Leading Emerging Sciences Conference, Giza, Egypt, 23–25 October 2021; pp. 370–375. [CrossRef]
20. Wang, F.S.; Chen, S.L. Geometric error measurement and compensation of a six-degree-of-freedom hybrid positioning stage. *Proc. Inst. Mech. Eng. Part B J. Eng. Manuf.* **2008**, *222*, 185–200. [CrossRef]

21. Fajardo-Pruna, M.; López-Estrada, L.; Pérez, H.; Diez, E.; Vizán, A. Analysis of a single-edge micro cutting process in a hybrid parallel-serial machine tool. *Int. J. Mech. Sci.* **2019**, *151*, 222–235. [CrossRef]
22. Klimchik, A.; Pashkevich, A. Serial vs. quasi-serial manipulators: Comparison analysis of elasto-static behaviors. *Mech. Mach. Theory* **2017**, *107*, 46–70. [CrossRef]
23. Zeng, Q.; Fang, Y. Structural synthesis and analysis of serial–parallel hybrid mechanisms with spatial multi-loop kinematic chains. *Mech. Mach. Theory* **2012**, *49*, 198–215. [CrossRef]
24. Huang, P.; Wang, J.; Wang, L.; Yao, R. Kinematical calibration of a hybrid machine tool with regularization method. *Int. J. Mach. Tools Manuf.* **2011**, *51*, 210–220. [CrossRef]
25. Chong, Z.; Xie, F.; Liu, X.J.; Wang, J.; Niu, H. Design of the parallel mechanism for a hybrid mobile robot in wind turbine blades polishing. *Robot. Comput. Integr. Manuf.* **2020**, *61*, 101857. [CrossRef]
26. Sun, P.; Li, Y.B.; Wang, Z.S.; Chen, K.; Chen, B.; Zeng, X.; Zhao, J.; Yue, Y. Inverse displacement analysis of a novel hybrid humanoid robotic arm. *Mech. Mach. Theory* **2020**, *147*, 103743. [CrossRef]
27. Singh, A.; Singla, A.; Soni, S. D-H parameters augmented with dummy frames for serial manipulators containing spatial links. In Proceedings of the 23rd IEEE International Symposium on Robot and Human Interactive Communication, Edinburgh, UK, 25–29 August 2014; pp. 975–980. [CrossRef]
28. Li, Q.; Fucai, L.; Lihuan, L. A novel hybrid humanoid dextrous manipulator for on-orbit servicing and its kinematics analysis. In Proceedings of the 2013 Third International Conference on Instrumentation, Measurement, Computer, Communication and Control, Shenyang, China, 21–23 September 2013; pp. 432–437. [CrossRef]
29. Zou, Q.; Zhang, D.; Huang, G. Kinematic models and the performance level index of a picking-and-placing hybrid robot. *Machines* **2023**, *11*, 979. [CrossRef]
30. Abarca, V.E.; Elias, D.A. A review of parallel robots: Rehabilitation, assistance, and humanoid applications for neck, shoulder, wrist, hip, and ankle joints. *Robotics* **2023**, *12*, 131. [CrossRef]
31. Kumar, S.; Wöhrle, H.; de Gea Fernández, J.; Müller, A.; Kirchner, F. A survey on modularity and distributivity in series-parallel hybrid robots. *Mechatronics* **2020**, *68*, 102367. [CrossRef]
32. Neumann, K.E. Robot. US Patent 4,732,525, 22 March 1988.
33. Thornton, G.S. The GEC Tetrabot—A new serial-parallel assembly robot. In Proceedings of the 1988 IEEE International Conference on Robotics and Automation, Philadelphia, PA, USA, 24–29 April 1988; pp. 437–439. [CrossRef]
34. Choi, B.O.; Lee, M.K. Development of a hybrid robot arm for propeller grinding. In *Intelligent Robots and Computer Vision XV: Algorithms, Techniques, Active Vision, and Materials Handling*; Casasent, D.P., Ed.; SPIE: Bellingham, WA, USA, 1996; pp. 517–527. [CrossRef]
35. Lee, M.K.; Park, K.W.; Choi, B.O. Kinematic and dynamic models of hybrid robot manipulator for propeller grinding. *J. Robot. Syst.* **1999**, *16*, 137–150. [CrossRef]
36. Zhao, D.; Dong, C.; Guo, H.; Tian, W. Kinematic calibration based on the multicollinearity diagnosis of a 6-DOF polishing hybrid robot using a laser tracker. *Math. Probl. Eng.* **2018**, *2018*, 5602397. [CrossRef]
37. Huang, T.; Zhao, D.; Yin, F.; Tian, W.; Chetwynd, D.G. Kinematic calibration of a 6-DOF hybrid robot by considering multi-collinearity in the identification Jacobian. *Mech. Mach. Theory* **2019**, *131*, 371–384. [CrossRef]
38. Ma, Y.; Liu, H.; Zhang, M.; Li, B.; Liu, Q.; Dong, C. Elasto-dynamic performance evaluation of a 6-DOF hybrid polishing robot based on kinematic modeling and CAE technology. *Mech. Mach. Theory* **2022**, *176*, 104983. [CrossRef]
39. Tian, W.; Xu, M.; Zhang, X.; Guo, X.; Wang, L.; Huang, T. Repeatability prediction of 6-DOF hybrid robot based on equivalent error model of actuated joint. *Measurement* **2023**, *207*, 112377. [CrossRef]
40. Han, J.; Shan, X.; Liu, H.; Xiao, J.; Huang, T. Fuzzy gain scheduling PID control of a hybrid robot based on dynamic characteristics. *Mech. Mach. Theory* **2023**, *184*, 105283. [CrossRef]
41. Han, J.; Cheng, H.; Shan, X.; Liu, H.; Xiao, J.; Huang, T. A novel multi-pulse friction compensation strategy for hybrid robots. *Mech. Mach. Theory* **2024**, *201*, 105726. [CrossRef]
42. Olazagoitia, J.L.; Wyatt, S. New PKM Tricept T9000 and its application to flexible manufacturing at aerospace industry. In Proceedings of the AeroTech Congress & Exhibition, Los Angeles, CA, USA, 17–20 September 2007; p. 2007-01-3820.
43. Siciliano, B. A study on the kinematics of a class of parallel manipulators. In *Advances in Robot Kinematics: Analysis and Control*; Lenarčič, J., Husty, M.L., Eds.; Springer: Dordrecht, The Netherlands, 1998; pp. 29–38. [CrossRef]
44. Siciliano, B. The Tricept robot: Inverse kinematics, manipulability analysis and closed-loop direct kinematics algorithm. *Robotica* **1999**, *17*, 437–445. [CrossRef]
45. Milutinović, M.; Slavković, N.; Milutinović, D. Kinematic modelling of hybrid parallel-serial five-axis machine tool. *FME Trans.* **2013**, *41*, 1–10.
46. Eastwood, S.; Webb, P. Compensation of thermal deformation of a hybrid parallel kinematic machine. *Robot. Comput. Integr. Manuf.* **2009**, *25*, 81–90. [CrossRef]
47. Callegari, M.; Gabrielli, A.; Palpacelli, M.C.; Principi, M. Robotised cell for the incremental forming of metal sheets. In Proceedings of the ASME 8th Biennial Conference on Engineering Systems Design and Analysis, Torino, Italy, 4–7 July 2006; Volume 1, pp. 749–756. [CrossRef]
48. Callegari, M.; Gabrielli, A.; Palpacelli, M.C.; Principi, M. Incremental forming of sheet metal by means of parallel kinematics machines. *J. Manuf. Sci. Eng.* **2008**, *130*, 054501. [CrossRef]

49. Callegari, M.; Forcellese, A.; Palpacelli, M.; Simoncini, M. Robotic friction stir welding of AA5754 aluminum alloy sheets at different initial temper states. *Key Eng. Mater.* **2014**, *622-623*, 540–547. [CrossRef]
50. Palpacelli, M.; Callegari, M.; Carbonari, L.; Palmieri, G. Theoretical and experimental analysis of a hybrid industrial robot used for friction stir welding. *Int. J. Mechatron. Manuf. Syst.* **2015**, *8*, 258. [CrossRef]
51. Dong, C.; Liu, H.; Huang, T.; Chetwynd, D.G. A lumped model for dynamic behavior prediction of a hybrid robot for optical polishing. In *Advances in Mechanism and Machine Science*; Uhl, T., Ed.; Springer: Cham, Switzerland, 2019; pp. 2007–2016. [CrossRef]
52. Dong, C.; Liu, H.; Huang, T.; Chetwynd, D.G. A screw theory-based semi-analytical approach for elastodynamics of the Tricept robot. *J. Mech. Robot.* **2019**, *11*, 031005. [CrossRef]
53. Jin, Z.; Cheng, G.; Chen, S.; Guo, F. Human-machine-environment information fusion and control compensation strategy for large optical mirror processing system. *Proc. Inst. Mech. Eng. Part C J. Mech. Eng. Sci.* **2021**, *235*, 2507–2523. [CrossRef]
54. Jin, Z.; Cheng, G.; Xu, S.; Yuan, D. Error prediction for large optical mirror processing robot based on deep learning. *Strojniški Vestn.-J. Mech. Eng.* **2022**, *68*, 175–184. [CrossRef]
55. Dong, K.; Li, J.; Lv, M.; Li, X.; Gu, W.; Cheng, G. Active disturbance rejection control algorithm for the driven branch chain of a polishing robot. *Strojniški Vestn.-J. Mech. Eng.* **2023**, *69*, 509–521. [CrossRef]
56. Kim, J.W.; Shin, C.R.; Kim, H.S.; Kyung, J.H.; Ha, Y.H.; Yu, H.S. Error model and kinematic calibration of a 5-axis hybrid machine tool. In Proceedings of the 2006 SICE-ICASE International Joint Conference, Busan, Republic of Korea, 18–21 October 2006; pp. 3111–3115. [CrossRef]
57. Tönshoff, H.K.; Grendel, H.; Kaak, R. Structure and characteristics of the hybrid manipulator Georg V. In *Parallel Kinematic Machines*; Boër, C., Molinari-Tosatti, L., Smith, K., Eds.; Springer: London, UK, 1999; pp. 365–376. [CrossRef]
58. Li, M.; Huang, T.; Zhang, D.; Zhao, X.; Hu, S.J.; Chetwynd, D.G. Conceptual design and dimensional synthesis of a reconfigurable hybrid robot. *J. Manuf. Sci. Eng.* **2005**, *127*, 647–653. [CrossRef]
59. Huang, T.; Li, M.; Zhao, X.M.; Mei, J.P.; Chetwynd, D.G.; Hu, S.J. Conceptual design and dimensional synthesis for a 3-DOF module of the TriVariant—A novel 5-DOF reconfigurable hybrid robot. *IEEE Trans. Robot.* **2005**, *21*, 449–456. [CrossRef]
60. Liu, H.; Huang, T.; Mei, J.; Zhao, X.; Chetwynd, D.G.; Li, M.; Hu, S.J. Kinematic design of a 5-DOF hybrid robot with large workspace/limb–stroke ratio. *J. Mech. Des.* **2007**, *129*, 530–537. [CrossRef]
61. Sun, T.; Song, Y.; Li, Y.; Zhang, J. Stiffness estimation for the 4-DOF hybrid module of a novel reconfigurable robot. In Proceedings of the 2009 ASME/IFToMM International Conference on Reconfigurable Mechanisms and Robots, London, UK, 22–24 June 2009; pp. 565–571.
62. Dong, C.; Liu, H.; Liu, Q.; Sun, T.; Huang, T.; Chetwynd, D.G. An approach for type synthesis of overconstrained 1T2R parallel mechanisms. In *Computational Kinematics*; Zeghloul, S., Romdhane, L., Laribi, M.E., Eds.; Springer: Cham, Switzerland, 2018; pp. 274–281. [CrossRef]
63. Wang, M.; Li, L.; Li, Z.; Liu, H.; Huang, T. Topological structure synthesis and optimization of 1T2R parallel mechanisms. *China Mech. Eng.* **2022**, *33*, 2395–2402. [CrossRef]
64. Li, J.; Dong, C.; Huang, S.; Zhao, H.; Shan, X.; Liu, H. Kinematic analysis and dimensional synthesis of a novel 3-DOF parallel mechanism. In *Advances in Mechanism and Machine Science*; Uhl, T., Ed.; Springer: Cham, Switzerland, 2019; pp. 1751–1760. [CrossRef]
65. Dong, C.; Liu, H.; Yang, J. Dimensional synthesis of a novel asymmetric 5-DOF hybrid robot. *China Mech. Eng.* **2021**, *32*, 2418–2426. [CrossRef]
66. Liu, X.; Wan, B.; Wang, Y.; Li, M.; Zhao, Y. Design, analysis and performance optimization of a novel super-redundantly actuated hybrid robot. *J. Mech. Eng.* **2024**, *60*, 55–67. [CrossRef]
67. Luo, J.; Wang, D.; Jiang, Y. Geometry optimization of a new hybrid robot manipulator. In Proceedings of the 2011 IEEE International Conference on Mechatronics and Automation, Beijing, China, 7–10 August 2011; pp. 881–886. [CrossRef]
68. Shan, Y.; He, N.; Li, L.; Yang, Y. Realization of spindle prompt normal posture alignment for assembly holemaking on large suspended panel. In Proceedings of the 2011 Third International Conference on Measuring Technology and Mechatronics Automation, Shanghai, China, 6–7 January 2011; Volume 2, pp. 956–960. [CrossRef]
69. Ganiev, R.F.; Glazunov, V.A.; Filippov, G.S. Urgent problems of machine science and ways of solving them: Wave and additive technologies, the machine tool industry, and robot surgery. *J. Mach. Manuf. Reliab.* **2018**, *47*, 399–406. [CrossRef]
70. Park, K.W.; Kim, T.S.; Lee, M.K.; Kyung, J.H. Study on kinematic optimization of a combined parallel-serial manipulator. In Proceedings of the 2006 SICE-ICASE International Joint Conference, Busan, Republic of Korea, 18–21 October 2006; pp. 1212–1216. [CrossRef]
71. Kyung, J.H.; Han, H.S.; Park, C.H.; Ha, Y.H.; Park, J.H. Dynamics of a hybrid serial-parallel robot for multi-tasking machining processes. In Proceedings of the 2006 SICE-ICASE International Joint Conference, Busan, Republic of Korea, 18–21 October 2006; pp. 3026–3030. [CrossRef]
72. Kyung, J.H.; Park, J.H.; Yu, H.S.; Han, H.S. Specification of driving constraints for dynamics simulation of a parallel-serial manipulator. In Proceedings of the 2007 International Conference on Control, Automation and Systems, Seoul, Republic of Korea, 17–20 October 2007; pp. 2283–2287. [CrossRef]
73. Huang, T.; Wang, P.F.; Zhao, X.M.; Chetwynd, D.G. Design of a 4-DOF hybrid PKM module for large structural component assembly. *CIRP Ann.* **2010**, *59*, 159–162. [CrossRef]

74. Wang, M.; Wang, P.; Song, Y.; Zhao, X.; Huang, T. Stiffness analysis of a 4-DOF hybrid robot. *J. Mech. Eng.* **2011**, *47*, 9–16. [CrossRef]
75. Li, M.; Huang, T.; Chetwynd, D.G.; Hu, S.J. Forward position analysis of the 3-DOF module of the TriVariant: A 5-DOF reconfigurable hybrid robot. *J. Mech. Des.* **2006**, *128*, 319–322. [CrossRef]
76. Bulej, V.; Uríček, J.; Poppeova, V.; Zahoranský, R.; Rupikova, M. Study of the workspace of hybrid mechanism Trivariant. *Appl. Mech. Mater.* **2013**, *436*, 366–373. [CrossRef]
77. Li, M.; Huang, T.; Mei, J.; Zhao, X.; Chetwynd, D.G.; Hu, S.J. Dynamic formulation and performance comparison of the 3-DOF modules of two reconfigurable PKM—The Tricept and the Trivariant. *J. Mech. Des.* **2005**, *127*, 1129–1136. [CrossRef]
78. Wang, Y.Y.; Huang, T.; Zhao, X.M.; Mei, J.P.; Chetwynd, D.G.; Hu, S.J. Finite element analysis and comparison of two hybrid robots—The Tricept and the TriVariant. In Proceedings of the 2006 IEEE/RSJ International Conference on Intelligent Robots and Systems, Beijing, China, 9–15 October 2006; pp. 490–495. [CrossRef]
79. Liu, H.T.; Huang, T.; Zhao, X.M.; Mei, J.P.; Chetwynd, D.G. Optimal design of the TriVariant robot to achieve a nearly axial symmetry of kinematic performance. *Mech. Mach. Theory* **2007**, *42*, 1643–1652. [CrossRef]
80. Huang, T.; Hong, Z.Y.; Mei, J.P.; Chetwynd, D.G. Kinematic calibration of the 3-DOF module of a 5-DOF reconfigurable hybrid robot using a double-ball-bar system. In Proceedings of the 2006 IEEE/RSJ International Conference on Intelligent Robots and Systems, Beijing, China, 9–15 October 2006; pp. 508–512. [CrossRef]
81. Liu, H.; Mei, J.; Zhao, X.; Huang, T.; Chetwynd, D.G. Inverse dynamics and servomotor parameter estimation of a 2-DOF spherical parallel mechanism. *Sci. China Ser. E Technol. Sci.* **2008**, *51*, 288–301. [CrossRef]
82. Wang, Y.; Huang, T.; Zhao, X.; Mei, J.; Chetwynd, D.G. A semi-analytical approach for stiffness modeling of PKM by considering compliance of machine frame with complex geometry. *Chin. Sci. Bull.* **2008**, *53*, 2565–2574. [CrossRef]
83. Sun, T.; Song, Y. Comparison between a 4-DOF hybrid module and Tricept module focusing on inverse kinematics and stiffness. In Proceedings of the 2009 IEEE International Conference on Robotics and Biomimetics, Guilin, China, 19–23 December 2009; pp. 1597–1602. [CrossRef]
84. Sun, T.; Song, Y.; Li, Y.; Zhang, J. Workspace decomposition based dimensional synthesis of a novel hybrid reconfigurable robot. *J. Mech. Robot.* **2010**, *2*, 031009. [CrossRef]
85. Sun, T.; Wu, H.; Lian, B.; Qi, Y.; Wang, P.; Song, Y. Stiffness modeling, analysis and evaluation of a 5 degree of freedom hybrid manipulator for friction stir welding. *Proc. Inst. Mech. Eng. Part C J. Mech. Eng. Sci.* **2017**, *231*, 4441–4456. [CrossRef]
86. Huang, T.; Dong, C.; Liu, H.; Sun, T.; Chetwynd, D.G. A simple and visually orientated approach for type synthesis of overconstrained 1T2R parallel mechanisms. *Robotica* **2019**, *37*, 1161–1173. [CrossRef]
87. Liu, Q.; Huang, T. Inverse kinematics of a 5-axis hybrid robot with non-singular tool path generation. *Robot. Comput. Integr. Manuf.* **2019**, *56*, 140–148. [CrossRef]
88. Liu, Q.; Tian, W.; Li, B.; Ma, Y. Kinematics of a 5-axis hybrid robot near singular configurations. *Robot. Comput. Integr. Manuf.* **2022**, *75*, 102294. [CrossRef]
89. Ma, Y.; Zhang, J.; Dong, C.; Liu, H.; Shan, X. Kinetostatic modelling and gravity compensation of the TriMule robot. In *Advances in Mechanism and Machine Science*; Uhl, T., Ed.; Springer: Cham, Switzerland, 2019; pp. 1731–1740. [CrossRef]
90. Wu, L.; Dong, C.; Wang, G.; Liu, H.; Huang, T. An approach to predict lower-order dynamic behaviors of a 5-DOF hybrid robot using a minimum set of generalized coordinates. *Robot. Comput. Integr. Manuf.* **2021**, *67*, 102024. [CrossRef]
91. Dong, C.; Liu, H.; Xiao, J.; Huang, T. Dynamic modeling and design of a 5-DOF hybrid robot for machining. *Mech. Mach. Theory* **2021**, *165*, 104438. [CrossRef]
92. Yue, W.; Liu, H.; Meng, S.; Bai, Y.; Li, G.; Song, Y. Kinetostatic modeling of a 5-DOF hybrid robot considering the gravitational effect. In *Advances in Mechanism and Machine Science*; Okada, M., Ed.; Springer: Cham, Switzerland, 2023; Volume 1, pp. 249–258. [CrossRef]
93. Liu, Q.; Yan, T.; Li, B.; Ma, Y. Dynamic formulation and inertia fast estimation of a 5-DOF hybrid robot. *Sci. Rep.* **2024**, *14*, 17252. [CrossRef]
94. Wu, L.; Wang, G.; Liu, H.; Huang, T. An approach for elastodynamic modeling of hybrid robots based on substructure synthesis technique. *Mech. Mach. Theory* **2018**, *123*, 124–136. [CrossRef]
95. Dong, C.; Liu, H.; Yue, W.; Huang, T. Stiffness modeling and analysis of a novel 5-DOF hybrid robot. *Mech. Mach. Theory* **2018**, *125*, 80–93. [CrossRef]
96. Zhao, Y.; Wang, C.; Niu, W.; Mei, Z. Stiffness modeling and analysis of a 3-DOF parallel kinematic machine. In *Advances in Mechanism and Machine Science*; Uhl, T., Ed.; Springer: Cham, Switzerland, 2019; pp. 2955–2964.
97. Shi, M.; Li, H.; Li, S.; Qin, X.; Liu, H. A rapid prediction method for the stiffness and the machining accuracy evaluation of a parallel kinematic mechanism. *J. Mech. Sci. Technol.* **2023**, *37*, 5965–5978. [CrossRef]
98. Wang, C.; Su, F.; Zhao, Y.; Liu, H.; Guo, Y.; Niu, W. A rapid performance evaluation approach for lower mobility hybrid robot based on gravity-center position. *Sci. Prog.* **2020**, *103*, 0036850420927135. [CrossRef]
99. Zhao, Y.; Mei, J.; Niu, W.; Wu, M.; Zhang, F. Coupling analysis of a 5-degree-of-freedom hybrid manipulator based on a global index. *Sci. Prog.* **2020**, *103*, 1–21. [CrossRef] [PubMed]
100. Zhao, Y.; Mei, J.; Jin, Y.; Niu, W. A new hierarchical approach for the optimal design of a 5-dof hybrid serial-parallel kinematic machine. *Mech. Mach. Theory* **2021**, *156*, 104160. [CrossRef]

101. Zhao, Y.; Mei, J.; Niu, W. Vibration error-based trajectory planning of a 5-dof hybrid machine tool. *Robot. Comput. Integr. Manuf.* **2021**, *69*, 102095. [CrossRef]
102. Li, G.; Liu, H.; Liu, S.; Xiao, J. A general C^2 continuous toolpath corner smoothing method for a 5-DOF hybrid robot. *Mech. Mach. Theory* **2022**, *169*, 104640. [CrossRef]
103. Liu, H.; Li, G.; Xiao, J. A C^3 continuous toolpath corner smoothing method for a hybrid machining robot. *J. Manuf. Process.* **2022**, *75*, 1072–1088. [CrossRef]
104. Li, G.; Liu, H.; Huang, T.; Han, J.; Xiao, J. An effective approach for non-singular trajectory generation of a 5-DOF hybrid machining robot. *Robot. Comput. Integr. Manuf.* **2023**, *80*, 102477. [CrossRef]
105. Li, G.; Liu, H.; Yue, W.; Xiao, J. Feedrate scheduling of a five-axis hybrid robot for milling considering drive constraints. *Int. J. Adv. Manuf. Technol.* **2021**, *112*, 3117–3136. [CrossRef]
106. Xiao, J.; Liu, S.; Liu, H.; Wang, M.; Li, G.; Wang, Y. A jerk-limited heuristic feedrate scheduling method based on particle swarm optimization for a 5-DOF hybrid robot. *Robot. Comput. Integr. Manuf.* **2022**, *78*, 102396. [CrossRef]
107. Li, G.; Liu, H.; Yue, W. Trajectory scheduling for a five-axis hybrid robot in flank milling of the S-shaped test piece. In *Advances in Mechanism, Machine Science and Engineering in China*; Liu, X., Ed.; Springer: Singapore, 2023; pp. 1713–1725. [CrossRef]
108. Tian, W.; Mou, M.; Yang, J.; Yin, F. Kinematic calibration of a 5-DOF hybrid kinematic machine tool by considering the ill-posed identification problem using regularisation method. *Robot. Comput. Integr. Manuf.* **2019**, *60*, 49–62. [CrossRef]
109. Fu, J.; Ding, Y.; Huang, T.; Liu, X. Hand-eye calibration method with a three-dimensional-vision sensor considering the rotation parameters of the robot pose. *Int. J. Adv. Rob. Syst.* **2020**, *17*, 172988142097729. [CrossRef]
110. Fu, J.; Ding, Y.; Huang, T.; Liu, H.; Liu, X. Hand–eye calibration method based on three-dimensional visual measurement in robotic high-precision machining. *Int. J. Adv. Manuf. Technol.* **2022**, *119*, 3845–3856. [CrossRef]
111. Liu, H.; Yan, Z.; Xiao, J. Pose error prediction and real-time compensation of a 5-DOF hybrid robot. *Mech. Mach. Theory* **2022**, *170*, 104737. [CrossRef]
112. Liu, Q.; Guo, H.; Ma, Y.; Tian, W.; Zhang, Z.; Li, B. Real-time error compensation of a 5-axis machining robot using externally mounted encoder systems. *Int. J. Adv. Manuf. Technol.* **2022**, *120*, 2793–2802. [CrossRef]
113. Wu, C.; Liu, H.; Yan, Z.; Huang, T.; Wu, H.; Ge, X. A local overfitting alleviation method for data-driven calibration applied in a 5-DOF hybrid robot. In *Advances in Mechanism and Machine Science*; Okada, M., Ed.; Springer: Cham, Switzerland, 2023; Volume 1, pp. 346–355. [CrossRef]
114. Liu, H.; Jia, Y.; Yan, Z. A new self-calibration method for the 5-DOF hybrid robot based on vision measurement. In *Advances in Mechanism, Machine Science and Engineering in China*; Liu, X., Ed.; Springer: Singapore, 2023; pp. 1883–1897. [CrossRef]
115. Yin, F.; Wang, L.; Tian, W.; Zhang, X. Kinematic calibration of a 5-DOF hybrid machining robot using an extended Kalman filter method. *Precis. Eng.* **2023**, *79*, 86–93. [CrossRef]
116. Song, Y.; Tian, W.; Tian, Y.; Liu, X. A task-oriented calibration method for a 5-DOF hybrid machining robot based on the equivalent system. *Measurement* **2023**, *216*, 112909. [CrossRef]
117. Yang, X.; Liu, H.; Xiao, J.; Zhu, W.; Liu, Q.; Gong, G.; Huang, T. Continuous friction feedforward sliding mode controller for a TriMule hybrid robot. *IEEE/ASME Trans. Mechatron.* **2018**, *23*, 1673–1683. [CrossRef]
118. Liu, Q.; Xiao, J.; Yang, X.; Liu, H.; Huang, T.; Chetwynd, D.G. An iterative tuning approach for feedforward control of parallel manipulators by considering joint couplings. *Mech. Mach. Theory* **2019**, *140*, 159–169. [CrossRef]
119. Wu, L.; Wang, G.; Liu, H.; Huang, T. An improved algorithm to predict the pose-dependent cutting stability in robot milling. *Int. J. Adv. Manuf. Technol.* **2022**, *120*, 2979–2991. [CrossRef]
120. Liu, H.; Yu, B.; Shan, X.; Yuan, H.; Meng, S. P-PI controller tuning for multi-axis motion control of hybrid robots. In *Advances in Mechanism, Machine Science and Engineering in China*; Liu, X., Ed.; Springer: Singapore, 2023; pp. 1871–1882. [CrossRef]
121. Qin, X.; Li, Y.; Feng, G.; Bao, Z.; Li, S.; Liu, H.; Li, H. A novel surface topography prediction method for hybrid robot milling considering the dynamic displacement of end effector. *Int. J. Adv. Manuf. Technol.* **2024**, *130*, 3495–3508. [CrossRef]
122. Li, H.; Xu, Q.; Wen, S.; Qin, X.; Huang, T. Deformation analysis and hole diameter error compensation for hybrid robot based helical milling. *J. Adv. Mech. Des. Syst. Manuf.* **2019**, *13*, JAMDSM0041. [CrossRef]
123. Xiao, J.L.; Zhao, S.L.; Guo, H.; Huang, T.; Lin, B. Research on the collaborative machining method for dual-robot mirror milling. *Int. J. Adv. Manuf. Technol.* **2019**, *105*, 4071–4084. [CrossRef]
124. Fei, J.; Lin, B.; Huang, T.; Xiao, J. Thin floor milling using moving support. *Int. J. Adv. Manuf. Technol.* **2022**, *120*, 1385–1397. [CrossRef]
125. Liu, S.; Xiao, J.; Tian, Y.; Ma, S.; Liu, H.; Huang, T. Chatter-free and high-quality end milling for thin-walled workpieces through a follow-up support technology. *J. Mater. Process. Technol.* **2023**, *312*, 117857. [CrossRef]
126. Ma, S.; Xiao, J.; Liu, H.; Liu, S.; Tian, Y. Modeling and analysis for time-varying dynamics of thin-walled workpieces in mirror milling considering material removal. *Sci. China Technol. Sci.* **2023**, *66*, 1883–1898. [CrossRef]
127. Xiao, J.; Wang, Y.; Liu, S.; Sun, Y.; Liu, H.; Huang, T.; Xu, J. Grinding trajectory generation of hybrid robot based on Cartesian direct teaching technology. *Ind. Robot* **2021**, *48*, 341–351. [CrossRef]
128. Sun, Y.; Xiao, J.; Liu, H.; Huang, T.; Wang, G. Deformation prediction based on an adaptive GA-BPNN and the online compensation of a 5-DOF hybrid robot. *Ind. Robot* **2020**, *47*, 915–928. [CrossRef]
129. Yue, W.; Liu, H.; Huang, T. An approach for predicting stiffness of a 5-DOF hybrid robot for friction stir welding. *Mech. Mach. Theory* **2022**, *175*, 104941. [CrossRef]

130. Yue, W.; Liu, H.; Li, G. An approach for optimizing the posture of a friction stir welding robotized equipment. In *Advances in Mechanism, Machine Science and Engineering in China*; Liu, X., Ed.; Springer: Singapore, 2023; pp. 1611–1631. [CrossRef]
131. Li, Z.; Zhao, H.; Zhang, X.; Dong, J.; Hu, L.; Gao, H. Multi-parameter sensing of robotic friction stir welding based on laser circular scanning. *J. Manuf. Process.* **2023**, *89*, 92–104. [CrossRef]
132. Xiao, J.; Wang, M.; Liu, H.; Liu, S.; Zhao, H.; Gao, J. A constant plunge depth control strategy for robotic FSW based on online trajectory generation. *Robot. Comput. Integr. Manuf.* **2023**, *80*, 102479. [CrossRef]
133. Gao, X.; Li, Z.; Zhao, H.; Dong, J.; Gao, H. Strain-based multi-dimensional force sensing system for robotic friction stir welding. *Measurement* **2024**, *236*, 115101. [CrossRef]
134. Zhang, Y.; Li, H.; Qin, X.; Liu, J.; Hou, Z. Analysis of vibration response and machining quality of hybrid robot based UD-CFRP trimming. *Proc. Inst. Mech. Eng. Part B J. Eng. Manuf.* **2021**, *235*, 974–986. [CrossRef]
135. Ding, Y.; Zhang, Z.; Liu, X.; Fu, J.; Huang, T. Development of a novel mobile robotic system for large-scale manufacturing. *Proc. Inst. Mech. Eng. Part B J. Eng. Manuf.* **2021**, *235*, 2300–2309. [CrossRef]
136. Zhang, Z.; Xiao, J.; Liu, H.; Huang, T. Base placement optimization of a mobile hybrid machining robot by stiffness analysis considering reachability and nonsingularity constraints. *Chin. J. Aeronaut.* **2023**, *36*, 398–416. [CrossRef]
137. Yan, Z.; Wang, Y.; Liu, H.; Xiao, J.; Huang, T. An improved data-driven calibration method with high efficiency for a 6-DOF hybrid robot. *Machines* **2023**, *11*, 31. [CrossRef]
138. Wang, M.; Wang, M. Dynamic modeling and performance evaluation of a new five-DOF hybrid robot. *J. Mech. Eng.* **2023**, *59*, 63–75. [CrossRef]
139. Yang, Y.; Wang, M. Modeling and analysis of position accuracy reliability of R(RPS&RP)& 2-UPS parallel mechanism. *J. Mech. Eng.* **2023**, *59*, 62–72. [CrossRef]
140. Antonov, A.; Fomin, A.; Glazunov, V.; Kiselev, S.; Carbone, G. Inverse and forward kinematics and workspace analysis of a novel 5-DOF (3T2R) parallel–serial (hybrid) manipulator. *Int. J. Adv. Robot. Syst.* **2021**, *18*, 1729881421992963. [CrossRef]
141. Laryushkin, P.; Antonov, A.; Fomin, A.; Essomba, T. Velocity and singularity analysis of a 5-DOF (3T2R) parallel-serial (hybrid) manipulator. *Machines* **2022**, *10*, 276. [CrossRef]
142. Wahl, J. Articulated Tool Head. US Patent 6,431,802, 13 August 2002.
143. Hunt, K.H. Structural kinematics of in-parallel-actuated robot-arms. *J. Mech. Trans. Autom.* **1983**, *105*, 705–712. [CrossRef]
144. Weck, M.; Staimer, D. Parallel kinematic machine tools—Current state and future potentials. *CIRP Ann.* **2002**, *51*, 671–683. [CrossRef]
145. San, H.; Ding, L.; Zhang, H.; Wu, X. Error analysis of a new five-degree-of-freedom hybrid robot. *Actuators* **2023**, *12*, 324. [CrossRef]
146. Wang, L.; Li, M.; Yu, G. A novel sensitivity analysis method for geometric errors of a parallel spindle head. In *Intelligent Robotics and Applications*; Yang, H., Liu, H., Zou, J., Yin, Z., Liu, L., Yang, G., Ouyang, X., Wang, Z., Eds.; Springer: Singapore, 2023; Volume 9, pp. 202–211. [CrossRef]
147. Wang, L.; Li, M.; Yu, G. A novel error sensitivity analysis method for a parallel spindle head. *Robotics* **2023**, *12*, 129. [CrossRef]
148. Ni, Y.; Cui, Y.; Lu, C.; Liu, H.; Zhang, L.; Lu, W. Semi-analytical static compliance modeling of hybrid equipment. *Proc. Inst. Mech. Eng. Part C J. Mech. Eng. Sci.* **2023**, *237*, 3444–3458. [CrossRef]
149. Li, M.; Wang, L.; Yu, G.; Li, W. A new calibration method for hybrid machine tools using virtual tool center point position constraint. *Measurement* **2021**, *181*, 109582. [CrossRef]
150. Li, M.; Wang, L.; Yu, G. Kinematic calibration of a hybrid machine tool with constrained least square method. In *Advances in Mechanism, Machine Science and Engineering in China*; Liu, X., Ed.; Springer: Singapore, 2023; pp. 1391–1402. [CrossRef]
151. Li, M.; Wang, L.; Yu, G.; Li, W.; Kong, X. A multiple test arbors-based calibration method for a hybrid machine tool. *Robot. Comput. Integr. Manuf.* **2023**, *80*, 102480. [CrossRef]
152. Wang, L.; Li, M.; Yu, G.; Li, W.; Kong, X. Automated measurement and hybrid adaptive identification method for kinematic calibration of hybrid machine tools. *Measurement* **2023**, *222*, 113638. [CrossRef]
153. Wang, L.; Kong, X.; Yu, G.; Li, W.; Li, M.; Jiang, A. Error estimation and cross-coupled control based on a novel tool pose representation method of a five-axis hybrid machine tool. *Int. J. Mach. Tools Manuf.* **2022**, *182*, 103955. [CrossRef]
154. Kong, X.; Wang, L.; Yu, G.; Li, W.; Li, M. Research on servo matching of a five-axis hybrid machine tool. *Int. J. Adv. Manuf. Technol.* **2023**, *129*, 983–997. [CrossRef]
155. Wang, L.; Kong, X.; Yu, G. Torque feedforward control of the parallel spindle head feed axes. In *Advances in Mechanism, Machine Science and Engineering in China*; Liu, X., Ed.; Springer: Singapore, 2023; pp. 1403–1418. [CrossRef]
156. Wang, D.; Wu, J.; Wang, L.; Liu, Y.; Yu, G. Research on the dynamic characteristics of a 3-DOF parallel tool head. *Ind. Robot* **2017**, *44*, 28–37. [CrossRef]
157. Huang, P.; Wang, J.; Wang, L.; Yao, R. Identification of structure errors of 3-PRS-XY mechanism with regularization method. *Mech. Mach. Theory* **2011**, *46*, 927–944. [CrossRef]
158. Liu, Y.; Wu, J.; Wang, L.; Wang, J.; Wang, D.; Yu, G. Kinematic calibration of a 3-DOF parallel tool head. *Ind. Robot* **2017**, *44*, 231–241. [CrossRef]
159. Wang, D.; Wang, L.; Wu, J. Physics-based mechatronics modeling and application of an industrial-grade parallel tool head. *Mech. Syst. Signal Process.* **2021**, *148*, 107158. [CrossRef]

160. Briones, J.A.; Castillo, E.; Carbone, G.; Ceccarelli, M. Position and force control of the CAPAMAN 2 bis parallel robot for drilling tasks. In Proceedings of the 2009 Electronics, Robotics and Automotive Mechanics Conference, Cuernavaca, Mexico, 22–25 September 2009; pp. 181–186. [CrossRef]
161. Chen, G.; Gao, S.; Li, H.; Yang, K.; Song, K. Kinematic analysis and experiments of the hybrid robot for the HTGR plugging weld. *Mech. Eng. J.* **2023**, *10*, 22-00458. [CrossRef]
162. Wang, R.; Ren, Y.Y.; Huang, X.S. Kinematics analysis of double-cutter & double-surface symmetrical machining tool for large-scale marine propeller. *Appl. Mech. Mater.* **2014**, *602–605*, 122–130. [CrossRef]
163. Ren, Y.Y.; Wang, R.; Zhong, S.S.; Wen, J.M. Kinematic calibration of hybrid machine tool for marine propellers processing. *Appl. Mech. Mater.* **2014**, *602–605*, 653–661. [CrossRef]
164. Yang, X.; Zhao, J.; Zhang, L.; Li, D.; Li, R. A novel surface self-adapting parallel machine tool for blade machining. In Proceedings of the 2009 International Conference on Mechatronics and Automation, Changchun, China, 9–12 August 2009; pp. 3921–3926. [CrossRef]
165. Fan, C.; Zhao, G.; Zhao, J.; Zhang, L.; Sun, L. Calibration of a parallel mechanism in a serial-parallel polishing machine tool based on genetic algorithm. *Int. J. Adv. Manuf. Technol.* **2015**, *81*, 27–37. [CrossRef]
166. Li, B.; Huang, T.; Zhang, L.; Zhao, X. Conceptual design and dimensional synthesis of a novel 5-DOF hybrid manipulator. *China Mech. Eng.* **2011**, *22*, 1900–1905.
167. Wang, M.; Liu, H.; Huang, T. Kinematics performance evaluation of a 3-SPR parallel manipulator. *J. Mech. Eng.* **2017**, *53*, 108–115. [CrossRef]
168. Wang, M.; Liu, H.; Huang, T.; Chetwynd, D.G. Compliance analysis of a 3-SPR parallel mechanism with consideration of gravity. *Mech. Mach. Theory* **2015**, *84*, 99–112. [CrossRef]
169. Wang, M.; Liu, H.; Huang, T. An approach for the lightweight design of a 3-SPR parallel mechanism. *J. Mech. Robot.* **2017**, *9*, 051016. [CrossRef]
170. Pan, B.; Song, Y.; Wang, P.; Dong, G.; Sun, T. Laser tracker based rapid home position calibration of a hybrid robot. *J. Mech. Eng.* **2014**, *50*, 31–37. [CrossRef]
171. Li, Q.; Wu, W.; Xiang, J.; Li, H.; Wu, C. A hybrid robot for friction stir welding. *Proc. Inst. Mech. Eng. Part C J. Mech. Eng. Sci.* **2015**, *229*, 2639–2650. [CrossRef]
172. Xu, D.; Dong, J.; Wang, G.; Cai, J.; Wang, H.; Yin, L. Redundant composite polishing robot with triangular parallel mechanism-assisted polishing to improve surface accuracy of thin-wall parts. *J. Manuf. Process.* **2024**, *124*, 147–162. [CrossRef]
173. Tian, X.; Zhao, T.; Wang, C.; Li, E.; Sheng, Y. Configuration and performance analysis of 3-RHUR/PUS+PP hybrid robot. *Trans. Chin. Soc. Agric. Mach.* **2021**, *52*, 386–396. [CrossRef]
174. Chen, J.; Xie, F.; Liu, X.J.; Chong, Z. Elasto-geometrical calibration of a hybrid mobile robot considering gravity deformation and stiffness parameter errors. *Robot. Comput. Integr. Manuf.* **2023**, *79*, 102437. [CrossRef]
175. Xie, F.; Chong, Z.; Liu, X.J.; Zhao, H.; Wang, J. Precise and smooth contact force control for a hybrid mobile robot used in polishing. *Robot. Comput. Integr. Manuf.* **2023**, *83*, 102573. [CrossRef]
176. Neumann, K.E. The key to aerospace automation. In Proceedings of the Aerospace Manufacturing and Automated Fastening Conference & Exhibition, Toulouse, France, 12–14 September 2006; p. 2006-01-3144. [CrossRef]
177. Neumann, K.E. Adaptive in-jig high load Exechon machining technology & assembly technology. In Proceedings of the Aerospace Manufacturing and Automated Fastening Conference & Exhibition, North Charleston, SC, USA, 16–18 September 2008; p. 2008-01-2308. [CrossRef]
178. Kong, Y.; Cheng, G.; Guo, F.; Gu, W.; Zhang, L. Inertia matching analysis of a 5-DOF hybrid optical machining manipulator. *J. Mech. Sci. Technol.* **2019**, *33*, 4991–5002. [CrossRef]
179. Jin, Y.; Bi, Z.; Higgins, C.; Price, M.; Chen, W.; Huang, T. Optimal design of a new parallel kinematic machine for large volume machining. In *Advances in Reconfigurable Mechanisms and Robots I*; Dai, J.S., Zoppi, M., Kong, X., Eds.; Springer: London, UK, 2012; pp. 343–354. [CrossRef]
180. Jin, Y.; McToal, P.; Higgins, C.; Brookes, H.; Summers, M. Parallel kinematic assisted automated aircraft assembly. *Int. J. Robot. Mechatron.* **2015**, *1*, 89–95. [CrossRef]
181. Jin, Y.; Bi, Z.M.; Liu, H.T.; Higgins, C.; Price, M.; Chen, W.H.; Huang, T. Kinematic analysis and dimensional synthesis of Exechon parallel kinematic machine for large volume machining. *J. Mech. Robot.* **2015**, *7*, 041004. [CrossRef]
182. Hu, B.; Shi, Y.; Xu, L.; Bai, P. Reconsideration of terminal constraint/mobility and kinematics of 5-DOF hybrid manipulators formed by one 2R1T PM and one RR SM. *Mech. Mach. Theory* **2020**, *149*, 103837. [CrossRef]
183. Bi, Z.M.; Jin, Y. Kinematic modeling of Exechon parallel kinematic machine. *Robot. Comput. Integr. Manuf.* **2011**, *27*, 186–193. [CrossRef]
184. Kang, R.; Chanal, H.; Bonnemains, T.; Pateloup, S.; Branson, D.T.; Ray, P. Learning the forward kinematics behavior of a hybrid robot employing artificial neural networks. *Robotica* **2012**, *30*, 847–855. [CrossRef]
185. Kang, R.; Chanal, H.; Dai, J.S.; Ray, P. Comparison of numerical and neural network methods for the kinematic modeling of a hybrid structure robot. *Proc. Inst. Mech. Eng. Part C J. Mech. Eng. Sci.* **2015**, *229*, 1162–1171. [CrossRef]
186. Bi, Z.M. Kinetostatic modeling of Exechon parallel kinematic machine for stiffness analysis. *Int. J. Adv. Manuf. Technol.* **2014**, *71*, 325–335. [CrossRef]

187. Zhang, J.; Zhao, Y.Q.; Jin, Y. Elastodynamic modeling and analysis for an Exechon parallel kinematic machine. *J. Manuf. Sci. Eng.* **2016**, *138*, 031011. [CrossRef]
188. Zhang, J.; Zhao, Y.; Jin, Y. Kinetostatic-model-based stiffness analysis of Exechon PKM. *Robot. Comput. Integr. Manuf.* **2016**, *37*, 208–220. [CrossRef]
189. Shen, N.; Geng, L.; Li, J.; Ye, F.; Yu, Z.; Wang, Z. Improved stiffness modeling for an Exechon-like parallel kinematic machine (PKM) and its application. *Chin. J. Mech. Eng.* **2020**, *33*, 40. [CrossRef]
190. Yang, S.H.; Lee, D.M.; Lee, H.H.; Lee, K.I. Sequential measurement of position-independent geometric errors in the rotary and spindle axes of a hybrid parallel kinematic machine. *Int. J. Precis. Eng. Manuf.* **2020**, *21*, 2391–2398. [CrossRef]
191. López-Custodio, P.C.; Dai, J.S.; Fu, R.; Jin, Y. Kinematic analysis of the Exechon robot accounting offsets in the joint axes. In Proceedings of the ASME 2019 International Design Engineering Technical Conferences and Computers and Information in Engineering Conference, Anaheim, CA, USA, 18–21 August 2019; Volume 5A, p. V05AT07A025. [CrossRef]
192. López-Custodio, P.C.; Dai, J.S.; Fu, R.; Jin, Y. Kinematics and constraints of the Exechon robot accounting offsets due to errors in the base joint axes. *J. Mech. Robot.* **2020**, *12*, 021109. [CrossRef]
193. Nagao, K.; Fujiki, N.; Morimoto, Y.; Hayashi, A. Calibration method of parallel mechanism type machine tools. *Int. J. Autom. Technol.* **2020**, *14*, 429–437. [CrossRef]
194. Nagao, K.; Fujiki, N.; Tanaka, H.; Hayashi, A.; Yamaoka, H.; Morimoto, Y. Machining performance of robot-type machine tool consisted of parallel and serial links based on calibration of kinematics parameters. *Int. J. Autom. Technol.* **2021**, *15*, 611–620. [CrossRef]
195. Tanaka, H.; Morimoto, Y.; Hayashi, A.; Yamaoka, H. Posture evaluation based on forward kinematics and inverse kinematics of parallel link type machine tool. *Int. J. Autom. Technol.* **2022**, *16*, 497–506. [CrossRef]
196. López-Custodio, P.C.; Fu, R.; Dai, J.S.; Jin, Y. Compliance model of Exechon manipulators with an offset wrist. *Mech. Mach. Theory* **2022**, *167*, 104558. [CrossRef]
197. Sagar, K.; Ramadoss, V.; Zoppi, M. Towards high dynamic operations with parallel-serial hybrid robots. In Proceedings of the ASME 2023 International Design Engineering Technical Conferences and Computers and Information in Engineering Conference, Boston, MA, USA, 20–23 August 2023; Volume 8, p. V008T08A064. [CrossRef]
198. Li, J.; Ye, F.; Shen, N.; Wang, Z.; Geng, L. Dimensional synthesis of a 5-DOF hybrid robot. *Mech. Mach. Theory* **2020**, *150*, 103865. [CrossRef]
199. Tengfei, T.; Yanqin, Z.; Jun, Z.; Yan, J. Conceptual design and workspace analysis of an Exechon-inspired parallel kinematic machine. In *Advances in Reconfigurable Mechanisms and Robots II*; Ding, X., Kong, X., Dai, J.S., Eds.; Springer: Cham, Switzerland, 2016; pp. 445–453. [CrossRef]
200. Tang, T.; Zhang, J.; Ceccarelli, M. Static performance analysis of an Exechon-like parallel kinematic machine. In *Mechanism and Machine Science*; Zhang, X., Wang, N., Huang, Y., Eds.; Springer: Singapore, 2017; pp. 831–843. [CrossRef]
201. Tang, T.; Zhang, J. Conceptual design and kinetostatic analysis of a modular parallel kinematic machine-based hybrid machine tool for large aeronautic components. *Robot. Comput. Integr. Manuf.* **2019**, *57*, 1–16. [CrossRef]
202. Jin, Y.; Kong, X.; Higgins, C.; Price, M. Kinematic design of a new parallel kinematic machine for aircraft wing assembly. In Proceedings of the IEEE 10th International Conference on Industrial Informatics, Beijing, China, 25–27 July 2012; pp. 669–674. [CrossRef]
203. Xu, Y.; Hu, J.; Zhang, D.; Yao, J.; Zhao, Y. A five-degree-of-freedom hybrid manipulator for machining of complex curved surface. In *Intelligent Robotics and Applications*; Huang, Y., Wu, H., Liu, H., Yin, Z., Eds.; Springer: Cham, Switzerland, 2017; Volume 2, pp. 48–58. [CrossRef]
204. Xu, Y.; Hu, J.; Zhang, D.; Hou, Z.; Yao, J.; Zhao, Y. A kind of five degrees of freedom hybrid robot with all rotating shafts continuous. *J. Mech. Eng.* **2018**, *54*, 19–24. [CrossRef]
205. Zhang, D.; Xu, Y.; Yao, J.; Zhao, Y. Inverse dynamic analysis of novel 5-DOF hybrid manipulator. *Trans. Chin. Soc. Agric. Mach.* **2017**, *48*, 384–391. [CrossRef]
206. Zhang, D.; Xu, Y.; Yao, J.; Zhao, Y. Static stiffness analysis of 2RPU/UPR+RP 5-DOF hybrid manipulators. *China Mech. Eng.* **2018**, *29*, 712–719. [CrossRef]
207. Zhang, D.S.; Xu, Y.D.; Yao, J.T.; Zhao, Y.S. Analysis and optimization of a spatial parallel mechanism for a new 5-DOF hybrid serial-parallel manipulator. *Chin. J. Mech. Eng.* **2018**, *31*, 54. [CrossRef]
208. Lu, L.; Zhang, D.; Xu, Y.; Yao, J.; Zhao, Y. Dimension and structure optimization design of 5-DOF hybrid manipulator. *Trans. Chin. Soc. Agric. Mach.* **2018**, *49*, 412–419. [CrossRef]
209. Ma, X.; He, X.; Wang, Y.; Jin, L.; Xu, Y.; Yao, J.; Zhao, Y. Error identification and accuracy compensation algorithm for improved 2RPU/UPR+R+P hybrid robot. *IEEE Robot. Autom. Lett.* **2024**, *9*, 8547–8554. [CrossRef]
210. Zhang, H.; Fang, H.; Fang, Y.; Jiang, B. Workspace analysis of a hybrid kinematic machine tool with high rotational applications. *Math. Probl. Eng.* **2018**, *2018*, 2607497. [CrossRef]
211. Zhang, D.; Xu, Y.; Yao, J.; Zhao, Y.; Chen, I.M. Rotational axes and inverse kinematics analysis of a novel 5-DOF hybrid manipulator. In Proceedings of the 2017 IEEE International Conference on Cybernetics and Intelligent Systems and IEEE Conference on Robotics, Automation and Mechatronics, Ningbo, China, 19–21 November 2017; pp. 350–355. [CrossRef]
212. Ye, H.; Wang, D.; Wu, J.; Yue, Y.; Zhou, Y. Forward and inverse kinematics of a 5-DOF hybrid robot for composite material machining. *Robot. Comput. Integr. Manuf.* **2020**, *65*, 101961. [CrossRef]

213. Xu, Y.; Yang, F.; Mei, Y.; Zhang, D.; Zhou, Y.; Zhao, Y. Kinematic, workspace and force analysis of a five-DOF hybrid manipulator R(2RPR)R/SP+RR. *Chin. J. Mech. Eng.* **2022**, *35*, 123. [CrossRef]
214. Zhang, D.; Xu, Y.; Yao, J.; Zhao, Y. Design of a novel 5-DOF hybrid serial-parallel manipulator and theoretical analysis of its parallel part. *Robot. Comput. Integr. Manuf.* **2018**, *53*, 228–239. [CrossRef]
215. Wang, X.; Wu, J.; Wang, Y. Dynamics evaluation of 2UPU/SP parallel mechanism for a 5-DOF hybrid robot considering gravity. *Robot. Auton. Syst.* **2021**, *135*, 103675. [CrossRef]
216. Wang, X.; Wu, J.; Zhou, Y. Dynamic modeling and performance evaluation of a 5-DOF hybrid robot for composite material machining. *Machines* **2023**, *11*, 652. [CrossRef]
217. Zhang, D.; Xu, Y.; Yao, J.; Zhou, Y.; Zhao, Y. Force analysis and mechanical design of a novel 3-DOF parallel mechanism. In Proceedings of the ASME 2018 International Design Engineering Technical Conferences and Computers and Information in Engineering Conference, Quebec City, QC, Canada, 26–29 August 2018; Volume 5B, pp. 2–7. [CrossRef]
218. Xu, Y.; Xu, Z.; Yang, F.; Zhao, Y.; Mei, Y.; Zhou, Y.; Yao, J.; Zhao, Y. Design and analysis of a new 5-DOF hybrid robot considering workspace and force transmission efficiency. *China Mech. Eng.* **2019**, *30*, 1996–2002. [CrossRef]
219. Xu, Y.; Xu, Z.; Yang, F.; Mei, Y.; Yue, Y.; Zhou, Y.; Yao, J.; Zhao, Y. Design and analysis of a new 5-DOF hybrid serial-parallel manipulator. In *Recent Advances in Mechanisms, Transmissions and Applications*; Wang, D., Petuya, V., Chen, Y., Yu, S., Eds.; Springer: Singapore, 2020; pp. 301–311. [CrossRef]
220. Ye, H.; Wu, J.; Wang, D. A general approach for geometric error modeling of over-constrained hybrid robot. *Mech. Mach. Theory* **2022**, *176*, 104998. [CrossRef]
221. Xu, L.; Chai, X.; Ding, Y. Design of a 2RRU-RRS parallel kinematic mechanism for an inner-cavity machining hybrid robot. *J. Mech. Robot.* **2024**, *16*, 054501. [CrossRef]
222. Yue, Y.; Zhang, Z.; Wei, B.; Zhu, J.; Li, X.; Liao, Z. Continuous rotational axes and workspace analysis of a novel 2UPU-2SPR parallel mechanism. In *Advances in Mechanism and Machine Science*; Okada, M., Ed.; Springer: Cham, Switzerland, 2023; Volume 1, pp. 632–640. [CrossRef]
223. Zhang, H.; Fang, H.; Zhang, D.; Luo, X.; Zou, Q. Forward kinematics and workspace determination of a novel redundantly actuated parallel manipulator. *Int. J. Aerosp. Eng.* **2019**, *2019*, 4769174. [CrossRef]
224. Zhang, H.; Fang, H.; Zhang, D.; Luo, X.; Zhao, F. Kinematics and dynamics simulation analysis of a 3-DOF parallel mechanism for application in hybrid machine. In *Recent Advances in Mechanisms, Transmissions and Applications*; Wang, D., Petuya, V., Chen, Y., Yu, S., Eds.; Springer: Singapore, 2020; pp. 247–258. [CrossRef]
225. Zhang, H.; Tang, J.; Yan, C.; Cui, G.; Zhang, M.; Yao, Y. Stiffness analysis of a 3-DOF parallel mechanism for engineering special machining. *Mech. Sci.* **2022**, *13*, 635–645. [CrossRef]
226. Zhang, H.; Tang, J.; Gao, Q.; Cui, G.; Shi, K.; Yao, Y. Multi-objective optimization of a redundantly actuated parallel robot mechanism for special machining. *Mech. Sci.* **2022**, *13*, 123–136. [CrossRef]
227. Li, J.; Shen, H.P.; Jiang, Y.X.; Deng, J.M.; Liu, S.S.; Ding, L.; Wang, W. Research and design of control system for a 3-DOF hybrid robot. *Appl. Mech. Mater.* **2011**, *43*, 207–210. [CrossRef]
228. Ma, X.; Xu, Y.; Wang, Y.; Yang, F.; Zhao, Y.; Yao, J.; Zhou, Y. Analysis of a five-degree-of-freedom hybrid robot RPR/RP + RR + P. In *Advances in Mechanism, Machine Science and Engineering in China*; Liu, X., Ed.; Springer: Singapore, 2023; pp. 367–379. [CrossRef]
229. Wang, M.; Wang, P.; Sun, T.; Chen, Y.; Lian, B.; Hou, B.; Zhao, X.; Song, Y. Teleoperation robot machining for large casting components. In *Intelligent Robotics and Applications*; Liu, X.J., Nie, Z., Yu, J., Xie, F., Song, R., Eds.; Springer: Cham, Switzerland, 2021; Volume 2, pp. 620–627. [CrossRef]
230. Wang, M.; Song, Y.; Wang, P.; Zhao, X.; Lian, B.; Chen, Y.; Sun, T. Master-slave robot system and its teleoperation machining approach for medium and large casting parts. *J. Mech. Eng.* **2022**, *58*, 93–103. [CrossRef]
231. Uchiyama, T.; Terada, H.; Mitsuya, H. Continuous path control of a 5-DOF parallel-serial hybrid robot. *J. Mech. Sci. Technol.* **2010**, *24*, 47–50. [CrossRef]
232. Guo, W.; Li, R.; Cao, C.; Gao, Y. Kinematics analysis of a novel 5-DOF hybrid manipulator. *Int. J. Autom. Technol.* **2015**, *9*, 765–774. [CrossRef]
233. Guo, W.; Li, R.; Cao, C.; Gao, Y. A novel method of dexterity analysis for a 5-DOF manipulator. *J. Robot.* **2016**, *2016*, 8901820. [CrossRef]
234. Guo, W.; Li, R.; Cao, C.; Tong, X.; Gao, Y. A new methodology for solving trajectory planning and dynamic load-carrying capacity of a robot manipulator. *Math. Probl. Eng.* **2016**, *2016*, 1302537. [CrossRef]
235. Guo, W.; Li, R.; Cao, C.; Gao, Y. Kinematics, dynamics, and control system of a new 5-degree-of-freedom hybrid robot manipulator. *Adv. Mech. Eng.* **2016**, *8*, 1–19. [CrossRef]
236. Guo, W.; Li, R.; Zhu, Y.; Yang, T.; Qin, R.; Hu, Z. A robotic deburring methodology for tool path planning and process parameter control of a five-degree-of-freedom robot manipulator. *Appl. Sci.* **2019**, *9*, 2033. [CrossRef]
237. Yang, G.; Chen, W.; Ho, E.H.L. Design and kinematic analysis of a modular hybrid parallel-serial manipulator. In Proceedings of the 7th International Conference on Control, Automation, Robotics and Vision, Singapore, 2–5 December 2002; Volume 1, pp. 45–50. [CrossRef]
238. Yang, G.; Chen, I.M.; Yeo, S.H.; Lin, W. Design and analysis of a modular hybrid parallel-serial manipulator for robotised deburring applications. In *Smart Devices and Machines for Advanced Manufacturing*; Wang, L., Xi, J., Eds.; Springer: London, UK, 2008; pp. 167–188. [CrossRef]

239. Antonov, A.V.; Fomin, A.S. Inverse kinematics of a 5-DOF hybrid manipulator. *Autom. Remote Control* **2023**, *84*, 281–293. [CrossRef]
240. Antonov, A.; Fomin, A. Velocity analysis of a 5-DOF hybrid manipulator. In *New Advances in Mechanisms, Transmissions and Applications*; Laribi, M.A., Nelson, C.A., Ceccarelli, M., Zeghloul, S., Eds.; Springer: Cham, Switzerland, 2023; pp. 161–170. [CrossRef]
241. Clavel, R. Device for Displacing and Positioning an Element in Space. International Patent WO 87/03528, 18 June 1987.
242. Yu, M.; Zhao, J.; Zhang, L.; Wang, Y. Study on the dynamic characteristics of a virtual-axis hybrid polishing machine tool by flexible multibody dynamics. *Proc. Inst. Mech. Eng. Part B J. Eng. Manuf.* **2004**, *218*, 1067–1076. [CrossRef]
243. Yu, M.; Zhao, J.; Ma, W.T. Study on the modeling and experiments for the virtual axis hybrid polishing machine tool by the flexible multibody dynamics. *Key Eng. Mater.* **2006**, *304–305*, 502–506. [CrossRef]
244. Wang, G.; Wang, Y. Research on polishing process of a special polishing machine tool. *Mach. Sci. Technol.* **2009**, *13*, 106–121. [CrossRef]
245. Xu, P.; Cheung, C.F.; Li, B.; Ho, L.T.; Zhang, J.F. Kinematics analysis of a hybrid manipulator for computer controlled ultra-precision freeform polishing. *Robot. Comput. Integr. Manuf.* **2017**, *44*, 44–56. [CrossRef]
246. Xu, P.; Cheung, C.F.; Wang, C.; Zhao, C. Novel hybrid robot and its processes for precision polishing of freeform surfaces. *Precis. Eng.* **2020**, *64*, 53–62. [CrossRef]
247. Xu, P.; Li, B.; Chueng, C.F. Dynamic analysis of a linear Delta robot in hybrid polishing machine based on the principle of virtual work. In Proceedings of the 2017 18th International Conference on Advanced Robotics, Hong Kong, China, 10–12 July 2017; pp. 379–384. [CrossRef]
248. Xu, P.; Cheung, C.F.; Li, B.; Wang, C.; Zhao, C. Design, dynamic analysis, and experimental evaluation of a hybrid parallel–serial polishing machine with decoupled motions. *J. Mech. Robot.* **2021**, *13*, 061008. [CrossRef]
249. Xu, P.; Cheung, C.F.; Li, B.; Wang, C.; Ho, L.T. Design, development, and analysis of a hybrid serial-parallel machine for precision polishing. In *Precision Machines*; Yang, S., Jiang, Z., Eds.; Springer: Singapore, 2020; pp. 171–205. [CrossRef]
250. Xu, P.; Li, B.; Cheung, C.F.; Zhang, J.F. Stiffness modeling and optimization of a 3-DOF parallel robot in a serial-parallel polishing machine. *Int. J. Precis. Eng. Manuf.* **2017**, *18*, 497–507. [CrossRef]
251. Xu, P.; Li, B.; Huang, H.; Xu, G. Error modeling and identification of a parallel robot in a hybrid machine for polishing. In Proceedings of the 2017 IEEE International Conference on Real-time Computing and Robotics, Okinawa, Japan, 14–18 July 2017; pp. 229–233. [CrossRef]
252. Li, Z.; Cheung, C.F.; Lam, K.M.; Lun, D.P.K. Active compliance smart control strategy of hybrid mechanism for bonnet polishing. *Sensors* **2024**, *24*, 421. [CrossRef]
253. Mohammadipanah, H.; Zohoor, H. Design and analysis of a novel 8-DOF hybrid manipulator. *Int. J. Mech. Ind. Aerosp. Sci.* **2009**, *3*, 1158–1164. [CrossRef]
254. Nguyen, V.L.; Kuo, C.H.; Lin, P.T. Compliance error compensation of a robot end-effector with joint stiffness uncertainties for milling: An analytical model. *Mech. Mach. Theory* **2022**, *170*, 104717. [CrossRef]
255. Gough, V.E. Contribution to discussion of papers on research in automobile stability, control and tyre performance. *Proc. Inst. Mech. Eng. Automob. Div.* **1957**, *171*, 392–395.
256. Stewart, D. A platform with six degrees of freedom. *Proc. Inst. Mech. Eng.* **1965**, *180*, 371–386. [CrossRef]
257. Merlet, J.P. *Parallel Robots*, 2nd ed.; Springer: Dordrecht, The Netherlands, 2006. [CrossRef]
258. Wu, H.; Pessi, P.; Handroos, H. Assembling and repairing for ITER vacuum vessel with mobile parallel robot. In Proceedings of the 2007 IEEE 22nd Symposium on Fusion Engineering, Albuquerque, NM, USA, 17–21 June 2007; pp. 1–4. [CrossRef]
259. Wang, Y.; Pessi, P.; Wu, H.; Handroos, H. Accuracy analysis of hybrid parallel robot for the assembling of ITER. *Fusion Eng. Des.* **2009**, *84*, 1964–1968. [CrossRef]
260. Li, M.; Wu, H.; Handroos, H. Static stiffness modeling of a novel hybrid redundant robot machine. *Fusion Eng. Des.* **2011**, *86*, 1838–1842. [CrossRef]
261. Li, M.; Wu, H.; Handroos, H. Stiffness-maximum trajectory planning of a hybrid kinematic-redundant robot machine. In Proceedings of the IECON 2011—37th Annual Conference of the IEEE Industrial Electronics Society, Melbourne, Australia, 7–10 November 2011; pp. 283–288. [CrossRef]
262. Wang, Y.; Wu, H.; Handroos, H.; Chen, B. On the error modeling of a novel mobile hybrid parallel robot. In Proceedings of the 2008 IEEE Conference on Robotics, Automation and Mechatronics, Chengdu, China, 21–24 September 2008; pp. 1217–1222. [CrossRef]
263. Wang, Y.; Wu, H.; Handroos, H. Identifiable parameter analysis for the kinematic calibration of a hybrid robot. In Proceedings of the ASME 2011 International Design Engineering Technical Conferences and Computers and Information in Engineering Conference, Washington, DC, USA, 28–31 August 2011; Volume 6, pp. 911–919. [CrossRef]
264. Wang, Y.; Wu, H.; Handroos, H. Markov Chain Monte Carlo (MCMC) methods for parameter estimation of a novel hybrid redundant robot. *Fusion Eng. Des.* **2011**, *86*, 1863–1867. [CrossRef]
265. Wang, Y.; Wu, H.; Handroos, H. Error modelling and differential-evolution-based parameter identification method for redundant hybrid robot. *Int. J. Modell. Simul.* **2012**, *32*, 255–264. [CrossRef]
266. Wang, Y.; Wu, H.; Handroos, H. Accuracy improvement of a hybrid robot for ITER application using POE modeling method. *Fusion Eng. Des.* **2013**, *88*, 1877–1880. [CrossRef]

267. Li, M.; Wu, H.; Handroos, H.; Yang, G. Software design of the hybrid robot machine for ITER vacuum vessel assembly and maintenance. *Fusion Eng. Des.* **2013**, *88*, 1872–1876. [CrossRef]
268. Wu, H.; Wang, Y.; Li, M.; Al-Saedi, M.; Handroos, H. Chatter suppression methods of a robot machine for ITER vacuum vessel assembly and maintenance. *Fusion Eng. Des.* **2014**, *89*, 2357–2362. [CrossRef]
269. Al-Saedi, M.I.; Wu, H.; Handroos, H. Intelligent controller of a flexible hybrid robot machine for ITER assembly and maintenance. *Fusion Eng. Des.* **2014**, *89*, 1795–1803. [CrossRef]
270. Li, M.; Wu, H.; Handroos, H.; Yang, G.; Wang, Y. Software protocol design: Communication and control in a multi-task robot machine for ITER vacuum vessel assembly and maintenance. *Fusion Eng. Des.* **2015**, *98–99*, 1532–1537. [CrossRef]
271. Li, C.; Wu, H.; Eskelinen, H. Design and multi-objective optimization of a dexterous mobile parallel mechanism for fusion reactor vacuum vessel assembly. *IEEE Access* **2021**, *9*, 153796–153810. [CrossRef]
272. Li, J.; Cheng, Y.; Ji, H.; Pan, H.; Yang, Y.; Zhang, X.; Zhong, Y.; Song, Y.; Wu, H.; Li, C. Experiments of vacuum vessel in-situ milling via mobile parallel robot machine. *Fusion Eng. Des.* **2024**, *205*, 114553. [CrossRef]
273. Ancuța, P.N.; Constantin, A.; Munteanu, I.S.; Gornoavă, V. Study on improving the measurement accuracy by touch probe with a cobotic multi-application platform. *Int. J. Mechatron. Appl. Mech.* **2022**, *2022*, 243–248. [CrossRef]
274. Mianowski, K.; Nazarczuk, K.; Wojtyra, M.; Szynkiewicz, W.; Zieliński, C.; Woźniak, A. Application of the RNT robot to milling and polishing. In *Romansy 13*; Morecki, A., Bianchi, G., Rzymkowski, C., Eds.; Springer: Vienna, Austria, 2000; pp. 421–429. [CrossRef]
275. Zieliński, C.; Szynkiewicz, W.; Mianowski, K.; Nazarczuk, K. Mechatronic design of open-structure multi-robot controllers. *Mechatronics* **2001**, *11*, 987–1000. [CrossRef]
276. Zieliński, C.; Mianowski, K.; Nazarczuk, K.; Szynkiewicz, W. A prototype robot for polishing and milling large objects. *Ind. Robot* **2003**, *30*, 67–76. [CrossRef]
277. Xie, F.; Mei, B.; Liu, X.; Zhang, J.; Yue, Y. Novel mode and equipment for machining large complex components. *J. Mech. Eng.* **2020**, *56*, 70–78. [CrossRef]
278. He, Y.; Xie, F.; Liu, X.J.; Xie, Z.; Zhao, H.; Yue, Y.; Li, M. Stiffness-performance-based redundant motion planning of a hybrid machining robot. *Machines* **2022**, *10*, 1157. [CrossRef]
279. He, Y.; Xie, F.; Xie, Z.; Wang, J.; Liu, X. Parameters and stiffness optimization of a five-axis parallel machining unit. *J. Mech. Eng.* **2024**, *60*, 308–315. [CrossRef]
280. Mei, B.; Xie, F.; Liu, X.J.; Xie, Z.; Zhao, H. A mobile hybrid robot and its accuracy issue in machining of large-scale structures. *IEEE/ASME Trans. Mechatron.* **2024**, *29*, 347–357. [CrossRef]
281. Lu, S.; Li, Y.; Ding, B. Kinematics and dynamics analysis of the 3PUS-PRU parallel mechanism module designed for a novel 6-DOF gantry hybrid machine tool. *J. Mech. Sci. Technol.* **2020**, *34*, 345–357. [CrossRef]
282. Tian, X.; Zhao, T.; Li, E. A novel 5-DOF hybrid robot without singularity configurations. In *Intelligent Robotics and Applications*; Yu, H., Liu, J., Liu, L., Ju, Z., Liu, Y., Zhou, D., Eds.; Springer: Cham, Switzerland, 2019; pp. 448–457. [CrossRef]
283. Li, R.; Wang, S.; Fan, D.; Du, Y.; Bai, S. Dynamic modeling of a 2-RPU+2-UPS hybrid manipulator for machining application. *Model. Identif. Control* **2017**, *38*, 169–184. [CrossRef]
284. Tian, X.; Zhao, T.; Peng, X.; Li, E. Singularity analysis and workspace optimization of a novel symmetrical 4-limb 5-DOF hybrid robot. *J. Mech. Sci. Technol.* **2023**, *37*, 2555–2567. [CrossRef]
285. Wang, G.; Wang, Y.; Zhao, J.; Chen, G. Process optimization of the serial-parallel hybrid polishing machine tool based on artificial neural network and genetic algorithm. *J. Intell. Manuf.* **2012**, *23*, 365–374. [CrossRef]
286. Dou, Y.; Wang, M.; Wang, P.; Huang, T. Stiffness analysis of a 6-DOF hybrid robot. *J. Mech. Eng.* **2015**, *51*, 38–44. [CrossRef]
287. Plitea, N.; Pisla, D.; Vaida, C. On kinematics of a parallel robot used for the minimally invasive surgery. *Proc. Appl. Math. Mech.* **2007**, *7*, 4010033–4010034. [CrossRef]
288. Pisla, D.; Vaida, C.; Plitea, N.; Hesselbach, J.; Raatz, A.; Simnofske, M.; Burisch, A.; Vlad, L. Modeling and simulation of a new parallel robot used in minimally invasive surgery. In Proceedings of the Fifth International Conference on Informatics in Control, Automation and Robotics, Funchal, Portugal, 11–15 May 2008; Volume 3, pp. 194–201. [CrossRef]
289. Pisla, D.; Plitea, N.; Vaida, C. Kinematic modeling and workspace generation for a new parallel robot used in minimally invasive surgery. In *Advances in Robot Kinematics: Analysis and Design*; Lenarčič, J., Wenger, P., Eds.; Springer: Dordrecht, The Netherlands, 2008; pp. 459–468. [CrossRef]
290. Gherman, B.; Vaida, C.; Pisla, D.; Plitea, N.; Gyurka, B.; Lese, D.; Glogoveanu, M. Singularities and workspace analysis for a parallel robot for minimally invasive surgery. In Proceedings of the 2010 IEEE International Conference on Automation, Quality and Testing, Robotics, Cluj-Napoca, Romania, 28–30 May 2010; Volume 1, pp. 1–6. [CrossRef]
291. Plitea, N.; Pisla, D.; Vaida, C.; Gherman, B.; Pisla, A. Dynamic modeling of a parallel robot used in minimally invasive surgery. In *Proceedings of EUCOMES 08*; Ceccarelli, M., Ed.; Springer: Dordrecht, The Netherlands, 2009; pp. 595–602. [CrossRef]
292. Vaida, C.; Pisla, D.; Plitea, N.; Gherman, B.; Gyurka, B.; Stancel, E.; Hesselbach, J.; Raatz, A.; Vlad, L.; Graur, F. Development of a control system for a parallel robot used in minimally invasive surgery. In *International Conference on Advancements of Medicine and Health Care through Technology*; Vlad, S., Ciupa, R.V., Nicu, A.I., Eds.; Springer: Berlin/Heidelberg, Germany, 2009; pp. 171–176. [CrossRef]
293. Vaida, C.; Pisla, D.; Plitea, N. Graphical simulation of a new concept of low sized surgical parallel robot for camera guidance in minimally invasive surgery. *Proc. Appl. Math. Mech.* **2007**, *7*, 2090005–2090006. [CrossRef]

294. Pisla, D.; Plitea, N.; Vaida, C.; Hesselbach, J.; Raatz, A.; Vlad, L.; Graur, F.; Gyurka, B.; Gherman, B.; Suciu, M. PARAMIS parallel robot for laparoscopic surgery. *Chirurgia* **2010**, *105*, 677–683.
295. Pisla, D.; Szilaghyi, A.; Vaida, C.; Plitea, N. Kinematics and workspace modeling of a new hybrid robot used in minimally invasive surgery. *Robot. Comput. Integr. Manuf.* **2013**, *29*, 463–474. [CrossRef]
296. Pisla, D.; Plitea, N.; Gherman, B.; Pisla, A.; Vaida, C. Kinematical analysis and design of a new surgical parallel robot. In *Computational Kinematics*; Kecskeméthy, A., Müller, A., Eds.; Springer: Berlin/Heidelberg, Germany, 2009; pp. 273–282. [CrossRef]
297. Pisla, D.; Plitea, N.; Gherman, B.G.; Vaida, C.; Pisla, A.; Suciu, M. Kinematics and design of a 5-DOF parallel robot used in minimally invasive surgery. In *Advances in Robot Kinematics: Motion in Man and Machine*; Lenarčič, J., Stanišić, M.M., Eds.; Springer: Dordrecht, The Netherlands, 2010; pp. 99–106. [CrossRef]
298. Pisla, D.; Gherman, B.; Vaida, C.; Plitea, N. Kinematic modelling of a 5-DOF hybrid parallel robot for laparoscopic surgery. *Robotica* **2012**, *30*, 1095–1107. [CrossRef]
299. Pisla, D.; Gherman, B.G.; Suciu, M.; Vaida, C.; Lese, D.; Sabou, C.; Plitea, N. On the dynamics of a 5 DOF parallel hybrid robot used in minimally invasive surgery. In *New Trends in Mechanism Science*; Pisla, D., Ceccarelli, M., Husty, M., Corves, B., Eds.; Springer: Dordrecht, The Netherlands, 2010; pp. 691–699. [CrossRef]
300. Gherman, B.; Pisla, D.; Vaida, C.; Plitea, N. Development of inverse dynamic model for a surgical hybrid parallel robot with equivalent lumped masses. *Robot. Comput. Integr. Manuf.* **2012**, *28*, 402–415. [CrossRef]
301. Stoica, A.; Gherman, B.; Vaida, C.; Pisla, D.; Plitea, N. Inverse dynamic model of a new parallel robot used in minimally invasive surgery. *Acta Tech. Napoc.* **2012**, *55*, 543–578.
302. Stoica, A.; Pisla, D.; Szilaghyi, A.; Gherman, B.; Plitea, N. Workspace and singularity analysis for a parallel robot used in surgical applications. In *New Trends in Mechanism and Machine Science*; Viadero, F., Ceccarelli, M., Eds.; Springer: Dordrecht, The Netherlands, 2013; pp. 149–157. [CrossRef]
303. Stoica, A.; Pisla, D.; Andras, S.; Gherman, B.; Gyurka, B.Z.; Plitea, N. Kinematic, workspace and singularity analysis of a new parallel robot used in minimally invasive surgery. *Front. Mech. Eng.* **2013**, *8*, 70–79. [CrossRef]
304. Szilaghyi, A.C.; Pisla, D. Matlab/Simulink simulation and validation of the kinematics model of a hybrid robot for minimally invasive surgery. *Acta Tech. Napoc.* **2012**, *55*, 513–518.
305. Szilaghyi, A.; Pisla, D.; Vaida, C.; Gyurka, B.; Plitea, N. Kinematics simulation and validation of a medical robot. In *New Advances in Mechanisms, Transmissions and Applications*; Petuya, V., Pinto, C., Lovasz, E.C., Eds.; Springer: Dordrecht, The Netherlands, 2014; pp. 139–147. [CrossRef]
306. Pisla, D.; Gherman, B.; Plitea, N.; Gyurka, B.; Vaida, C.; Vlad, L.; Graur, F.; Radu, C.; Suciu, M.; Szilaghi, A.; et al. PARASURG hybrid parallel robot for minimally invasive surgery. *Chirurgia* **2011**, *108*, 619–625.
307. Suciu, M.; Pisla, D.; Vaida, C.; Plitea, N. Design and structural analysis of PARASURG-9M parallel hybrid surgical robotic system. *Acta Tech. Napocensis* **2012**, *54*, 245–250.
308. Suciu, M.; Gherman, B.; Vaida, C.; Plitea, N.; Stoica, A.; Pisla, D. On the kinematics of a hybrid parallel robot used in minimally invasive surgery. In *Mechanisms, Transmissions and Applications*; Lovasz, E.C., Corves, B., Eds.; Springer: Dordrecht, The Netherlands, 2012; pp. 255–262. [CrossRef]
309. Pisla, D.; Gherman, B.; Vaida, C.; Suciu, M.; Plitea, N. An active hybrid parallel robot for minimally invasive surgery. *Robot. Comput. Integr. Manuf.* **2013**, *29*, 203–221. [CrossRef]
310. Gyurka, B.; Pisla, D.; Stancel, E.; Vaida, C.; Kovacs, I.; Gherman, B.; Balogh, S.; Plitea, N. Integrated control techniques for PARASURG 9M parallel robot. In Proceedings of the 2012 IEEE International Conference on Automation, Quality and Testing, Robotics, Cluj-Napoca, Romania, 24–27 May 2012; pp. 461–466. [CrossRef]
311. Gyurka, B.; Kovacs, I.; Pisla, D. Presentation of the mixt control unit for PARMIS parallel robotic system. In Proceedings of the 2014 IEEE International Conference on Automation, Quality and Testing, Robotics, Cluj-Napoca, Romania, 22–24 May 2014; pp. 1–6. [CrossRef]
312. Peng, Y.; Yu, H.; Du, Z. Design and kinematic analysis of a hybrid manipulator for spine surgery. In Proceedings of the 2016 IEEE International Conference on Mechatronics and Automation, Harbin, China, 7–10 August 2016; pp. 884–889. [CrossRef]
313. Li, S.; Du, Z.; Yu, H. A robot-assisted spine surgery system based on intraoperative 2D fluoroscopy navigation. *IEEE Access* **2020**, *8*, 51786–51802. [CrossRef]
314. Degirmenci, A.; Hammond, F.L.; Gafford, J.B.; Walsh, C.J.; Wood, R.J.; Howe, R.D. Design and control of a parallel linkage wrist for robotic microsurgery. In Proceedings of the 2015 IEEE/RSJ International Conference on Intelligent Robots and Systems, Hamburg, Germany, 28 September–2 October 2015; pp. 222–228. [CrossRef]
315. Tucan, P.; Gherman, B.; Andras, I.; Vaida, C.; Pisla, D. Kinematic modelling of a parallel robot used in single incision laparoscopic surgery. In *ROMANSY 24—Robot Design, Dynamics and Control*; Kecskeméthy, A., Parenti-Castelli, V., Eds.; Springer: Cham, Switzerland, 2022; pp. 115–122. [CrossRef]
316. Cao, W.; Xu, S.; Rao, K.; Ding, T. Kinematic design of a novel two degree-of-freedom parallel mechanism for minimally invasive surgery. *J. Mech. Des.* **2019**, *141*, 104501. [CrossRef]
317. Li, J.; Xing, Y.; Liang, K.; Wang, S. Kinematic design of a novel spatial remote center-of-motion mechanism for minimally invasive surgical robot. *J. Med. Devices* **2015**, *9*, 011003. [CrossRef]
318. Yang, Y.; Chen, Z.; Guang, C.; Zheng, Y.; Lin, C. Design and kinematics analysis of a serial-parallel hybrid mechanism used for intraocular surgeries. *J. Mech. Eng.* **2022**, *58*, 36–44. [CrossRef]

319. Lin, C.; Guang, C.; Zheng, Y.; Ma, K.; Yang, Y. Preliminary evaluation of a novel vision-guided hybrid robot system for capsulotomy in cataract surgery. *Displays* **2022**, *74*, 102262. [CrossRef]
320. Tao, Q.; Liu, J.; Zheng, Y.; Yang, Y.; Lin, C.; Guang, C. Evaluation of an active disturbance rejection controller for ophthalmic robots with piezo-driven injector. *Micromachines* **2024**, *15*, 833. [CrossRef] [PubMed]
321. Tanev, T.K. Minimally-invasive-surgery parallel robot with non-identical limbs. In Proceedings of the 2014 IEEE/ASME 10th International Conference on Mechatronic and Embedded Systems and Applications, Senigallia, Italy, 10–12 September 2014; pp. 1–6. [CrossRef]
322. Tanev, T.K.; Cammarata, A.; Marano, D.; Sinatra, R. Elastostatic model of a new hybrid minimally-invasive-surgery robot. In Proceedings of the 14th IFToMM World Congress, Taipei, Taiwan, 25–30 October 2015; pp. 449–458. [CrossRef]
323. Tanev, T.K. Singularity analysis of a novel minimally-invasive-surgery hybrid robot using geometric algebra. In *New Trends in Medical and Service Robots*; Wenger, P., Chevallereau, C., Pisla, D., Bleuler, H., Rodić, A., Eds.; Springer: Cham, Switzerland, 2016; pp. 15–29. [CrossRef]
324. Phan, V.T.; Nguyen, P.S.; Le, H.N. Kinematic analysis of a hybrid Delta- remote center of motion (RCM) robot assisting minimally invasive surgery. *Univ. Danang-J. Sci. Technol.* **2017**, *11*, 90–94.
325. Hong, Z.D.; Yun, C.; Zhao, L. Modeling and mechanical design of a MRI-guided robot for neurosurgery. In Proceedings of the 13th International Conference on Biomedical Engineering, Singapore, 3–6 December 2008; Lim, C.T., Goh, J.C.H., Eds.; Springer: Berlin/Heidelberg, Germany, 2009; pp. 1004–1008. [CrossRef]
326. Chung, G.B.; Chung, J.H.; Choi, D.G.; Yi, B.J.; Han, S.Y.; Kim, S.J. Development of a 5-DOF hybrid micro-manipulator and implementation to needle manipulation process in medical applications. *Key Eng. Mater.* **2006**, *326–328*, 773–776. [CrossRef]
327. Puglisi, L.J.; Saltaren, R.; Rey Portolés, G.; Moreno, H.; Cárdenas, P.F.; Garcia, C. Design and kinematic analysis of 3PSS-1S wrist for needle insertion guidance. *Rob. Auton. Syst.* **2013**, *61*, 417–427. [CrossRef]
328. Ceccarelli, M.; Ottaviano, E.; Carbone, G. A study of feasibility for a novel parallel-serial manipulator. *J. Robot. Mechatron.* **2002**, *14*, 304–312. [CrossRef]
329. Carbone, G.; Ceccarelli, M. A stiffness analysis for a hybrid parallel-serial manipulator. *Robotica* **2004**, *22*, 567–576. [CrossRef]
330. Carbone, G.; Marini, G.; Ceccarelli, M. Experimental validation and tests of operation characteristics of a parallel-serial manipulator. In *Romansy 14*; Bianchi, G., Guinot, J.C., Rzymkowski, C., Eds.; Springer: Vienna, Austria, 2002; pp. 331–338. [CrossRef]
331. Carbone, G.; Ceccarelli, M. A serial-parallel robotic architecture for surgical tasks. *Robotica* **2005**, *23*, 345–354. [CrossRef]
332. Gómez-Bravo, F.; Carbone, G.; Fortes, J.C. Collision free trajectory planning for hybrid manipulators. *Mechatronics* **2012**, *22*, 836–851. [CrossRef]
333. Carbone, G.; Ceccarelli, M.; Ottaviano, E.; Checcacci, D.; Frisoli, A.; Avizzano, C.A.; Bergamasco, M. A study of feasibility for a macro-milli serial-parallel robotic manipulator for surgery operated by a 3 Dofs haptic device. In Proceedings of the 12th International Workshop on Robotics in Alpe-Andria-Danube Region, Cassino, Italy, 7–10 May 2003; p. 006RAAD03.
334. Carbone, G.; Ottaviano, E.; Ceccarelli, M. Experimental stiffness evaluation of a serial-parallel macro-milli manipulator for medical applications. In *Proceedings of the 11th World Congress in Mechanism and Machine Science*; Huang, T., Ed.; China Machine Press: Tianjin, China, 2004; Volume 4, pp. 1862–1867.
335. Feng, Y.; Fan, J.; Tao, B.; Wang, S.; Mo, J.; Wu, Y.; Liang, Q.; Chen, X. An image-guided hybrid robot system for dental implant surgery. *Int. J. Comput. Assist. Radiol. Surg.* **2022**, *17*, 15–26. [CrossRef] [PubMed]
336. Tosi, D.; Legnani, G.; Pedrocchi, N.; Righettini, P.; Giberti, H. Cheope: A new reconfigurable redundant manipulator. *Mech. Mach. Theory* **2010**, *45*, 611–626. [CrossRef]
337. Tao, B.; Feng, Y.; Fan, X.; Zhuang, M.; Chen, X.; Wang, F.; Wu, Y. Accuracy of dental implant surgery using dynamic navigation and robotic systems: An in vitro study. *J. Dent.* **2022**, *123*, 104170. [CrossRef] [PubMed]
338. Fan, X.; Feng, Y.; Tao, B.; Shen, Y.; Wu, Y.; Chen, X. A hybrid robotic system for zygomatic implant placement based on mixed reality navigation. *Comput. Methods Programs Biomed.* **2024**, *249*, 108156. [CrossRef]
339. Raabe, D.; Dogramadzi, S.; Atkins, R. Semi-automatic percutaneous reduction of intra-articular joint fractures—An initial analysis. In Proceedings of the 2012 IEEE International Conference on Robotics and Automation, Saint Paul, MN, USA, 14–18 May 2012; pp. 2679–2684. [CrossRef]
340. Dagnino, G.; Georgilas, I.; Kohler, P.; Atkins, R.; Dogramadzi, S. Image-based robotic system for enhanced minimally invasive intra-articular fracture surgeries. In Proceedings of the 2016 IEEE International Conference on Robotics and Automation, Stockholm, Sweden, 16–21 May 2016; pp. 696–701. [CrossRef]
341. Dagnino, G.; Georgilas, I.; Morad, S.; Gibbons, P.; Tarassoli, P.; Atkins, R.; Dogramadzi, S. Image-guided surgical robotic system for percutaneous reduction of joint fractures. *Ann. Biomed. Eng.* **2017**, *45*, 2648–2662. [CrossRef]
342. Dagnino, G.; Georgilas, I.; Morad, S.; Gibbons, P.; Tarassoli, P.; Atkins, R.; Dogramadzi, S. Intra-operative fiducial-based CT/fluoroscope image registration framework for image-guided robot-assisted joint fracture surgery. *Int. J. Comput. Assist. Radiol. Surg.* **2017**, *12*, 1383–1397. [CrossRef]
343. Dagnino, G.; Georgilas, I.; Tarassoli, P.; Atkins, R.; Dogramadzi, S. Vision-based real-time position control of a semi-automated system for robot-assisted joint fracture surgery. *Int. J. Comput. Assist. Radiol. Surg.* **2016**, *11*, 437–455. [CrossRef]
344. Dagnino, G.; Georgilas, I.; Köhler, P.; Morad, S.; Atkins, R.; Dogramadzi, S. Navigation system for robot-assisted intra-articular lower-limb fracture surgery. *Int. J. Comput. Assist. Radiol. Surg.* **2016**, *11*, 1831–1843. [CrossRef]

345. Ye, R.; Chen, Y. Development of a six degree of freedom (DOF) hybrid robot for femur shaft fracture reduction. In Proceedings of the 2008 IEEE International Conference on Robotics and Biomimetics, Bangkok, Thailand, 21–26 February 2009; pp. 306–311. [CrossRef]
346. Cai, S.; Lei, J.; Rao, J. Configuration design and load capacity analysis of pelvic fracture reduction robot. *J. Vibroeng.* **2023**, *25*, 996–1010. [CrossRef]
347. Ye, R.; Chen, Y. Path planning for robot assisted femur shaft fracture reduction: A preliminary investigation. In Proceedings of the 2009 IEEE International Conference on Virtual Environments, Human-Computer Interfaces and Measurements Systems, Hong Kong, China, 11–13 May 2009; pp. 113–117. [CrossRef]
348. Ye, R.; Chen, Y.; Yau, W. A simple and novel hybrid robotic system for robot-assisted femur fracture reduction. *Adv. Robot.* **2012**, *26*, 83–104. [CrossRef]
349. Wang, S.; Chen, Y.; Zhang, P. Control simulation of a six DOF parallel-serial robot for femur fracture reduction. In Proceedings of the 2009 IEEE International Conference on Virtual Environments, Human-Computer Interfaces and Measurements Systems, Hong Kong, China, 11–13 May 2009; pp. 330–335. [CrossRef]
350. Wang, S.; Chen, Y.; Ye, R.; Yau, W. Kinematic analysis in robot assisted femur fracture reduction: Fuzzy logic approach. In Proceedings of the 26th Southern Biomedical Engineering Conference SBEC 2010, College Park, MD, USA, 30 April–2 May 2010; Herold, K.E., Vossoughi, J., Bentley, W.E., Eds.; Springer: Berlin/Heidelberg, Germany, 2010; pp. 118–121. [CrossRef]
351. Ye, R.; Wang, S.; Chen, Y. Tele-operation and simulation for a new surgical robot design. *Comput. Aided Des. Applic.* **2011**, *8*, 325–334. [CrossRef]
352. Shi, X.; Ren, L.; Liao, Z.; Zhu, J.; Wang, H. Design & analysis of the mechanical system for a spacial 4-DOF series-parallel hybrid lower limb rehabilitation robot. *J. Mech. Eng.* **2017**, *53*, 48–54. [CrossRef]
353. Zhang, P.C.; Niu, J.Y.; Liu, C.L.; Song, J.K.; Wang, L.P.; Zhang, J.J. Mechanism parameter optimization and trajectory planning of traction lower limb rehabilitation robot. *Chin. J. Eng. Des.* **2022**, *29*, 695–704. [CrossRef]
354. Wang, L.; Tian, J.; Du, J.; Zheng, S.; Niu, J.; Zhang, Z.; Wu, J. A hybrid mechanism-based robot for end-traction lower limb rehabilitation: Design, analysis and experimental evaluation. *Machines* **2022**, *10*, 99. [CrossRef]
355. Tian, J.; Wang, H.; Zheng, S.; Ning, Y.; Zhang, X.; Niu, J.; Vladareanu, L. sEMG-based gain-tuned compliance control for the lower limb rehabilitation robot during passive training. *Sensors* **2022**, *22*, 7890. [CrossRef] [PubMed]
356. Tian, J.; Wang, H.; Lu, H.; Yang, Y.; Li, L.; Niu, J.; Cheng, B. Force/position-based velocity control strategy for the lower limb rehabilitation robot during active training: Design and validation. *Front. Bioeng. Biotechnol.* **2024**, *11*, 1335071. [CrossRef]
357. Li, R.; Fan, X.; Li, X.; Bai, S.; Zhang, J. Kinematic design of a 2-SPS/PU&R 4-DOF hybrid robot for ankle rehabilitation. In *Advances in Mechanism and Machine Science*; Uhl, T., Ed.; Springer: Cham, Switzerland, 2019; pp. 1849–1858. [CrossRef]
358. Qu, S.; Li, R.; Yao, W.; Ma, C.; Guo, Z. Structure design, kinematics analysis, and effect evaluation of a novel ankle rehabilitation robot. *Appl. Sci.* **2023**, *13*, 6109. [CrossRef]
359. Mohanta, J.; Mohan, S.; Deepasundar, P.; Kiruba-Shankar, R. Development and control of a new sitting-type lower limb rehabilitation robot. *Comput. Electr. Eng.* **2018**, *67*, 330–347. [CrossRef]
360. Vasanthakumar, M.; Vinod, B.; Mohanta, J.K.; Mohan, S. Design and robust motion control of a planar 1P-2P RP hybrid manipulator for lower limb rehabilitation applications. *J. Intell. Robot. Syst.* **2019**, *96*, 17–30. [CrossRef]
361. Wang, H.B.; Ishimatsu, T.; Schaerer, C.; Huang, Z. Kinematics of a five degree-of-freedom prosthetic arm. *Mech. Mach. Theory* **1998**, *33*, 895–908. [CrossRef]
362. Larbi, M.; Belharet, K.; Guechi, E.H. LQR feedback linearization method to control the motions of a spherical serial mechanism. In Proceedings of the 2020 IEEE/ASME International Conference on Advanced Intelligent Mechatronics, Boston, MA, USA, 6–9 July 2020; pp. 1216–1221. [CrossRef]
363. Nadour, H.; Bozorg Grayeli, A.; Poisson, G.; Belharet, K. CochleRob: Parallel-serial robot to position a magnetic actuator around a patient's head for intracochlear microrobot navigation. *Sensors* **2023**, *23*, 2973. [CrossRef]
364. Kucuk, S.; Gungor, B.D. Inverse kinematics solution of a new hybrid robot manipulator proposed for medical purposes. In Proceedings of the 2016 Medical Technologies National Congress, Antalya, Turkey, 27–29 October 2016; pp. 1–4. [CrossRef]
365. Singh, A.; Singla, A.; Soni, S. Extension of D-H parameter method to hybrid manipulators used in robot-assisted surgery. *Proc. Inst. Mech. Eng. Part H J. Eng. Med.* **2015**, *229*, 703–712. [CrossRef] [PubMed]
366. Singh, A.; Singla, E.; Soni, S.; Singla, A. Kinematic modeling of a 7-degree of freedom spatial hybrid manipulator for medical surgery. *Proc. Inst. Mech. Eng. Part H J. Eng. Med.* **2018**, *232*, 12–23. [CrossRef]
367. Gupta, S.; Singla, E.; Soni, S.; Singla, A. Singularity analysis of a 7-DOF spatial hybrid manipulator for medical surgery. *Int. J. Nonlinear Sci. Numer. Simul.* **2022**, *23*, 419–431. [CrossRef]
368. Singh, A.; Singla, A.; Soni, S. Gravity balancing of a seven-DOFs hybrid manipulator. In Proceedings of the 2nd International and 17th National Conference on Machines and Mechanisms, Kanpur, India, 16–19 December 2015; pp. 5–14.
369. Antonov, A.; Fomin, A. Mechanism design and inverse kinematics of a 5-DOF medical assistive manipulator. In *New Trends in Medical and Service Robotics*; Tarnita, D., Dumitru, N., Pisla, D., Carbone, G., Geonea, I., Eds.; Mechanisms and Machine Science; Springer: Cham, Switzerland, 2023; pp. 334–342. [CrossRef]
370. Antonov, A.V.; Fomin, A.S. A screw theory approach for instantaneous kinematic analysis of parallel–serial manipulators. *J. Mech. Robot.* **2025**, *17*, 031009. [CrossRef]
371. Liu, N.; Wu, J. Kinematics and application of a hybrid industrial robot—Delta-RST. *Sens. Transducers* **2014**, *169*, 186–192.

372. Wu, Y.; Fu, Z.; Xu, J.N.; Yan, W.X.; Liu, W.H.; Zhao, Y.Z. Kinematic analysis of 5-DOF hybrid parallel robot. In *Intelligent Robotics and Applications*; Liu, H., Kubota, N., Zhu, X., Dillmann, R., Zhou, D., Eds.; Springer: Cham, Switzerland, 2015; pp. 153–163. [CrossRef]
373. Wu, Y.; Fu, Z.; Xu, J.N.; Yan, W.X.; Liu, W.H.; Zhao, Y.Z. Dynamics analysis of hybrid parallel robot. In Proceedings of the 2015 International Conference on Fluid Power and Mechatronics, Harbin, China, 5–7 August 2015; pp. 1272–1275. [CrossRef]
374. Wu, Y.; Yang, Z.; Fu, Z.; Fei, J.; Zheng, H. Kinematics and dynamics analysis of a novel five-degrees-of-freedom hybrid robot. *Int. J. Adv. Robot. Syst.* **2017**, *14*, 172988141771663. [CrossRef]
375. Deng, F.; Liu, X.; Zhang, N.; Zhang, F. Dimension synthesis of a 3T2R labelling robot with hybrid mechanism. *J. Eur. Syst. Autom.* **2019**, *52*, 509–514. [CrossRef]
376. Lei, J.; San, H.; Zhao, J.; He, W. Trajectory planning and simulation of 5-DOF hybrid robot based on ADAMS. In Proceedings of the 2017 9th International Conference on Modelling, Identification and Control, Kunming, China, 10–12 July 2017; pp. 237–241. [CrossRef]
377. Chen, J.; San, H.; Chen, M.; Zhang, K.; Zhang, D. Mobility analysis of a hybrid mechanism based on POC equations and its kinematic. In Proceedings of the 2019 IEEE 8th Data Driven Control and Learning Systems Conference, Dali, China, 24–27 May 2019; pp. 1360–1367. [CrossRef]
378. Yao, Y.; Lin, J.; Zhang, B.; Jiang, D.; Chen, L. Improved strong tracking extended Kalman filter for identifying load disturbances and model uncertainties of serial–parallel mechanism. *Mech. Syst. Signal Process.* **2022**, *171*, 108819. [CrossRef]
379. Qiong, L.; Changyong, C.; Xiaodong, Z.; Kang, L.; Wenlei, X. Design of strawberry picking hybrid robot based on kinect sensor. In Proceedings of the 2018 International Conference on Sensing, Diagnostics, Prognostics, and Control, Xi'an, China, 15–17 August 2018; pp. 248–251. [CrossRef]
380. Huang, T.; Li, Z.; Li, M.; Chetwynd, D.G.; Gosselin, C.M. Conceptual design and dimensional synthesis of a novel 2-DOF translational parallel robot for pick-and-place operations. *J. Mech. Des.* **2004**, *126*, 449–455. [CrossRef]
381. Huang, T.; Mei, J.; Li, Z.; Zhao, X.; Chetwynd, D.G. A method for estimating servomotor parameters of a parallel robot for rapid pick-and-place operations. *J. Mech. Des.* **2005**, *127*, 596–601. [CrossRef]
382. Moosavian, S.A.A.; Pourreza, A.; Alipour, K. Kinematics and dynamics of a hybrid serial-parallel mobile robot. In Proceedings of the 2009 IEEE International Conference on Robotics and Automation, Kobe, Japan, 12–17 May 2009; pp. 1358–1363. [CrossRef]
383. Moosavian, S.A.A.; Pourreza, A.; Alipour, K. Dynamics and stability of a hybrid serial-parallel mobile robot. *Math. Comput. Modell. Dyn. Syst.* **2010**, *16*, 35–56. [CrossRef]
384. Shen, H.; Ji, E.; Ding, W.; Deng, J.; Hua, Y.; Li, T. Mechanism design and dynamic balance analysis of 6-DOF hybrid robot for tea-picking. *Trans. Chin. Soc. Agric. Mach.* **2023**, *54*, 416–426. [CrossRef]
385. Lv, C.; Hu, Y.; Wan, Z.; Zhang, J. The kinematics analysis for a five DOF serial-parallel manipulator with RP-(2-RRU/1-RUU) structure. In Proceedings of the 2011 IEEE International Conference on Mechatronics and Automation, Beijing, China, 7–10 August 2011; pp. 743–748. [CrossRef]
386. Moosavian, S.A.A.; Nazari, A.A.; Hasani, A. Kinematics and workspace analysis of a novel 3-DOF spatial parallel robot. In Proceedings of the 2011 19th Iranian Conference on Electrical Engineering, Tehran, Iran, 17–19 May 2011; pp. 1–6.
387. Lian, B.; Feng, P.; Wu, J.; Ma, J.; Zhang, Y.; Song, Y. Light-weight design of five-degree-of-freedom hybrid robot for assembling in the cabin. *J. Mech. Robot.* **2024**, *16*, 031010. [CrossRef]
388. Golla, P.; Ramesh, S.; Bandyopadhyay, S. Kinematics of the hybrid 6-Axis (H6A) manipulator. *Robotica* **2023**, *41*, 2251–2282. [CrossRef]
389. Hou, C.; Zhang, P.; Hu, Y.; Zhang, J. The dynamics analysis for a five DOF serial-parallel manipulator with RP-(2-RRU/1-RUU) structure. In Proceedings of the 2012 IEEE International Conference on Robotics and Biomimetics, Guangzhou, China, 11–14 December 2012; pp. 1564–1569. [CrossRef]
390. Nazari, A.A.; Moosavian, S.A.A.; Hasani, A. Kinematics analysis, dynamic modeling and verification of a CRRR 3-DOF spatial parallel robot. In Proceedings of the 2nd International Conference on Control, Instrumentation and Automation, Shiraz, Iran, 27–29 December 2011; pp. 1067–1073. [CrossRef]
391. Moosavian, S.A.A.; Hoseyni, S.S. Dynamics modeling and tipover stability of a hybrid serial-parallel mobile robot. In Proceedings of the 2nd International Conference on Control, Instrumentation and Automation, Shiraz, Iran, 27–29 December 2011; pp. 1024–1029. [CrossRef]
392. Lian, B.; Guo, J.; He, Z.; Song, Y. Optimal design of assembling robot considering different limb topologies and layouts. *J. Mech. Des.* **2025**, *147*, 013305. [CrossRef]
393. Waldron, K.J.; Raghavan, M.; Roth, B. Kinematics of a hybrid series-parallel manipulation system. *J. Dyn. Sys. Meas. Control* **1989**, *111*, 211–221. [CrossRef]
394. Khatib, O.; Roth, B.; Waldron, K.J. The design of a high-performance force-controlled manipulator. In Proceedings of the Eighth World Congress on the Theory of Machines and Mechanisms, Prague, Czechoslovakia, 26–31 August 1991; Volume 2, pp. 475–478.
395. Choi, H.S.; Han, C.S.; Lee, K.Y.; Lee, S.H. Development of hybrid robot for construction works with pneumatic actuator. *Autom. Constr.* **2005**, *14*, 452–459. [CrossRef]
396. Elsamanty, M.; Faidallah, E.M.; Hossameldin, Y.H.; Rabbo, S.A.; Maged, S.A.; Yang, H.; Guo, K. Workspace analysis and path planning of a novel robot configuration with a 9-DOF serial-parallel hybrid manipulator (SPHM). *Appl. Sci.* **2023**, *13*, 2088. [CrossRef]

397. Liang, F.; Zhang, G.; Zhang, T.; Guan, Y.; Liu, G. Kinematics analysis of a hybrid robot consisting of a SCARA and a parallel wrist. In Proceedings of the 2019 IEEE International Conference on Robotics and Biomimetics, Dali, China, 6–8 December 2019; pp. 558–563. [CrossRef]
398. Goubej, M.; Švejda, M. Research and design of modular robotic manipulator for chemical aggressive environment. In Proceedings of the 2011 12th International Carpathian Control Conference, Velke Karlovice, Czech Republic, 25–28 May 2011; pp. 374–378. [CrossRef]
399. Švejda, M.; Goubej, M. Innovative design and control of robotic manipulator for chemically aggressive environments. In Proceedings of the 13th International Carpathian Control Conference, High Tatras, Slovakia, 28–31 May 2012; pp. 715–720. [CrossRef]
400. Goubej, M.; Švejda, M. Dynamic analysis and control of robotic manipulator for chemically aggressive environments. In Proceedings of the 2013 IEEE International Conference on Mechatronics, Vicenza, Italy, 27 February–1 March 2013; pp. 273–278. [CrossRef]
401. Cheng, M.; Han, Z.; Ding, R.; Zhang, J.; Xu, B. Development of a redundant anthropomorphic hydraulically actuated manipulator with a roll-pitch-yaw spherical wrist. *Front. Mech. Eng.* **2021**, *16*, 698–710. [CrossRef]
402. Cheng, H.H. Real-time manipulation of a hybrid serial-and-parallel-driven redundant industrial manipulator. In Proceedings of the 1993 American Control Conference, San Francisco, CA, USA, 2–4 June 1993; pp. 1801–1805. [CrossRef]
403. Cheng, H.H. Real-time manipulation of a hybrid serial-and-parallel-driven redundant industrial manipulator. *J. Dyn. Sys. Meas. Control* **1994**, *116*, 687–701. [CrossRef]
404. Cheng, H.H.; Lee, J.J.; Penkar, R. Kinematic analysis of a hybrid serial-and-parallel-driven redundant industrial manipulator. *Int. J. Robot. Autom.* **1995**, *10*, 159–166.
405. Cheng, H.H.; Penkar, R. Stacking irregular-sized packages by a robot manipulator. *IEEE Rob. Autom. Mag.* **1995**, *2*, 12–20. [CrossRef]
406. Cheng, H.H. Real-time four-dimensional collision detection for an industrial robot manipulator. *J. Appl. Mech. Robot.* **1995**, *2*, 20–33.
407. Wang, Y.; Zhang, H.; Xu, S.; Zhu, Z.; Tang, Q.; He, Y.; Wei, C. A capture method based on series-parallel manipulator for satellite on-orbit service. In Proceedings of the 2016 35th Chinese Control Conference, Chengdu, China, 27–29 July 2016; pp. 6284–6289. [CrossRef]
408. He, J.; Gao, F.; Sun, Q. Design and kinematic analysis of a novel hybrid kinematic mechanism with seven-degrees-of-freedom and variable topology for operation in space. *J. Mech. Robot.* **2019**, *11*, 011003. [CrossRef]
409. He, J.; Ding, Q.; Gao, F.; Zhang, H. Kinematic calibration methodology of hybrid manipulator containing parallel topology with main limb. *Measurement* **2020**, *152*, 107334. [CrossRef]
410. Souza-Jimenez, J.A.; Gonzalez-Villela, V.J. Kinematics and tip-over stability analysis for a hybrid serial-parallel mobile manipulator. In Proceedings of the ASME 2011 International Mechanical Engineering Congress and Exposition, Denver, CO, USA, 11–17 November 2011; Volume 7, pp. 1237–1246. [CrossRef]
411. Kim, Y.Y.; Hwang, H.; Cho, S.I. A hybrid robotic system for harvesting heavy produce. *Eng. Agric. Environ. Food* **2008**, *1*, 18–23. [CrossRef]
412. Wang, X.; Yu, H.; Wang, H.; Sang, L.; Wang, X. Kinematics analysis for the leg mechanism of a wheel-leg hybrid rescue robot. In Proceedings of the 2013 International Conference on Advanced Mechatronic Systems, Luoyang, China, 25–27 September 2013; pp. 369–373. [CrossRef]
413. Wang, X.; Wang, X.; Yu, H.; Wang, H.; Lu, L.; Vladareanu, L.; Melinte, D.O. Dynamic analysis for the leg mechanism of a wheel-leg hybrid rescue robot. In Proceedings of the 2014 UKACC International Conference on Control, Loughborough, UK, 9–11 July 2014; pp. 504–508. [CrossRef]
414. Niu, J.; Wang, H.; Shi, H.; Pop, N.; Li, D.; Li, S.; Wu, S. Study on structural modeling and kinematics analysis of a novel wheel-legged rescue robot. *Int. J. Adv. Robot. Syst.* **2018**, *15*, 172988141775275. [CrossRef]
415. Niu, J.; Wang, H.; Jiang, Z.; Chen, L.; Zhang, J.; Feng, Y.; Guo, S. Kinematic analysis of a serial-parallel hybrid mechanism and its application to a wheel-legged robot. *IEEE Access* **2020**, *8*, 111931–111944. [CrossRef]
416. So, B.R.; Yi, B.J.; Kim, W.; Oh, S.R.; Park, J.; Kim, Y.S. Design of a redundantly actuated leg mechanism. In Proceedings of the 2003 IEEE International Conference on Robotics and Automation, Taipei, Taiwan, 14–19 September 2003; Volume 3, pp. 4348–4353. [CrossRef]
417. Zhang, W.; Guo, X.; Huang, H.; Huang, Q. Novel design of a 3-DOF series-parallel torso for humanoid robots. In Proceedings of the 2016 IEEE International Conference on Mechatronics and Automation, Harbin, China, 7–10 August 2016; pp. 1149–1154. [CrossRef]
418. Alfayad, S.; Ouezdou, F.B.; Namoun, F. New 3-DOFs hybrid mechanism for ankle and wrist of humanoid robot: Modeling, simulation, and experiments. *J. Mech. Des.* **2011**, *133*, 021005. [CrossRef]
419. Abdellatif, A.; Alfayad, S.; Hildebrandt, A.C.; Ouezdou, F.B.; Mechbal, N.; Zweiri, Y. Development of a new hydraulic ankle for HYDROïD humanoid robot. *J. Intell. Robot. Syst.* **2018**, *92*, 293–308. [CrossRef]
420. Li, Y.; Wang, Z.; Sun, P.; Xu, T.; Qin, S. Dynamic load distribution optimization for a 4-DOF redundant and series-parallel hybrid humanoid arm. *J. Mech. Eng.* **2020**, *56*, 45–54. [CrossRef]
421. Li, Y.; Wang, L.; Chen, B.; Wang, Z.; Sun, P.; Zheng, H.; Xu, T.; Qin, S. Optimization of dynamic load distribution of a serial-parallel hybrid humanoid arm. *Mech. Mach. Theory* **2020**, *149*, 103792. [CrossRef]

422. Wang, Z.; Li, Y.; Luo, Y.; Sun, P.; Chen, B.; Zheng, H. Dynamic analysis of a 7-DOF redundant and hybrid mechanical arm. *J. Zhejiang Univ. (Eng. Sci.)* **2020**, *54*, 1505–1515. [CrossRef]
423. Gao, J.S.; Li, M.X.; Li, Y.Y.; Wang, B.T. Singularity analysis and dimensional optimization on a novel serial-parallel leg mechanism. *Procedia Eng.* **2017**, *174*, 45–52. [CrossRef]
424. Feller, D.; Siemers, C. Topological analysis of a novel compact omnidirectional three-legged robot with parallel hip structures regarding locomotion capability and load distribution. *Robotics* **2021**, *10*, 117. [CrossRef]
425. Russo, M.; Ceccarelli, M. Design and simulation of a parallel-serial LARMbot arm. In *New Advances in Mechanism and Machine Science*; Doroftei, I., Oprisan, C., Pisla, D., Lovasz, E., Eds.; Springer: Cham, Switzerland, 2018; pp. 379–386. [CrossRef]
426. Ding, W.; Detert, T.; Corves, B.; Yao, Y.A. Reconbot: A reconfigurable rescue robot composed of serial-parallel hybrid upper humanoid body and track mobile platform. In *New Advances in Mechanisms, Mechanical Transmissions and Robotics*; Corves, B., Lovasz, E., Hüsing, M., Maniu, I., Gruescu, C., Eds.; Springer: Cham, Switzerland, 2017; pp. 241–249. [CrossRef]
427. Alfayad, S.; Ouezdou, F.B.; Namoun, F.; Bruneau, O.; Henaff, P. Three DOF hybrid mechanism for humanoid robotic application: Modeling, design and realization. In Proceedings of the 2009 IEEE/RSJ International Conference on Intelligent Robots and Systems, St. Louis, MO, USA, 10–15 October 2009; pp. 4955–4961. [CrossRef]
428. Alfayad, S.; Tayba, A.M.; Ouezdou, F.B.; Namoun, F. Kinematic synthesis and modeling of a three degrees-of-freedom hybrid mechanism for shoulder and hip modules of humanoid robots. *J. Mech. Robot.* **2016**, *8*, 041017. [CrossRef]
429. Tayba, A.; Alfayad, S.; Ouezdou, F.B.; Namoun, F. Kinematic modelling for glenohumeral shoulder of humanoid robot. *WSEAS Trans. Syst.* **2017**, *16*, 218–224.
430. Ghandour, M.; Jleilaty, S.; Oufroukh, N.A.; Olaru, S.; Alfayad, S. Real-time EtherCAT-based control architecture for electro-hydraulic humanoid. *Mathematics* **2024**, *12*, 1405. [CrossRef]
431. Ibrahim, A.A.H.; Ammounah, A.; Alfayad, S.; Tliba, S.; Ouezdou, F.B.; Delaplace, S. Hydraulic robotic leg for HYDROïD Robot: Modeling and control. *J. Robot. Mechatron.* **2022**, *34*, 576–587. [CrossRef]
432. Qin, L.; Liu, F.; Hou, T.; Liang, L. Kinematics analysis of serial-parallel hybrid humanoid robot in reaching movement. *J. Robot. Mechatron.* **2014**, *26*, 592–599. [CrossRef]
433. Qin, L.; Liu, F.; Liang, L. The application of adaptive backstepping sliding mode for hybrid humanoid robot arm trajectory tracking control. *Adv. Mech. Eng.* **2014**, *6*, 307985. [CrossRef]
434. Qin, L.; Liu, F.; Liang, L.; Jin, Z. Hybrid humanoid space mechanical arm trajectory tracking control based on sliding mode. *China Mech. Eng.* **2015**, *26*, 435–441. [CrossRef]
435. Wang, Z.; Li, Y.; Sun, P.; Luo, Y.; Chen, B.; Zhu, W. A multi-objective approach for the trajectory planning of a 7-DOF serial-parallel hybrid humanoid arm. *Mech. Mach. Theory* **2021**, *165*, 104423. [CrossRef]
436. Wang, Z.; Li, Y.; Shuai, K.; Zhu, W.; Chen, B.; Chen, K. Multi-objective trajectory planning method based on the improved elitist non-dominated sorting genetic algorithm. *Chin. J. Mech. Eng.* **2022**, *35*, 7. [CrossRef]
437. Sun, P.; Li, Y.; Shuai, K.; Yue, Y.; Wei, B. Workspace optimization of a humanoid robotic arm based on the multi-parameter plane model. *Robotica* **2022**, *40*, 3088–3103. [CrossRef]
438. Sun, P.; Li, Y.; Zhang, C.; Shan, X.; Yue, Y.; Wei, B. Scale optimization of humanoid robotic arms based on kinematic performance analysis. *China Mech. Eng.* **2022**, *33*, 2331–2340. [CrossRef]
439. Gao, J.; Wang, Y.; Yu, Q.; Zuo, W. Study on gait planning and simulation of a novel hybrid quadruped robot. In *Advances in Mechanical Design*; Tan, J., Gao, F., Xiang, C., Eds.; Springer: Singapore, 2018; pp. 1225–1239. [CrossRef]
440. Feller, D.; Siemers, C. Mechanical design and analysis of a novel three-legged, compact, lightweight, omnidirectional, serial–parallel robot with compliant agile legs. *Robotics* **2022**, *11*, 39. [CrossRef]
441. Feller, D. Dexterity, workspace and performance analysis of the conceptual design of a novel three-legged, redundant, lightweight, compliant, serial-parallel robot. *J. Intell. Rob. Syst.* **2023**, *109*, 6. [CrossRef]
442. Feller, D. Kinematics of a novel serial-parallel, compliant, three-legged robot. *IEEE Access* **2023**, *11*, 100729–100754. [CrossRef]
443. Fort, A.; Ceccarelli, M.; Laribi, M.A. Prototype and testing of LARMbot PK arm. In *Advances in Mechanism Design III*; Beran, J., Bílek, M., Václavík, M., Žabka, P., Eds.; Springer: Cham, Switzerland, 2022; pp. 210–219. [CrossRef]
444. Fort, A.; Laribi, M.A.; Ceccarelli, M. Design and performance of a LARMbot PK arm prototype. *Int. J. Humanoid Robot.* **2022**, *19*, 2250009. [CrossRef]
445. Ceccarelli, M.; Beaumont, S.; Russo, M. Design of a tripod LARMbot arm. *Actuators* **2024**, *13*, 211. [CrossRef]
446. Ceccarelli, M. A history of LARMbot humanoid. In *Explorations in the History and Heritage of Machines and Mechanisms*; Ceccarelli, M., Aslan Seyhan, I., Eds.; Springer: Cham, Switzerland, 2024; pp. 360–370. [CrossRef]
447. Giri, G.S.; Maddahi, Y.; Zareinia, K. An application-based review of haptics technology. *Robotics* **2021**, *10*, 29. [CrossRef]
448. Li, J.R.; Fu, J.L.; Wu, S.C.; Wang, Q.H. An active and passive combined gravity compensation approach for a hybrid force feedback device. *Proc. Inst. Mech. Eng. Part C J. Mech. Eng. Sci.* **2021**, *235*, 4368–4381. [CrossRef]
449. Li, Y.; Yan, Z.; Wang, H.; Du, Z.; Zhang, Y. Design and optimization of a haptic manipulator using series-parallel mechanism. In Proceedings of the 2012 IEEE International Conference on Mechatronics and Automation, Chengdu, China, 5–8 August 2012; pp. 2140–2145. [CrossRef]
450. Hao, J.L.; Xie, X.L.; Bian, G.B.; Hou, Z.G.; Zhou, X.H. Development and evaluation of a 7-DOF haptic interface. *IEEE/CAA J. Autom. Sin.* **2018**, *5*, 261–269. [CrossRef]

451. Bilgincan, T.; Dede, M.I.C. Development of an R-CUBE based general purpose haptic device system. In Proceedings of the ASME 2010 10th Biennial Conference on Engineering Systems Design and Analysis, Istanbul, Turkey, 12–14 July 2010; Volume 3, pp. 675–682. [CrossRef]
452. Dede, M.I.C.; Maaroof, O.W.; Ceccarelli, M. Analytical dynamic analysis of a kinesthetic haptic device. *J. Sci. Eng.* **2018**, *20*, 492–508. [CrossRef]
453. Tang, Z.; Payandeh, S. Design and modeling of a novel 6 degree of freedom haptic device. In Proceedings of the Third Joint EuroHaptics Conference and Symposium on Haptic Interfaces for Virtual Environment and Teleoperator Systems, Salt Lake City, UT, USA, 18–20 March 2009; pp. 523–528. [CrossRef]
454. Payandeh, S.; Tang, Z. Inverse kinematics solution of a class of hybrid manipulators. In *Intelligent Robotics and Applications*; Jeschke, S., Liu, H., Schilberg, D., Eds.; Springer: Berlin/Heidelberg, Germany, 2011; Volume 1, pp. 230–239. [CrossRef]
455. Tang, Z.; Payandeh, S. Modeling and experimental studies of a novel 6-DOF haptic device. In *Haptics: Generating and Perceiving Tangible Sensations*; Kappers, A.M.L., van Erp, J.B.F., Bergmann Tiest, W.M., van der Helm, F.C.T., Eds.; Springer: Berlin/Heidelberg, Germany, 2010; pp. 73–80. [CrossRef]
456. Tang, Z.; Payandeh, S. Experimental studies of a novel 6-DOF haptic device. In Proceedings of the 2013 IEEE International Conference on Systems, Man, and Cybernetics, Manchester, UK, 13–16 October 2013; pp. 3372–3377. [CrossRef]
457. Lu, S.; Li, Y. Kinematic analysis and performance evaluation of the 3-PUU parallel module of a 3D printing manipulator. In Proceedings of the 2014 13th International Conference on Control Automation Robotics & Vision, Singapore, 10–12 December 2014; pp. 1847–1852. [CrossRef]
458. Lu, S.; Li, Y. Dynamic analysis of a 3-DOF 3-PUU parallel manipulator based on the principle of virtual work. In Proceedings of the 2015 IEEE International Conference on Advanced Intelligent Mechatronics, Busan, Republic of Korea, 7–11 July 2015; pp. 1445–1450. [CrossRef]
459. Lu, S.; Li, Y. Dynamic dexterity evaluation of a 3-DOF 3-PUU parallel manipulator based on generalized inertia matrix. In Proceedings of the 2015 IEEE International Conference on Robotics and Biomimetics, Zhuhai, China, 6–9 December 2015; pp. 1506–1511. [CrossRef]
460. Zhou, H.; Ding, R.; Qin, Y.; Cao, Y. Hybrid kinematics mechanisms and its kinematic analysis oriented to multi 3D printing. *China Mech. Eng.* **2017**, *28*, 505–511. [CrossRef]
461. Liu, J.; Zhai, M.; Wang, B.; Lin, M.; Li, W.; Cao, Y. Dynamics analysis of 3-CPaR&R_1R_2 hybrid mechanism with joint clearance. In *Intelligent Robotics and Applications*; Yu, H., Liu, J., Liu, L., Ju, Z., Liu, Y., Zhou, D., Eds.; Springer: Cham, Switzerland, 2019; Volume 5, pp. 660–672. [CrossRef]
462. Cao, Y.; Liu, J.; Zhai, M.; Wang, B.; Sheng, Y.; Ju, Y. Wear performance analysis of 3-CPaR&R_1R_2 hybrid mechanism with joint clearance. *J. Harbin Eng. Univ.* **2021**, *42*, 893–901. [CrossRef]
463. Antonov, A.V.; Chernetsov, R.A.; Ulyanov, E.E.; Ivanov, K.A. Use of the chord method for analyzing workspaces of a parallel structure mechanism. *IOP Conf. Ser. Mater. Sci. Eng.* **2020**, *747*, 012079. [CrossRef]
464. Antonov, A. Stiffness evaluation and dimensional synthesis of a 5-DOF parallel-serial robot. In *Mechanism Design for Robotics*; Lovasz, E.C., Ceccarelli, M., Ciupe, V., Eds.; Springer: Cham, Switzerland, 2024; pp. 99–107. [CrossRef]
465. Cong, M.; Liu, D.; Du, Y.; Wen, H.; Wu, Y. Application of triune parallel-serial robot system for full-mission tank training. *Ind. Robot* **2011**, *38*, 533–544. [CrossRef]
466. Wang, X.; Chen, W. Command assignment method of a serial-parallel hybrid flight simulator. In Proceedings of the 27th Chinese Control and Decision Conference, Qingdao, China, 23–25 May 2015; pp. 3539–3544. [CrossRef]
467. Wang, X.; Chen, W. Kinematics analysis of a high dynamic serial-parallel hybrid flight simulator. In Proceedings of the 2015 34th Chinese Control Conference, Hangzhou, China, 28–30 July 2015; pp. 8667–8672. [CrossRef]
468. Jaberi, A.; Nahvi, A.; Hasanvand, M.; Tale Masouleh, M.; Arbabtafti, M.R.; Yazdani, M.; Lagha, M.; Hemmatabadi, M.; Samiezadeh, S. Design and kinematic analysis of a 4-DOF serial-parallel manipulator for urban bus driving simulator. In Proceedings of the 2013 First RSI/ISM International Conference on Robotics and Mechatronics, Tehran, Iran, 13–15 February 2013; pp. 407–412. [CrossRef]
469. Qazani, M.R.C.; Mohammadi, V.; Asadi, H.; Mohamed, S.; Nahavandi, S. Development of gantry-Tau-3R mechanism using a neuro PID controller. In Proceedings of the Australasian Conference on Robotics and Automation, Adelaide, Australia, 9–11 December 2019; pp. 1–8. Available online: https://ssl.linklings.net/conferences/acra/acra2019_proceedings/views/includes/files/pap103s1-file1.pdf (accessed on 6 November 2017). [CrossRef]
470. Nabavi, S.N.; Enferadi, J. Implementation of Gibbs-Appell method in dynamic analysis of a novel serial-parallel hybrid robot PP-(3RSS-PS). *J. Appl. Comput. Sci. Mech.* **2024**, *36*, 77–92. [CrossRef]
471. Qazani, M.R.C.; Asadi, H.; Nahavandi, S. A new Gantry-Tau-based mechanism using spherical wrist and model predictive control-based motion cueing algorithm. *Robotica* **2020**, *38*, 1359–1380. [CrossRef]
472. Gao, Z.; Xiao, J.; Wang, H.; Jin, Z. Dynamics analysis on a 3-DOF rotational platform with serial-parallel structure. *China Mech. Eng.* **2012**, *23*, 18–21. 38. [CrossRef]
473. Xu, Y.; Chen, L.; Yan, W.; Wang, B.; Zhao, Y. Type synthesis of the hybrid rotary platform mechanism with three degrees of freedom. In *Mechanism and Machine Science*; Zhang, X., Wang, N., Huang, Y., Eds.; Springer: Singapore, 2017; pp. 379–387. [CrossRef]

474. Xu, Y.; Ni, S.; Wang, B.; Wang, Z.; Yao, J.; Zhao, Y. Design and calibration experiment of serial–parallel hybrid rotary platform with three degrees of freedom. *Proc. Inst. Mech. Eng. Part C J. Mech. Eng. Sci.* **2019**, *233*, 1807–1817. [CrossRef]
475. Zhang, G.; Hou, Y.; Zeng, D.; Dou, Y.; Duan, Y. Motion characteristics analysis of 4-DOF hybrid antenna mechanisms. *China Mech. Eng.* **2020**, *31*, 2566–2572. [CrossRef]
476. Zhang, G.; Zheng, D.; Guo, J.; Hou, Y.; Zeng, D. Dynamic modeling and mobility analysis of the 3-R(RRR)R+R antenna mechanism. *Robotica* **2021**, *39*, 1485–1503. [CrossRef]
477. Deng, Y.; Duan, Y.; Li, J.; Dou, Y.; Zeng, D.; Hou, Y. Parametric design of hybrid polarization antenna mechanism based on workspace and its mechanical analysis. *J. Mech. Eng.* **2021**, *57*, 81–89. [CrossRef]
478. Wang, A.; Wei, Y.; Han, H.; Guan, L.; Zhang, X.; Xu, X. Ocean wave active compensation analysis of inverse kinematics for hybrid boarding system based on fuzzy algorithm. In Proceedings of the 2018 OCEANS—MTS/IEEE Kobe Techno-Oceans, Kobe, Japan, 28–31 May 2018; pp. 1–6. [CrossRef]
479. Yin, L.; Qiao, D.; Li, B.; Liang, H.; Yan, J.; Tang, G.; Ou, J. Modeling and controller design of an offshore wind service operation vessel with parallel active motion compensated gangway. *Ocean Eng.* **2022**, *266*, 112999. [CrossRef]
480. Tian, C.; Wei, Y.; Han, H.; Wang, A. Ocean wave active compensation analysis of hybrid boarding system based on multitask motion planning. In Proceedings of the OCEANS 2019—Marseille, Marseille, France, 17–20 June 2019; pp. 1–7. [CrossRef]
481. Wei, Y.; Wang, A.; Han, H. Ocean wave active compensation analysis of inverse kinematics for hybrid boarding system based on fuzzy algorithm. *Ocean Eng.* **2019**, *182*, 577–583. [CrossRef]
482. Wang, Y.; Wei, Y.; Gao, W.; Ma, T.; Han, Y. Ocean wave active compensation analysis for redundant hybrid boarding system: A multi-task motion planning method. *J. Mar. Sci. Eng.* **2023**, *11*, 708. [CrossRef]
483. Niu, A.; Wang, S.; Sun, Y.; Qiu, J.; Qiu, W.; Chen, H. Dynamic modeling and analysis of a novel offshore gangway with 3UPU/UP-RRP series-parallel hybrid structure. *Ocean Eng.* **2022**, *266*, 113122. [CrossRef]
484. Tang, G.; Lei, J.; Li, F.; Zhu, W.; Xu, X.; Yao, B.; Claramunt, C.; Hu, X. A modified 6-DOF hybrid serial–parallel platform for ship wave compensation. *Ocean Eng.* **2023**, *280*, 114336. [CrossRef]
485. Wu, J.; Gao, Y.; Zhang, B.; Wang, L. Workspace and dynamic performance evaluation of the parallel manipulators in a spray-painting equipment. *Robot. Comput. Integr. Manuf.* **2017**, *44*, 199–207. [CrossRef]
486. Yu, G.; Wu, J.; Wang, L.; Gao, Y. Optimal design of the three-degree-of-freedom parallel manipulator in a spray-painting equipment. *Robotica* **2020**, *38*, 1064–1081. [CrossRef]
487. Wang, X.; Zhang, B.; Xu, S.; Li, C.; Wu, T.; Zhang, C. Spatial arc interpolation analysis of novel 5-DOF hybrid mechanism. *Trans. Chin. Soc. Agric. Mach.* **2017**, *48*, 403–411. [CrossRef]
488. Karim, S.; Piano, S.; Leach, R.; Tolley, M. Error analysis for a high-precision five degree of freedom hybrid mechanism for high-power high-repetition rate laser operations. In Proceedings of the 32nd Annual Meeting of the American Society for Precision Engineering, Charlotte, NC, USA, 29 October–3 November 2017; pp. 372–377.
489. Karim, S.; Piano, S.; Leach, R.; Branson, D.; Tolley, M. Calibration and adjustment of a high-precision five degree-of-freedom hybrid mechanism. In Proceedings of the 33rd Annual Meeting of the American Society for Precision Engineering, Las Vegas, NV, USA, 4–9 November 2018; pp. 32–37.
490. Karim, S.; Piano, S.; Leach, R.; Tolley, M. Error modelling and validation of a high-precision five degree of freedom hybrid mechanism for high-power high-repetition rate laser operations. *Precis. Eng.* **2018**, *54*, 182–197. [CrossRef]
491. Karim, S.; Piano, S.; Branson, D.; Santoso, T.; Leach, R.; Tolley, M. Real-time target alignment system for high-power high-repetition rate laser operations using a five degree-of-freedom hybrid mechanism. *Int. J. Control* **2022**, *95*, 867–885. [CrossRef]
492. Vossoughi, G.R.; Bagheri, S.; Tavakoli, M.; Zakerzadeh, M.R.; Hosseinzadeh, M. Design, modeling and kinematics analysis of a novel serial/parallel pole climbing and manipulating robot. In Proceedings of the ASME 7th Biennial Conference on Engineering Systems Design and Analysis, Manchester, UK, 19–22 July 2004; Volume 2, pp. 399–408. [CrossRef]
493. Zakerzadeh, M.R.; Tavakoli, M.; Vossoughi, G.R.; Bagheri, S. Inverse kinematic/dynamic analysis of a new 4-DOF hybrid (serial-parallel) pole climbing robot manipulator. In *Climbing and Walking Robots*; Springer: Berlin/Heidelberg, Germany, 2005; pp. 919–934. [CrossRef]
494. Tavakoli, M.; Vosoughi, G.R.; Bagheri, S.; Zakerzadeh, M.R.; Salarieh, H. A novel serial/parallel pole climbing/manipulating robot: Design, kinematic analysis and workspace optimization with genetic algorithm. In Proceedings of the 21st International Symposium on Automation and Robotics in Construction, Jeju, Republic of Korea, 21–25 September 2004. [CrossRef]
495. Tavakoli, M.; Zakerzadeh, M.R.; Vossoughi, G.R.; Bagheri, S. Design and prototyping of a hybrid pole climbing and manipulating robot with minimum DOFs for construction and service applications. In *Climbing and Walking Robots*; Springer: Berlin/Heidelberg, Germany, 2005; pp. 1071–1080. [CrossRef]
496. Tavakoli, M.; Zakerzadeh, M.R.; Vossoughi, G.R.; Bagheri, S. A hybrid pole climbing and manipulating robot with minimum DOFs for construction and service applications. *Ind. Robot* **2005**, *32*, 171–178. [CrossRef]
497. Yan, L.; Chen, I.M.; Yeo, S.H.; Chen, Y.; Yang, G.L. A high-dexterity low-degree-of-freedom hybrid manipulator structure for robotic lion dance. *J. Zhejiang Univ. Sci. A* **2010**, *11*, 240–249. [CrossRef]
498. Chablat, D.; Wenger, P.; Angeles, J. The isoconditioning loci of a class of closed-chain manipulators. In Proceedings of the 1998 IEEE International Conference on Robotics and Automation, Leuven, Belgium, 16–20 May 1998; Volume 3, pp. 1970–1975. [CrossRef]

499. Chablat, D.; Wenger, P.; Angeles, J. The kinematic design of a 3-DOF hybrid manipulator. In *Integrated Design and Manufacturing in Mechanical Engineering '98*; Batoz, J.L., Chedmail, P., Cognet, G., Fortin, C., Eds.; Springer: Dordrecht, The Netherlands, 1999; pp. 225–232. [CrossRef]
500. Huang, M.Z.; Ling, S.H.; Sheng, Y. A study of velocity kinematics for hybrid manipulators with parallel-series configurations. In Proceedings of the 1993 IEEE International Conference on Robotics and Automation, Atlanta, GA, USA, 2–6 May 1993; Volume 1, pp. 456–461. [CrossRef]
501. Lee, S.; Kim, S. Efficient inverse kinematics for serial connections of serial and parallel manipulators. In Proceedings of the 1993 IEEE/RSJ International Conference on Intelligent Robots and Systems, Yokohama, Japan, 26–30 July 1993; Volume 3, pp. 1635–1641. [CrossRef]
502. Huang, M.Z.; Ling, S.H. Kinematics of a class of hybrid robotic mechanisms with parallel and series modules. In Proceedings of the 1994 IEEE International Conference on Robotics and Automation, San Diego, CA, USA, 8–13 May 1994; Volume 3, pp. 2180–2185. [CrossRef]
503. Chen, S. Dynamic model of a hybrid robot manipulator based on Stewart platform. In Proceedings of the ASME 1994 Design Technical Conferences Collocated with the ASME 1994 International Computers in Engineering Conference and Exhibition and the ASME 1994 8th Annual Database Symposium, Minneapolis, MN, USA, 11–14 September 1994; pp. 249–253. [CrossRef]
504. Cha, S.H.; Lasky, T.A.; Velinsky, S.A. Kinematic redundancy resolution for serial-parallel manipulators via local optimization including joint constraints. *Mech. Based Des. Struct. Mach.* **2006**, *34*, 213–239. [CrossRef]
505. Meng, X.; Gao, F.; Wu, S.; Ge, Q.J. Type synthesis of parallel robotic mechanisms: Framework and brief review. *Mech. Mach. Theory* **2014**, *78*, 177–186. [CrossRef]
506. Ye, W.; Li, Q. Type synthesis of lower mobility parallel mechanisms: A review. *Chin. J. Mech. Eng.* **2019**, *32*, 38. [CrossRef]
507. Chakarov, D.; Parushev, P. Synthesis of parallel manipulators with linear drive modules. *Mech. Mach. Theory* **1994**, *29*, 917–932. [CrossRef]
508. Campos, A.; Budde, C.; Hesselbach, J. A type synthesis method for hybrid robot structures. *Mech. Mach. Theory* **2008**, *43*, 984–995. [CrossRef]
509. Zeng, Q.; Fang, Y. Structural synthesis of serial-parallel hybrid mechanisms via group theory and representation of logical matrix. In Proceedings of the 2009 International Conference on Information and Automation, Zhuhai/Macau, China, 22–24 June 2009; pp. 1392–1397. [CrossRef]
510. Zeng, Q.; Fang, Y. Structural synthesis of serial-parallel hybrid mechanisms based on representation and operation of logical matrix. *J. Mech. Robot.* **2009**, *1*, 041003. [CrossRef]
511. Zeng, Q.; Fang, Y. Algorithm for topological design of multi-loop hybrid mechanisms via logical proposition. *Robotica* **2012**, *30*, 599–612. [CrossRef]
512. Shen, H.; Zhao, H.; Deng, J.; Meng, Q.; Zhu, W.; Yang, T. Type design method and the application for hybrid robot based on freedom distribution and position and orientation characteristic set. *J. Mech. Eng.* **2011**, *47*, 56–64. [CrossRef]
513. Shen, H.; Yang, T.; Ma, L. Synthesis and structure analysis of kinematic structures of 6-dof parallel robotic mechanisms. *Mech. Mach. Theory* **2005**, *40*, 1164–1180. [CrossRef]
514. Qin, Y.; Hai, Y.C.; Zhou, C.H.; Cao, Y. Structural synthesis of 3T2R five-degree-of-freedom (DoF) hybrid mechanism. In Proceedings of the 2015 IEEE International Conference on Cyber Technology in Automation, Control, and Intelligent Systems, Shenyang, China, 8–12 June 2015; pp. 65–70. [CrossRef]
515. Cao, Y.; Qin, Y.; Chen, H.; Ge, S.; Zhou, H. Structural synthesis of 5-DOF hybrid mechanisms based on G_F set. *Trans. Chin. Soc. Agric. Mach.* **2015**, *46*, 392–398. [CrossRef]
516. Qin, Y.; Cao, Y.; Chen, H.; Cao, H. Structural synthesis of fully-decoupled two-translational and three-rotational hybrid robotic manipulators. *J. Xi'an Jiaotong Univ.* **2016**, *50*, 92–99. [CrossRef]
517. Qin, Y.; Cao, Y.; Chen, H. Type synthesis of two-translational and three-rotational hybrid mechanisms. *China Mech. Eng.* **2016**, *27*, 1001–1006. [CrossRef]
518. Zhou, H.; Qin, Y.; Chen, H.; Ge, S.; Cao, Y. Structural synthesis of five-degree-of-freedom hybrid kinematics mechanism. *J. Eng. Des.* **2016**, *27*, 390–412. [CrossRef]
519. Xie, F.; Liu, X.J.; Li, T. Type synthesis and typical application of 1T2R-type parallel robotic mechanisms. *Math. Probl. Eng.* **2013**, *2013*, 206181. [CrossRef]
520. Zhang, D.; Zheng, Y.; Wei, L.; Wu, J.; Xu, Y.; Zhao, Y. Type synthesis of 2T1R planar parallel mechanisms and their moduling development applications. *IEEE Access* **2021**, *9*, 72217–72227. [CrossRef]
521. Zhang, L.; Qi, Y. Topology synthesis of hybrid space control mechanism based on FIS theory. *IEEE Access* **2023**, *11*, 48749–48767. [CrossRef]
522. Antonov, A.; Fomin, A.; Glazunov, V.; Petelin, D.; Filippov, G. Type synthesis of 5-DOF hybrid (parallel-serial) manipulators designed from open kinematic chains. *Robotics* **2023**, *12*, 98. [CrossRef]
523. Zanganeh, K.E.; Angeles, J. A formalism for the analysis and design of modular kinematic structures. *Int. J. Robot. Res.* **1998**, *17*, 720–730. [CrossRef]
524. Shukla, D.; Paul, F.W. Motion kinematics of series-parallel robots using a virtual link concept. In Proceedings of the 22nd Biennial Mechanisms Conference: Robotics, Spatial Mechanisms, and Mechanical Systems, Scottsdale, AZ, USA, 13–16 September 1992; pp. 49–58. [CrossRef]

525. Li, Q.; Yang, C.; Xu, L.; Ye, W. *Performance Analysis and Optimization of Parallel Manipulators*; Springer: Singapore, 2023. [CrossRef]
526. Carmichael, M.G.; Liu, D.; Waldron, K.J. A framework for singularity-robust manipulator control during physical human-robot interaction. *Int. J. Rob. Res.* **2017**, *36*, 861–876. [CrossRef]
527. Sklar, M.; Tesar, D. Dynamic analysis of hybrid serial manipulator systems containing parallel modules. *J. Mech. Transm. Autom. Des.* **1988**, *110*, 109–115. [CrossRef]
528. Chung, G.B.; Yi, B.J.; Lim, D.J.; Kim, W. An efficient dynamic modeling methodology for general type of hybrid robotic systems. In Proceedings of the 2004 IEEE International Conference on Robotics and Automation, New Orleans, LA, USA, 26 April–1 May 2004; Volume 2, pp. 1795–1802. [CrossRef]
529. Zhang, X.; Wang, H.; Rong, Y.; Niu, J.; Tian, J.; Li, S. Dynamic modeling of a class of parallel-serial mechanisms by the principle of virtual work. *Meccanica* **2023**, *58*, 303–316. [CrossRef]
530. Etemadi-Zanganeh, K.; Angeles, J. Instantaneous kinematics of modular parallel manipulators. In Proceedings of the ASME 1994 Design Technical Conferences Collocated with the ASME 1994 International Computers in Engineering Conference and Exhibition and the ASME 1994 8th Annual Database Symposium, Minneapolis, MN, USA, 11–14 September 1994; pp. 271–277. [CrossRef]
531. Etemadi-Zanganeh, K.; Angeles, J. Instantaneous kinematics of general hybrid parallel manipulators. *J. Mech. Des.* **1995**, *117*, 581–588. [CrossRef]
532. Monsarrat, B.; Gosselin, C.M. Jacobian matrix of general parallel and hybrid mechanisms with rigid and flexible links: A software-oriented approach. In Proceedings of the ASME 2002 International Design Engineering Technical Conferences and Computers and Information in Engineering Conference, Montreal, QC, Canada, 29 September–2 October 2002; Volume 5, pp. 461–470. [CrossRef]
533. Sun, P.; Li, Y.; Chen, K.; Zhu, W.; Zhong, Q.; Chen, B. Generalized kinematics analysis of hybrid mechanisms based on screw theory and Lie groups Lie algebras. *Chin. J. Mech. Eng.* **2021**, *34*, 98. [CrossRef]
534. Cho, W.; Tesar, D.; Freeman, R.A. The dynamic and stiffness modeling of general robotic manipulator systems with antagonistic actuation. In Proceedings of the 1989 International Conference on Robotics and Automation, Scottsdale, AZ, USA, 14–19 May 1989; pp. 1380–1387. [CrossRef]
535. Cho, W. Constraint embedding in kinematics and dynamics of hybrid manipulator systems. *KSME J.* **1994**, *8*, 6–18. [CrossRef]
536. Rosyid, A.; El-Khasawneh, B.; Alazzam, A. Review article: Performance measures of parallel kinematics manipulators. *Mech. Sci.* **2020**, *11*, 49–73. [CrossRef]
537. Russo, M. Measuring performance: Metrics for manipulator design, control, and optimization. *Robotics* **2022**, *12*, 4. [CrossRef]
538. Lee, S.; Kim, S. Manipulabilities of serial-parallel manipulator systems. In Proceedings of the IEEE/RSJ International Conference on Intelligent Robots and Systems, Raleigh, NC, USA, 7–10 July 1992; Volume 2, pp. 1185–1192. [CrossRef]
539. Lewis, F.L.; Dawson, D.M.; Abdallah, C.T. *Robot Manipulator Control: Theory and Practice*, 2 ed.; CRC Press: Boca Raton, FL, USA, 2003. [CrossRef]
540. Ajwad, S.A.; Iqbal, J.; Ullah, M.I.; Mehmood, A. A systematic review of current and emergent manipulator control approaches. *Front. Mech. Eng.* **2015**, *10*, 198–210. [CrossRef]
541. Majarena, A.C.; Santolaria, J.; Samper, D.; Aguilar, J.J. An overview of kinematic and calibration models using internal/external sensors or constraints to improve the behavior of spatial parallel mechanisms. *Sensors* **2010**, *10*, 10256–10297. [CrossRef]
542. Chen, G.; Li, T.; Chu, M.; Xuan, J.Q.; Xu, S.H. Review on kinematics calibration technology of serial robots. *Int. J. Pre. Eng. Manuf.* **2014**, *15*, 1759–1774. [CrossRef]
543. Ye, H.; Wu, J.; Huang, T. Kinematic calibration of over-constrained robot with geometric error and internal deformation. *Mech. Mach. Theory* **2023**, *185*, 105345. [CrossRef]
544. Ye, H.; Wu, J. Residual index for measurement configuration optimization in robot kinematic calibration. *Sci. China Technol. Sci.* **2023**, *66*, 1899–1915. [CrossRef]
545. Moser, B.L.; Gordon, J.A.; Petruska, A.J. Unified parameterization and calibration of serial, parallel, and hybrid manipulators. *Robotics* **2021**, *10*, 124. [CrossRef]